1999

# Modeling the response of groundwater levels in wells to changes in barometric pressure

Hyejoung Han Seo
*Iowa State University*

# INFORMATION TO USERS

This manuscript has been reproduced from the microfilm master. UMI films the text directly from the original or copy submitted. Thus, some thesis and dissertation copies are in typewriter face, while others may be from any type of computer printer.

**The quality of this reproduction is dependent upon the quality of the copy submitted.** Broken or indistinct print, colored or poor quality illustrations and photographs, print bleedthrough, substandard margins, and improper alignment can adversely affect reproduction.

In the unlikely event that the author did not send UMI a complete manuscript and there are missing pages, these will be noted. Also, if unauthorized copyright material had to be removed, a note will indicate the deletion.

Oversize materials (e.g., maps, drawings, charts) are reproduced by sectioning the original, beginning at the upper left-hand corner and continuing from left to right in equal sections with small overlaps.

Photographs included in the original manuscript have been reproduced xerographically in this copy. Higher quality 6" x 9" black and white photographic prints are available for any photographs or illustrations appearing in this copy for an additional charge. Contact UMI directly to order.

Bell & Howell Information and Learning
300 North Zeeb Road, Ann Arbor, MI 48106-1346 USA

UMI®
800-521-0600

# Modeling the response of groundwater levels in wells to changes in barometric pressure

by

Hyejoung Han Seo

A dissertation submitted to the graduate faculty

in partial fulfillment of the requirements for the degree of

DOCTOR OF PHILOSOPHY

Co-majors: Civil Engineering (Environmental Engineering); Water Resources

Major Professors: LaDon C. Jones and Robert Horton

Iowa State University

Ames, Iowa

1999

UMI Number: 9950118





Bell & Howell Information and Learning Company
300 North Zeeb Road
P.O. Box 1346
Ann Arbor, MI 48106-1346

Graduate College
Iowa State University

This is to certify that the Doctoral dissertation of

Hyejoung Han Seo

Has meet the dissertation requirement of Iowa State University

Signature was redacted for privacy.

Co-major Professor

Signature was redacted for privacy.

Co-major Professor

Signature was redacted for privacy.

For the Co-Major Program

Signature was redacted for privacy.

For the Co-Major Program

Signature was redacted for privacy.

For the Graduate College

# DEDICATION

I would like to dedicate this dissertation to my parents.

## TABLE OF CONTENTS

## LIST OF FIGURES

# LIST OF TABLES

# NOTATION

| Symbol | Description | Unit |
|---|---|---|
| $\rho$ | density of water | $(M/L^3)$ |
| $\alpha$ | confined compressibility of porous medium | $(LT^2/M)$ |
| $\alpha'$ | bulk compressibility of porous medium (drained) | $(LT^2/M)$ |
| $\beta$ | compressibility of water | $(LT^2/M)$ |
| $\gamma$ | compressibility of solid skeleton | $(LT^2/M)$ |
| $\gamma_w$ | specific weight of water | $(M/L^2T^2)$ |
| $\delta$ | error term | |
| $\varphi$ | angle of phase lag | |
| $\varepsilon$ | parameter varying 0 to 1 | |
| $\eta$ | constituent of phase lag | |
| $\lambda$ | parameter varying 0 to 2/3 | |
| $\nu$ | Poisson's ratio | |
| $\Phi(t)$ | hydraulic head in the porous medium at time = t | (L-water) |
| $\Phi_m$ | amplitude of sinusoidal head perturbation | (L_water) |
| $\Phi_0$ | initial hydraulic head for all r and z at t = 0 | (L_water) |
| A | A constant of well discharge factor | (1/T) |
| $\Delta BP$ | change in barometric pressure between time = t and t $+\Delta t$ | (L_water) |
| (r, z) | radial and vertical location | (L) |
| $\sigma_T$ | normal stress | $(M/LT^2)$ |
| $\Delta w$ | water level change in the well between time = t and t $+\Delta t$ | (L_water) |
| $B_e$ | barometric efficiency | |
| BP(t) | barometric pressure at time = t | (L_water) |
| $BP_m$ | Amplitude of barometric pressure frequency function | (L_water) |
| $BP_0$ | initial barometric pressure at t = 0 | (L_water) |
| C | well discharge factor | (1/L) |
| c | speed of sound | (L/T) |
| D | depth of well from the water table | (L) |
| $D_f$ | hydraulic diffusivity | $(L^2/T)$ |
| $d\sigma_e$ | change in effective stress | $(M/LT^2)$ |
| dp | change in fluid pressure | $(M/LT^2)$ |
| $dV_T$ | volume reduction of the porous medium | $(L^3)$ |
| $dV_{w1}$ | change in volume due to compression of porous medium | $(L^3)$ |
| $dV_{w2}$ | change in volume due to expansion of water | $(L^3)$ |
| $E_v$ | bulk modulus of water | $(M/LT^2)$ |

| | | |
|---|---|---|
| f | external source term | (L_water) |
| g | gravitational constant | (L/T2) |
| g(u) | well response function | |
| H(t) | Water level displcacement in well recovery | (L) |
| i | hydraulic gradient | |
| K | hydraulic conductivity | (L/T) |
| $K_0$ | Bessel function | |
| $K_r$ | horizontal hydraulic conductivity | (L/T) |
| $K_z$ | vertical hydraulic conductivity | (L/T) |
| L | Length of well screen | (L) |
| $l_i$ | water slug length based on well casing radius | (L) |
| n | porosity | |
| p | fluid pressure (incremental) | ($M/LT^2$) |
| $p_m$ | amplitude of sinusoidal pressure perturbation | (L_water) |
| Q | total groundwater flowrate out of the well | (L3/T) |
| q | Darcy's groundwater velocity | (L/T) |
| $r_c$ | radius of well casing | (L) |
| $r_w$ | radius of well borehole | (L) |
| $S_s$ | specific storage | (1/L) |
| $S_s'$ | three dimensional storage coefficient | (1/L) |
| T | period | (T) |
| t | time | (T) |
| WP | continuous function of water supply into a well | (L_water) |
| w(t) | water surface elevation in the well at time = t | (L_water) |
| $w_0$ | initial water surface elevation in the well at t = 0 | (L_water) |
| $\varpi$ | angular frequency | (1/T) |
| $z_1$ | vertical coordinates of the bottom of well screen | (L) |
| $z_2$ | vertical coordinates of the top of well screen | (L) |

## ABSTRACT

For many practical situations, the effect of barometric pressure variations on the water level in a well has been ignored. However, in many cases, water levels in wells are observed to fluctuate significantly in response to changes in barometric pressure. In this study, a physically based conceptual model for the influence of barometric pressure on groundwater wells was developed and tested.

It is proposed that water level fluctuations in response to barometric pressure are due, in large part, to the different manner in which the pressure is propagated through the water column in the well and the porous media outside the well. Changes in pressure transmit through the water column in the well to the screened region with essentially negligible loss in pressure. On the contrary, pressure changes transferred through the porous media to the screened elevation outside the well undergo an irreversible transformation of fluid potential (head loss). Consequently, the loss in pressure head through the porous medium causes a lateral hydraulic head gradient to be developed around the well-screen region, as well as a vertical one through the porous medium. In response to the head gradient developed due to changes in barometric pressure, groundwater flows are induced through the well screen, with subsequent changes in well-casing storage. In the proposed model the well itself is an essential element. The well-water flux across the screen and the consequent change in well-casing storage were appropriately linked with groundwater flow in the surrounding porous medium and estimated through an iteration technique. This approach incorporates the traditional governing theories on groundwater flow: conservation of mass and Darcy's law. Groundwater flow was modeled as two-dimensional (radial and vertical) unsteady flow, and

solved by using finite element approximations. The basic concept of the model was successfully applied to the modeling of slug tests through simple modification of boundary and initial conditions. Furthermore, it was demonstrated that a series of slug/bail tests and barometric pressure are theoretically related to each other in physical and numerical senses.

The results suggest that the physically based model in this study is very effective in estimating the water level fluctuations in a well due to changes in barometric pressure. The magnitude and behavior of well response varies with the hydraulic properties (hydraulic conductivity and specific storage) and well geometry (casing radius, screened length, and depth of well). Moreover, the model relating the barograph and responding water levels can potentially serve as a tool for estimation of unknown hydraulic parameters. Conclusively, the influence of barometric pressure on groundwater wells can be solved by relevant integration of three parts: i) the solution of the differential equation governing groundwater flow, ii) the use of the well screen as a boundary condition, where the fluctuating water levels and head perturbation in surrounding formation are coupled, iii) the estimation of the exact amount of well-water flux across the screen and changes in well-casing storage.

# CHAPTER 1. INTRODUCTION

## 1.1 Background

Wells are the primary instrument used to measure groundwater pressures over space and time. The water level in a well measures the average hydrostatic pressure over the well screen. In fact, groundwater levels in wells and fluid pressures in the porous medium are not constant. They are subject to natural and man-made forces that cause changes in the hydraulic head. Several natural phenomena can affect the water level in a well over a period of a few days: infiltration from precipitation, evapotranspiration, phreatophtic consumption, earth tides, atmospheric pressure and even tectonics of earth crust material. Measurement and analysis of these types of stress on the subsurface hydrologic system have been reported (Bredehoeft, 1967; Johnson et al., 1973; Marine, 1975; Bower and Heaton, 1978; Rhoads and Robinson, 1979; Hanson, 1980; Bower, 1983). Parameter estimation techniques have been applied to measurements of naturally occurring pressure fluctuations in order to assess hydrogeologic properties (Carr and van der Kamp, 1969; Pinder et al., 1969; Davis, 1972; van der Kamp and Gale, 1983; Keller et al., 1989; Rojstaczer, 1998a; Furbish, 1988; Ritzi et al., 1991). Among the natural causes for well-water fluctuations, the change in barometric pressure (b.p.) is continuous and ubiquitous and the related data are obtainable without much cost and man-power. Thus, the influence of b.p. on groundwater has a high potential to serve as an in-situ hydraulic test.

However, the physical mechanisms or physics, describing the relationship between b.p. and groundwater levels in a well, has not been fully explored or understood. In fact, looking for the influence of b.p. on a well has not been a popular research topic for hydrologists,

because of its perceived lack of practical implications. The influence of b.p. effects on aquifers has long been recognized (Meinzer, 1928). Meinzer proposed the elastic property of confined aquifers as a mechanism for a variety of responses to changes in b.p. between aquifers. Based on his argument, most previous research has been limited to consideration of the elastic properties of aquifers (Jacob, 1940; Todd, 1959; Tuinzaad, 1954, Gilliland, 1969). In other previous works, most of the descriptions and explanations for the mechanics of b.p. induced water level fluctuations in wells have been applicable only for limited cases; entrapped air in the capillary zone (Peck, 1960; Turk, 1975) or well intake region (Keller and van der Kamp, 1992), and air flow in the unsaturated zone (Weeks, 1979).

None of the above studies paid attention to the conservation of mass and Darcy's law, with incorporation of the well itself as a boundary condition, in their model or explanation. In many cases, hydrostatic equilibrium of heads between the well and surrounding porous media were assumed to be quickly restored after exertion of b.p. on the groundwater system, so the actual water flow process through the well screen and storage changes within the well were not taken into account.

Some textbooks (e.g., Sen, 1995) address the topic of b.p. effects on static water levels and aquifer tests, suggesting simultaneous monitoring of b.p. and the water level in a well prior to aquifer tests. A simple linear model (Walton, 1970; Freeze and Cherry, 1974) is generally used in an attempt to correct for possible barometric influences on measured water level data. However, this simple linear model is essentially a curve fitting between changes in b.p. and the water level in a well. This model is not enough to explain the mechanics or physics for the observed strong relation between groundwater head and b.p.

In practice, fluctuations of the groundwater level in wells due to changes in b.p. are often encountered in the simultaneous records of the two. The water surface elevation in a well is inversely related to b.p.; it decreases (increases) with an increase (decrease) in b.p. In some cases, the water levels in observation wells show almost the mirror image of b.p. fluctuation, with a very high efficiency (Furbish, 1991; Hare and Morse, 1997). A groundwater well can act like a barometer under certain conditions.

Recently the importance of b.p. in terms of groundwater hydrology has focused on many aspects. The significant impacts of b.p. variations on water level monitoring in a containment system has been reported by Hare and Morse (1997). Considerable fluctuations in static water levels in wells due to changes in b.p. can lead to erroneous estimates of hydraulic gradient, and consequently, erroneous parameters for contaminant transport at sites with monitoring programs and remedial measures. The b.p. effects on well recovery during slug tests were observed and its potential for misleading estimation of hydraulic conductivity pointed out (Supardi, 1993). Correction of b.p. effects in the water level measurements through determination of barometric efficiency is getting more attention than before (Furbish and Lyverse, 1988; Davis and Rasmussen, 1993; Rasmussen and Crawford, 1997).

The effect of b.p. variation on groundwater conditions is typically observed through the change in water level elevation in a well. A well occupies a particular volume in the subsurface porous system, with storage of water within it. A groundwater well is usually vented to the atmosphere at the top and open to water flow at the bottom through a screened section. Barometric pressure simultaneously exerts forces on water both inside and outside of a well, but in quite different manners. A well acts as a shortcut to carry the full changes in

b.p. directly to the saturated porous system because water has filled the well column, whereas b.p. transmits vertically through the porous media outside the well with loss of its potential. The resultant pressure imbalance of hydraulic head, between the inside and outside of a well, across the screen, initiates changes in well-casing storage through groundwater flow into or out of the surrounding formation. The well itself is an essential factor which affects the influence of b.p. on the well responses. Conceptually, the direct exertion of varying b.p. on wells, which is convertible to terms of water head, can be considered to be equivalent to dynamic slug/bail tests, with an oscillating water supply into/out of the well.

In the following recent works, well-aquifer communication and pressure imbalances has been proposed as a possible mechanism for water level fluctuations in response to b.p. variations. Rojstaczer (1988b) adequately summarized, through frequency analyses, general theory on the effects of b.p. on various groundwater conditions. In other works (Gieske, 1986; Furbish, 1991), the interaction between b.p. and an aquifer was clarified in terms of the pressure potential difference established at the section of well screen directly by changes in b.p. in the well. Their studies are theoretical or analytical trials for explanation of the b.p. influence on fully penetrating wells under confined conditions. The uniqueness of Furbish's work is to seek a well response function to b.p. loadings from an existing solution for slug tests, implying a theoretical analogy between b.p. effects and a series of slug /bail tests. Although the approaches, assumed conditions, and solution methods of the above the models are different from those in this work, the concepts for the relationship between b.p. and groundwater wells is complementary. B.p. induced water level fluctuations are a response to a pressure imbalance across the well screen and concurrent groundwater flow in the

surrounding porous material. However, specifically, none of the previous studies have developed a physically based conceptual model for the influence of b.p. on groundwater well, using mass conservation, Darcy's law, and incorporating the well as a boundary condition, including exact well geometry and well-casing storage (in contrast to treating the well as a line source).

Given the shortcomings of the linear model and previous works, a new conceptual model is introduced in this dissertation in order to describe the phenomenon responsible for fluctuations of water level in wells in response to barometric pressure. This model incorporates accurate well physics with traditional governing theories for groundwater flow. Groundwater flow in response to changes in b.p are assumed to result from two pressure imbalances: i) between the well and the surrounding aquifer and ii) between the water table and porous medium. Conceptually, the lateral movement of water around the well, affected by vertical flow from the water table, are responsible for well water fluctuations; flow through the well screen into/out of porous medium and subsequent changes in well-casing storage are appropriately coupled in the model. The proposed model is solved in terms of saturated groundwater flow, neglecting air movement in the overlying vadose zone. A deep and partially penetrating well in an unconfined condition is assumed, but the governing theory of a confining flow is applied to solve b.p. induced pore pressure changes, with the assumption of no water table fluctuation. Thus, any confining or leaky confining aquifer condition can be simulated by applying appropriate hydraulic properties.

The model structure, as mentioned earlier, is based on the integration of distinct physical phenomena due to b.p. variations between a well (direct input of b.p. and well-casing storage

changes) and in the surrounding porous medium (increasing head losses of b.p. with depths). The model can be used for simulation or parameter estimation; water level changes in a well are predicted for given hydraulic properties, or conversely hydraulic parameters of the formation are to be estimated when we have observed water level and b.p. data. In the application of the model, it will be evaluated whether optimal analysis of the natural fluctuations of groundwater levels due to b.p. changes can serve as an in-situ hydraulic test for unsteady groundwater flow.

### 1.2 Objectives of Study

An understanding of physical phenomenon and hydraulic properties in subsurface hydrologic systems is necessary to locate, extract, treat, and protect groundwater, so current and future generations can depend on this resource to enhance their quality of life. Therefore, the influence of b.p. on water level in wells and groundwater conditions should also be realized in order to: i) explain the observed strong correlation between them, ii) get an accurate estimation of groundwater level with the b.p. effect filtered out and iii) evaluate the potential use of the observed data set of b.p. and responding water levels for estimation of hydraulic properties. Moreover, from a scientific perspective, it is highly valuable to comprehend the nature and cause of the observed fluctuations in wells due to b.p., even if they were not significant on a practical basis.

The objectives of this study are:

- to develop and test a new model for the response of water level in wells to changes in b.p.

- to investigate factors, such as hydraulic properties of screened formation and well geometry, controlling the magnitude and behavior of b.p. induced water fluctuations in wells through sensitivity analyses
- to evaluate the suggested model as a tool for hydraulic property estimation
- to relate the concept of slug/bail tests to b.p. effects on wells through new modeling of slug test.

It is hoped that information from this study will lead to a better understanding of groundwater modeling and well hydraulics with respect to the influence of barometric pressure on groundwater conditions.

### 1.3 Scope of Study

It is proposed in this study that the influence of b.p. on the water level in a well can be described by traditional concepts of groundwater flow, with the well itself as a boundary condition, including well-casing storage. This well boundary condition is distinct from the traditional concepts of the well as a line-source. The accurate estimation of well-water flux and well-casing storage variations are completed by inclusion of exact well geometry in the model. The groundwater flow portion of the model is assumed to be described by a two-dimensional (radial–vertical) unsteady groundwater flow, without loss of generality. The groundwater model was solved numericaly using Galerkin's finite element approximations. The techniques discussed in this study may offer a method of obtaining the hydrologic parameters necessary for evaluating aquifer systems, using stresses imposed by nature on groundwater systems. In addition, a new model for slug tests is also developed through the

modification of boundary conditions of the main model for the b.p. effect on wells. This outcome makes the simulation of b.p. effect on well recovery during slug tests feasible in this study. Furthermore, extensions of conventional slug tests to more exotic tests are introduced in order to support the basic concept of the model for b.p. effect and then relate it into slug/bail tests. Verification of the model against available analytical solutions supports the fact that the numerical procedures and handing of the well boundary condition employed in the models are correct and valid.

Field data that are presented in this study are mainly hydrologic data obtained from a glacial till area, the Ames Till Hydrology Site (ATHS), in central Iowa. The data include hydrographs from wells penetrating part of the porous medium, barographs, well geometry, and well recovery data during slug tests. Field data of b.p. and responding water levels in a well in a sandy aquifer material in New York are also included for validation of the model. This was obtained from other researchers who are working on related topics about b.p. effects on wells (Hare and Morse, 1997; Hare, 1998).

In the section of model application, theoretical simulations are first presented to support the postulated hypotheses of the model, assuming a sinusoidal fluctuation of b.p. over a range of days. All cases simulated are for a single well, where the radial-vertical groundwater flow model is appropriate. The factors controlling water level fluctuation due to changes in b.p. are examined through the sensitivity studies about well and hydraulic parameters. Supplementary discussions focus on: i) comparison of b.p. effects between the cases of with and without a well in the porous medium, ii) importance of hydraulic diffusivity in b.p. propagation, iii) effects of well depth (or water table) on well response to changes in b.p., and

iv) limitations of the linear model as a post-step for correction for b.p. induced water level variations. The model is then applied to actual field cases that showed strong evidence of correlation between changes in b.p. and water levels (or heads). Actual case studies consist of: i) b.p. effect on head changes in the porous medium without a well, ii) b.p. effect on static water level in a well, iii) b.p. effect on water level in a well in a containment system, and iv) b.p. effects on well recovery in slug tests. Simulated results will support the validity of adopting the model of this study in various ways. Optimization of unknown hydraulic parameters will prove the effectiveness of the model as a tool for estimation of hydraulic properties of the tested formation.

In brief, the approach of this study is theoretical in terms of well physics and groundwater hydrology applied in the conceptual model, and pragmatic as well through use of the most common numerical tool for groundwater problems. However, it should be noted that there are practical limitations on the applicability of this model, depending on the degree to which the assumptions of the model will actually be valid.

### 1.4 Dissertation Organization

This dissertation includes eight main chapters and six appendix sections: Introduction (Chapter 1), Literature Review (Chapter 2), Physically Based Conceptual Model for the Response of Wells to Barometric Pressure (Chapter 3), Method (Chapter 4), Revision of Model for Slug Tests (Chapter, 5), Model Application (Chapter 6), Results and Discussion (Chapter 7), and Conclusion (Chapter 8). All tables and figures appear in the middle of text, usually in a separated page, following the first point referred to in the text. Reference style

follows the format of the journal, *Ground Water*. Governing equation and its solution, computer codes, and other additional works are included in the appendix after the conclusion chapter. References cited are close to the end of document just before the acknowledgements.

# CHAPTER 2. LITERATURE REVIEW

## 2.1 Theoretical Background of Barometric Pressure Effects on Porous Media

Barometric fluctuations of water levels in wells imply that fluid pressure in a well and a saturated porous formation are rarely constant over appreciable periods of time under the continuous changes in b.p. Because b.p. is a source for change in stress of the subsurface hydrologic system, changes in b.p. lead to changes in the pore fluid pressure of the formation. The general theory about pore fluid pressure changes in response to the applied stress needs to be reviewed before the study of b.p. effects on groundwater wells.

The response of pore pressure to changes in stress due to b.p. is a particular case of the interactions between *fluid pressure*, *stress* and *strain* in a porous formation system. Such interactions are influenced by the physical, mechanical, and hydraulic properties of a formation. The theory of consolidation is based on five principles (Verruijt, 1977): 1) conservation of mass in the pore fluid; 2) Darcy's law for the movement of the pore fluid; 3) equilibrium of the porous medium as a whole; 4) Hooke's law for the deformation of the solid skeleton; and 5) Terzaghi's principle of effective stress (Figure 1).

In the context of soil mechanics, Terzaghi (1923) first concisely summed up the phenomenon of deformation of a porous medium as a whole, accompanied by the flow of fluid in the pores due to changes in stress. He also presented the theory of effective stress to describe the changes in fluid pressure responding to the applied stress. Biot (1941) extended Terzaghi's work in a more physical way, based on consistent assumptions.

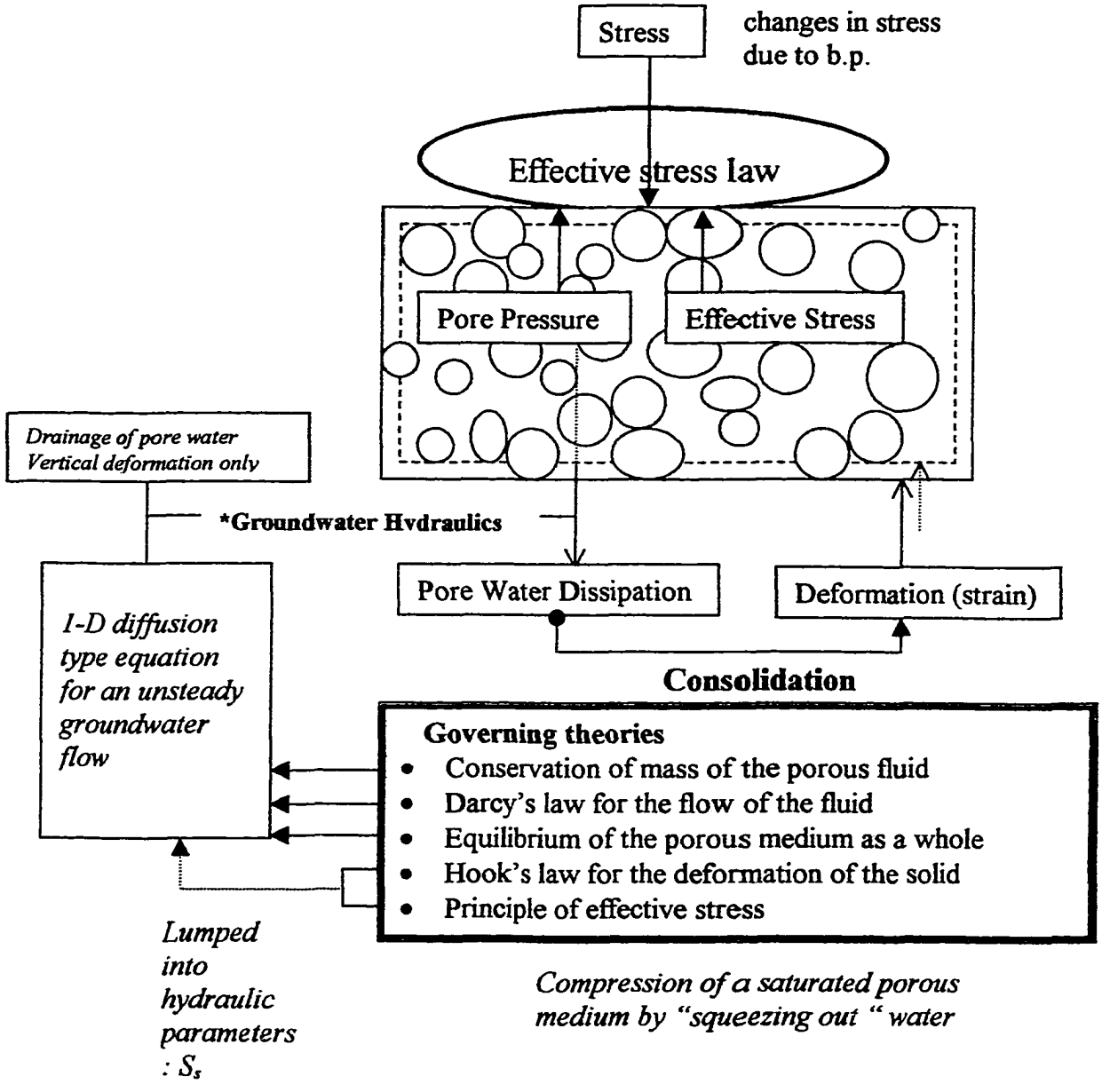


Figure 2.1. Theoretical background on one-dimensional diffusion-type groundwater flow due to changes in barometric pressure.

Biot assumed that a porous medium behaves as a perfectly elastic material and presented the most general three-dimensional equations for the interaction of pore fluid pressure, stress, and strain. His work primarily composed the basis for many theoretical works in soil mechanics, and more generally for the theory of flow through elastic porous media. However, the behavior of real porous medium is more complicated than the behavior of a perfect elastic material, so his theory provides an approximate description of the mechanical behavior of the porous formation. In fact, consolidation is not an immediate response of formations to transient pressure. Rather, consolidation is manifested in the gradual settlement, or subsidence of soil under long term loading, such as that due to a permanent structure. Hence the practical importance of consolidation lies not so much in groundwater hydraulics as in soil mechanics, where the amount and uniformity of settlement are of interest in the stability of soil.

As a part of consolidation, pore water moves in response to changes in fluid pressure distribution. In other words, water dissipated during the consolidation process must find its way out from an unevenly distributed load. This results in different hydrostatic pressures, at various points in the soil, due to the complex space-variable and time-variable nature of the consolidation. Describing the behavior of this pore fluid due to change in stress is less erroneous than that of a solid, because its sensitivity to changes in stress can be solved clearly in physical way.

In the concept of groundwater hydraulics, elastic properties of porous formation was first recognized as a controlling factor for various responses of aquifers to changes in stress due to b.p by Meinzer (1928). Later, Jacob (1940) derived equations for the elastic storage

coefficient and porosity of an aquifer based on one-dimensional (vertical) aquifer elasticity. Since his analysis, the diffusion-type partial differential equation developed has served as the governing theory on the subsequent unsteady groundwater flow due to changes in b.p. In the theory of groundwater flow, the Biot's theory reduces to Jacob's under assumptions of no horizontal deformation and one-directional groundwater movement. Verruijt (1969) showed mathematically how Biot's theory reduces to Jacob's. Nur and Byerlee (1971) derived an exact expression for strain of a formation due to pore fluid pressure. Based on Nur and Byerlee's works, van der Kamp and Gale (1983) generalized earlier derivations on the hydraulic behavior of a fluid under the applied stress changes in a compressible porous medium. It was confirmed that vertical groundwater flow induced by b.p. can be described with a simple diffusion-type equation involving pore pressure only under certain assumptions.

The following is a brief summary of works by van der Kamp and Gale (1983). The generalized three-dimensional equations for the interaction of stress and fluid pressure are written in the form of equations 2-1 and 2-2. The variables $\sigma_T$, p, denote only deviation from the initial undisturbed state.

$$K\nabla^2 p = S_s' \frac{\partial}{\partial t}(p - \varepsilon\sigma_T) \qquad (2\text{-}1)$$

$$\nabla^2 \sigma_T = \lambda \nabla^2 p \qquad (2\text{-}2)$$

where $$S_s' = \rho g\{(\alpha - \gamma) + n(\beta - \gamma)\} \qquad (2\text{-}3)$$

$$\varepsilon = \alpha' - \gamma[\alpha' - \gamma + n(\beta - \gamma)]^{-1} \qquad (2\text{-}4)$$

$$\lambda = \frac{2\left(1 - \frac{\gamma}{\alpha'}\right)(1 - 2\nu)}{3(1 - \nu)} \qquad (2\text{-}5)$$

$K$ = hydraulic conductivity

$S'_s$ = three dimensional storage coefficient

$p$ = fluid pressure (incremental)

$\varepsilon$ = parameter varying 0 to 1

$\sigma_T$ = normal stress

$\alpha$ = confined compressibility of porous medium

$\beta$ = compressibility of water

$\gamma$ = compressibility of solid skeleton

$\alpha'$ = bulk compressibility of porous medium (drained)

$\lambda$ = parameter varying 0 to 1

$\nu$ = Poisson ratio

$n$ = porosity

$\rho$ = density of water

$g$ = gravitational constant

Equations 2-1 and 2-2 constitute a pair of equations for the interaction of pore pressure and stress in a homogeneous formation with compressible solid grains. For the undrained case, i.e., if there is no flow induced by the stress changes, then

$$\nabla^2 p = 0 \tag{2-6}$$

and thus,

$$P = \varepsilon \sigma_T \tag{2-7}$$

The pore pressure transient is a direct measure of changes in the normal stress. Under the assumption of ideal confined conditions of the aquifer, the static response of the well to deformation due to b.p. and earth tides has been used for determination of elastic properties of aquifer material (Bodvarsson, 1970; Bisop, 1973; Rhoads and Robinson, 1979; Furbish, 1988; Rojstaczer and Agnew, 1989). However, problems always arise when using a groundwater well as a strain meter, because there is no ideal static or confined response of the well to given stress changes. For example, the b.p. influence on the water table and seasonal fluctuations of the water table due to precipitation can easily disguise the quality of the strain signal in the well.

For the special case of fluid flow, in which no horizontal strain is assumed during the transient flow process, the normal stress is expressed in the following equation:

$$\sigma_T = \lambda P \qquad (2\text{-}8)$$

Now the above-coupled equations, 2-1 and 2-2, are reduced to one equation, a diffusion-type equation:

$$\nabla^2 p = \frac{S_s}{K}\frac{\partial p}{\partial t} \qquad (2\text{-}9)$$

$$S_s = S'(1-\lambda\varepsilon) = \rho g\{(\alpha-\gamma')(1-\gamma)+n(\beta-\gamma)\} \qquad (2\text{-}10)$$

where $S_s$ = specific storage

In equation 2-10, if the compressibility of solid is ignored ($\gamma = 0$), then

$$S_s = \rho g(\alpha + n\beta) \qquad (2\text{-}11)$$

The expression of $S_s$ in equation 2-11 is commonly encountered in groundwater hydrology texts. Based on the compressibility of formations reported in literature (Freeze and Cherry, 1979), the range of $S_s$ is illustrated in Figure 2.2.

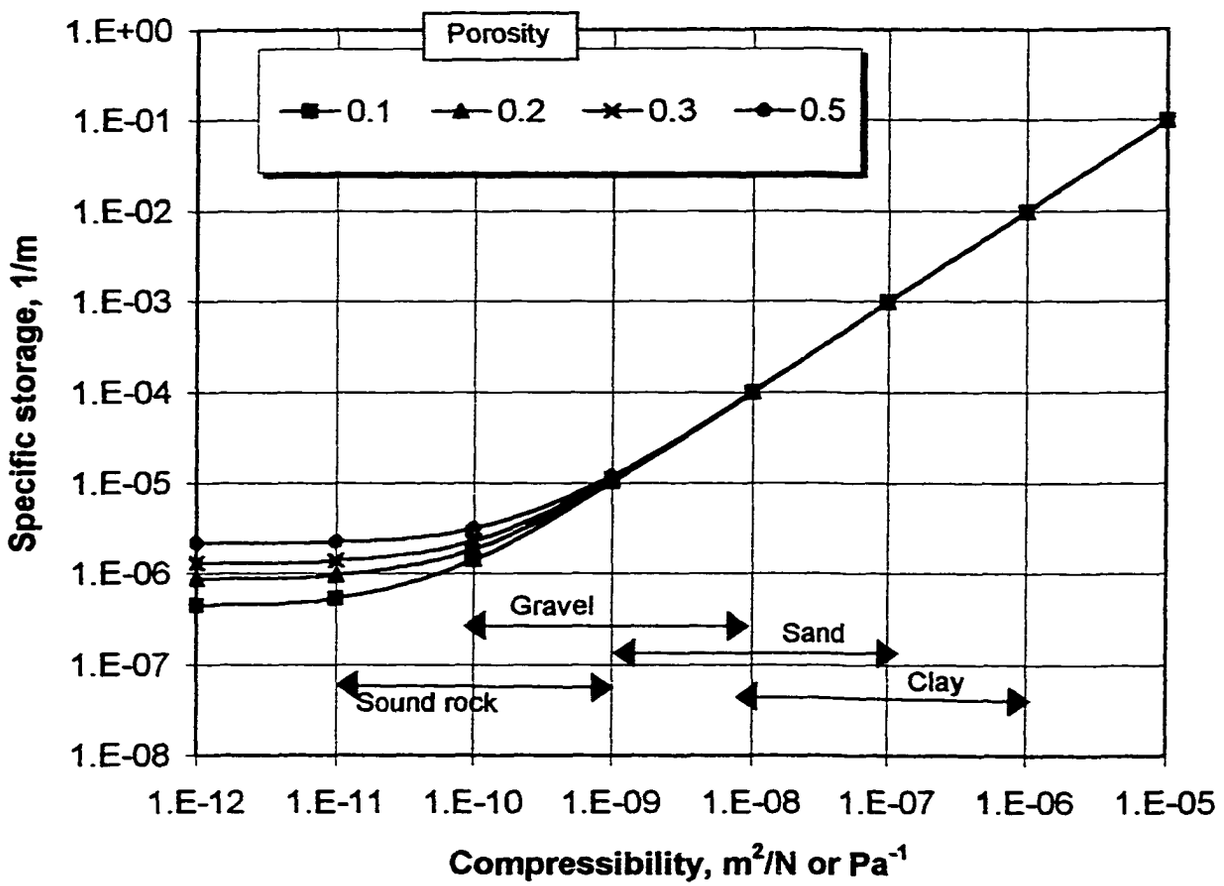


Figure 2.2. Specific storage values for various geologic units.

Specific storage ranges from 1E-01 $m^{-1}$ to 1E-06 $m^{-1}$ for various types of geologic materials. It is also clearly seen that changes in porosity has a minor influence on the $S_s$ of a formation at a given compressibility. Since equation 2-9 is used when pore fluid flow is present, the basic concepts behind the equation are conservation of mass and Darcy's law. This means equation 2-9 constitutes the standard form of a governing equation for unsteady groundwater flow. In fact, measurements of b.p. effects on subsurface porous medium using the above diffusion-type governing equation has been suggested as possible in-situ hydraulic tests for the characterization of bulk formation properties, such as hydraulic conductivity, specific storage, and porosity (Bredehoef, 1967; van der Kamp and Gale, 1983; Hsieh et al., 1987; Furbish, 1988; Rojastaczer, 1988a).

Atmospheric pressure changes are exerted simultaneously over formations of large horizontal extent. Thus, for a homogeneous formation with no lateral variations of the formation properties, horizontal displacements due to atmospheric pressure changes may be assumed to be negligible. Under no horizontal displacements, the change of total vertical stress is equal to the change of atmospheric pressure at the ground surface. Neglecting changes in pneumatic potential in the unsaturated zone, vertical groundwater flow due to barometric loading may occur when the top boundary of the flow is the water table. The water table itself constitutes a boundary condition at the top surface for pore pressure in an unconfined groundwater flow condition. In such a case, the pressure potential associated with the vertical flow will satisfy the one-dimensional diffusion-type equation.

$$\frac{\partial^2 p}{\partial z^2} = \frac{S_s}{K}\frac{\partial p}{\partial t} = \frac{1}{D_f}\frac{\partial p}{\partial t} \qquad (2\text{-}12)$$

where $D_f$ = hydraulic diffusivity

The above equation is valid for the one-dimensional case when fluid flow and deformation occur in one direction. The vertical propagation of changes in b.p. from the water table can be considered to be a groundwater flow process governed by the hydraulic properties of the porous formation, called hydraulic diffusivity ($D_f$), which is defined as hydraulic conductivity divided by specific storage in units of $L^2/T$.

The mathematical solution for equation 2-12 is readily available (e.g. Keller et al. 1989). If the head fluctuation at the upper boundary is assumed to be a sinusoidal wave, the boundary condition for the source head fluctuations is:

$$p = p_m \cos\left(\frac{2\pi t}{T}\right) \qquad \text{at } z=0 \tag{2-13}$$

$$p=0 \qquad \text{at } z=\infty \tag{2-14}$$

The solution is:
$$p(z, t) = p_m\, e^{-\eta z} \cos\left(\frac{2\pi t}{T} - \eta z\right) \tag{2-15}$$

where
$$\eta = \left(\frac{\pi S_s}{T K_z}\right) \tag{2-16}$$

$$\varphi = \eta z \tag{2-17}$$

$p_m$ = amplitude of external pressure source

T = period of frequency function

$\eta$ = constituent of phase lag

$\varphi$ = angle of phase lag

## 2.2 Analytical Approaches for Barometric Pressure and Groundwater Wells

Three studies (Geiske, 1986; Rojstaczer, 1988a; Furbish; 1991), which have contributed to the study of b.p. effects on groundwater wells, will be introduced in this section. Their contribution is mainly adoption of pressure imbalance between the well and aquifer and consequent unsteady groundwater flow as a possible mechanism for barometric fluctuation of water in wells. Other previous works have not properly taken into account the actual well-aquifer interaction based on governing theories on groundwater flow due to changes in b.p.

The problem of b.p. influence on wells can analytically become manageable by casting it into a frequency domain, so a periodic rate of well discharge is obtainable (Cooper et al., 1965; Geiske, 1986; Rojstaczer, 1988a). In the studies by Geiske (1986) and Rojstaczer (1988a), it was demonstrated that the amplitudes and phases of the well fluctuations depend on the frequency characteristics of b.p.

In Gieske's work (1986), interaction between the barometric pressure and well response has been analytically solved in terms of a continuous frequency response function by assuming only the lateral movement of groundwater through the well screen region.

The governing equation for the transient groundwater flow is the diffusion-type equation:

$$\nabla^2\Phi=\frac{S_s}{K}\frac{\partial\Phi}{\partial t} \qquad (2\text{-}18)$$

The assumed boundary conditions are external b.p. variations and the total head fluctuations at the well boundary ($r = r_c$), respectively:

$$BP(r, t) = BP_m \exp(i\ \varpi t) \qquad (2\text{-}19)$$

$$\Phi(r, t) = \Phi_m \exp[i(\varpi t + \varphi)] \qquad (2\text{-}20)$$

$$\Phi(r,t) = w(t) + BP(r,t) \qquad (2\text{-}21)$$

where $\Phi$ = hydraulic head

w = water level

BP = barometric pressure

$\varpi$ = angular frequency

Then the well flux created by BP(t) was estimated using the conservation of mass and Darcy's flux at the well boundary. The final form of the water level transient, w(t), is:

$$w(t) = BP_m \cos\varphi \cos(\varpi t + \varphi) - BP_m \cos(\varpi t) \qquad (2\text{-}22)$$

where $$\tan\varphi = A/\varpi = \frac{2LK}{r_c^{\,2}\varpi K_0(C r_c)} \qquad (2\text{-}23)$$

A = constant of well discharge factor

L = length of well screen

K = hydraulic conductivity

$K_0$= Bessel function

C = well discharge factor

$r_c$ = well casing diameter

$\varphi$ = angle of phase lag

As seen in equations 2-22 and 2-23, attenuation and phase shift in the well response to b.p. vary with the frequency function applied. Geiske's model allows explicit solutions for the amplitude and phase shift of well water fluctuation arising from sinusoidal motion of b.p., yielding very useful information on the aquifer properties of K and $S_s$.

An integral study on the well water response to b.p. loading, also in the frequency domain, was presented by Rojstaczer (1988b). He analyzed different types of responses of water levels in wells under various groundwater conditions: static confined, leaky confined, and unconfined conditions. In his study, all the possible responses of subsurface fluids are specified and then integrated for understanding b.p. induced water level fluctuations.

For example, in a leaky (partially) confined aquifer condition (Rojstaczer, 1988a), the whole track of b.p. propagation from the top of the land surface to the bottom of the well was introduced in terms of four different fluid flows responsible for the well response into periodic b.p. variations: air flow in the unsaturated zone, vertical water flow through the confining layer, vertical flow through the aquifer, and lateral groundwater flow between the well itself and the surrounding aquifer. The water level in a well due to changes in b.p. was inferred from solutions for the traditional governing equations, such as one-dimensional diffusion of air flow, one-dimensional diffusion type leakage flow in the confining layer, and vertical and lateral groundwater flow in the aquifer. The resulting frequency of b.p. dynamics was shown to be a partial controlling factor on the response of subsurface hydrologic system in terms of attenuation and phase lagging. The well response at a high frequency of b.p. is controlled mainly by the well radius and horizontal hydraulic diffusivity of the aquifer, implying that influence of the air flow and vertical leakage on well responses can be ignored under certain situations. Such circumstances were assumed in the work by Furbish (1991), which focused only on the well-aquifer interaction responding to b.p. changes in time domain. At the intermediate b.p. frequency, the response of the well is subject to the loading efficiency of the

aquifer, whereas at low b.p. frequency, it is largely governed by the air diffusivity and thickness of the unsaturated zone.

Under the unconfined condition, significant attenuation of well responses to b.p. were shown to attribute to interference of flow from the water table. In further discussion, it was demonstrated that unconfined responses can be assumed to be equivalent to the above partial confined condition, under certain conditions which minimize the effects of water table. For example, for a deep well in a very low vertical hydraulic diffusivity formation, the vertical average of the well responses are similar to a partially confined condition. Additionally, a very high frequency of b.p. and high lateral hydraulic diffusivity of the formation allow for the assumption of confined response of a well in the unconfined condition.

The mathematical solution for b.p. induced water level transient in a confined well is obtained by inferring that b.p. influence on a well is conceptually equivalent to a continuous series of slug or bail tests (Furbish, 1991). Furbish employed the mathematical concept of impulse response function and the convolution integral for explaining b.p. effect on water level in wells, assuming a groundwater well as a linear system. The convolution integral equation which relates the water level response to changes in b.p. is given as:

$$w(t) = \int_0^\infty g(u)\, BP(t-u)\, du \qquad (2\text{-}24)$$

where $g(u)$ = well response function

Furbish demonstrated the impulse response function of pressure variation within the well can be obtained from traditional solutions to slug tests. Slug impact can be thought of as a step change in pressure and b.p. dynamics can be expressed as a series of slug impacts on the well. A series of step functions in a very small time interval was applied for an approximation of

continuously changing atmospheric pressure. It is mathematically clear that the impulse well response function is the first derivative of the step response function. In Furbish's derivation of the impulse response function, the approximate solution (Hvsorlev, 1951) was applied instead of the complete Cooper et al. solution (1967) due to its computational complexity. The final solution for water level fluctuation responding to b.p. change was obtained by the principle of superposition: proportionality and additivity. It was concluded that well response to b.p. fluctuation depends on not only the hydraulic properties (specific storage and hydraulic conductivity), but also well geometry parameters (casing radius and screened length).

**2.3 Other Previous Works**

Another mechanism for the response of groundwater wells to b.p. effects were described by vertical air movement in the unsaturated zone (Yusa, 1969; Weeks 1979; Rojstaczer, 1988a). In the above studies, b.p. induced air movement and the attendant pressure lag and attenuation in the unsaturated zone, which is reflected in water levels in wells, were utilized to determine the pneumatic diffusivity of materials. Week's explanation was that the resistance of solid particles in the unsaturated zone prevent changes in b.p. from propagating to the water table at once and without head loss, whereas b.p. reaches the water inside the well instantaneously. He explored the b.p. effects on fully screened wells below the water table and developed his own model, in which water level fluctuations are computed by the solution of the governing equation for the air flow in the unsaturated zone. He did not extend the resistance concept to head losses in the saturated zone, where the well is generally partially screened and groundwater movement actually occurs.

Rojstaczer (1988a) included air flow in the unsaturated zone as a partial component affecting well responses to b.p. frequency signals. In his further study (Rojstazer and Tunks, 1995), in-situ analysis of the soil air pressure transient in responding to changes in b.p. are utilized to determine temporal and spatial variability in soil air diffusivity.

Entrapped air in the unsaturated zone, capillary pores, or well-screened region was alternatively proposed as a mechanism for water level fluctuations due to b.p. (Peck, 1960; Turk, 1975; Keller and van der Kamp, 1992). The mechanism and their postulated situations are entirely different from that suggested in this study. The mechanism of air entrapment below the water table would work only for the case of a shallow well in unconfined aquifers. Air entrapment in well bore region is also not a common case in groundwater well installation. Furthermore, considering the solubility of air in water and the duration of monitoring wells, fluctuations due to entrapped air are somewhat suspicious in many cases. Therefore, they are not adequate to explain the ubiquitous correlation between changes in b.p. and water levels in a well.

## 2.4 Simple Linear Model and Barometric Efficiency

A simple linear model for the response of a well to b.p. is:

$$\Delta w = B_e \Delta BP \qquad (2\text{-}25)$$

where $\Delta w$ = changes in water level in the well

$\Delta BP$ = changes in the barometric pressure

$B_e$ = barometric efficiency

The barometric efficiency ($B_e$) assumes a linear relationship between changes in the b.p. and the resulting changes in the water level:

$$B_e = \frac{\Delta w}{\Delta BP} \qquad (2\text{-}26)$$

To estimate the effect of changes in b.p. on the water levels in the wells, b.p and responding water levels in the well need to be measured simultaneously. Then the barometric efficiency of a well is estimated by applying linear regression to the measured water level response, using $\Delta BP$ as the independent variable and $\Delta w$ as the dependent variable. The slope of the regression line represents the barometric efficiency of the well. The inverse relationship between b.p. and water level yields the negative sign of $B_e$, which was reported usually to fall in a range of –0.20 to -0.75 (Freeze and Cherry, 1979).

However, as pointed out in the studies of frequency analyses, b.p. effects on wells is subject to a lagging problem, as well as attenuation (Geiske, 1986; Rojstaczer, 1988a). For such a situation, simple linear regression between b.p. and water level data, without any statistical correction, may result in significant errors in estimates of the barometric efficiency for a well.

# CHAPTER 3. PHYSICALLY BASED CONCEPTUAL MODEL FOR THE RESPONSE OF WELLS TO BAROMETRIC PRESSURE

We will now develop and describe the proposed physically based conceptual model for the response of wells to barometric pressure. The assumptions and physical concepts are covered. The model is expressed in mathematical form, as a coupled governing differential equation for groundwater flow, groundwater flux through the well screen, and a volume balance for the water level in the well.

## 3.1 Hypotheses

The effects of b.p. on groundwater pressures are typically observed through a common hydrogeologic measurement: the water level elevation in a well. The top of a well usually has a vent hole open to the atmosphere, and changes in b.p. can act directly on the water surface in the well. The change in b.p. at the water surface in the well transmit through the free standing water in the well. Disturbances in a fluid column propagate at the speed of sound in the fluid, where the velocity is determined by changes in the pressure and also the density of the fluid as described by the following equation (Munson et al., 1990, see p. 27).

$$c=\sqrt{\frac{dp}{d\rho}} \qquad \text{or} \qquad c=\sqrt{\frac{E_v}{\rho}} \tag{3-1}$$

where $c$ = speed of sound

$p$ = pressure

$\rho$ = density of fluid

$E_v$ = bulk modulus of fluid

For water at 10 °C, for instance, $E_v = 2.09 \times 10^9$ N/m$^2$ and $\rho = 999.7$ kg/m$^3$, and the pressure propagation velocity is 1447 m/s or 4747 ft/s. The changes in b.p. on the water surface in a well are transmitted very rapidly (i.e., essentially instantaneously with respect to the velocity of groundwater flow) through the water column inside the well casing. Hence, in analyzing the barometric response of the water level in a well, the fact that b.p. acts directly on the water in contact with the surrounding formation at the well screen should be born in mind. For practical purposes, a change in b.p. at the water surface in a well can be assumed to be instantly transmitted throughout the free water column in the well.

On the other hand, b.p. changes acting on the porous media outside the well must be transmitted through the unsaturated and saturated porous medium. The vadose zone, which is usually oxidized and unsaturated soil, often contains a variety of openings such as fractures, joints, and pore spaces between solid particles. Since these openings are connected to each other, changes of b.p. in the atmosphere is assumed to transmit instantly, and without loss, as pressure changes at the groundwater table. During the pressure propagation in the saturated porous media, head loss will occur. Head losses occur by the resistance on boundaries between particles. The head loss is the conversion of a part of the energy (or pressure head), which is usually transformed into thermal energy within the system (usually not significant enough to affect the temperature of the groundwater system). With a change in b.p., without head loss in the saturated porous media, the pore pressure changes in the porous media would be equal to the fluid pressure changes in the free standing water in the well. Consequently, the change in pressure both inside and outside of the well would cancel each other, and changes in b.p. would not induce any movement of the water level in the well. However, the reduced

transferability of pressure heads over depth in the saturated porous media (head loss), in contrast to the prompt addition of b.p. into head in a well, cause the development of two pressure imbalances: i) across the well screen and ii) between the water table and porous medium. In brief, distinct and different head responses to changes in b.p between the inside and the outside of the well are believed to be responsible for the water level fluctuations in the well in response to barometric pressure.

The analysis of a physical process that involves groundwater flow always requires the recognition of a head gradient in porous media. The pressure imbalance mentioned above produces a hydraulic gradient at the contact between the well screen and aquifer in response to changes in b.p. In response to the head gradient, a well-flux is created through the well screen, where the water level variation (i.e. changes in well casing storage) directly depends on the flux over the screen and well geometry (surface area of the well screen). Accurate assessment of the well-flux is feasible through appropriate handling of boundary heads on the well, which satisfy both aspects of well heads responding to b.p. and concurrent groundwater flows in the surrounding porous medium. According to Darcy's law and conservation of mass, the flowrate into or from the well can be mathematically determined.

Consequently, the total head changes in a well due to b.p. is not the result of b.p. change alone, but is the sum of the b.p. change and the consequent change in water level, expressed in a consistent unit. Continuous changes in b.p., responding well water level fluctuations, and concurrent head perturbations within the surrounding formation are coupled, simultaneous, transient phenomenon.. Specifically, the situation investigated is the case of two-dimensional (radial and vertical) unsteady groundwater flow. The well itself is included as part of the

model, accounting for changes in well storage. This also benefits inclusion of exact well dimension and partial penetration of it in the proposed model.

Overall, the model in this study is based on, without loss of generality, the following hypotheses: a) atmospheric pressure acts directly on the water surface in the well. b) b.p. changes at the water surface in the well are transmitted instantly, and without loss, through the free water column in the well, c) head losses in the well filter pack are assumed to be negligible; d) head losses occurs during the propagation of b.p. changes through a saturated porous media and is described by the physics of saturated groundwater flow in a porous media; e) the combination of hydrologic features in b) and d) lead to pressure imbalances across the screen, which is responsible for the water level fluctuations due to changes in b.p. In addition to the above hypotheses, the following assumptions were made for the development of a feasible conceptual physical model: i) water is drainable in the system and vertical deformation occur only due to changes in b.p.; ii) the air movement by b.p. and head loss of b.p. in the unsaturated zone are ignored; and iii) the seasonal fluctuation of water table are ignored in describing b.p. effects on wells in a short period (less than two weeks).

### 3.2 Governing Equation

When the presence of the well is ignored, the response of groundwater flow to b.p. variations on the water table can be described by a one-dimensional diffusion-type equation. An analytical solution for the one-dimensional diffusion-type equation is readily available by assuming a sinusoidal change of b.p. However, inclusion of the well itself and the physical phenomena hypothesized, which is an essential part of the proposed model, requires use of the

two-dimensional (radial and vertical) model. A schematic view for the structure of the proposed model is presented in Figure 3.1.

The physical model for b.p. effects in this study consists of three parts: a) unsteady groundwater flow in the saturated porous medium; b) changes in water storage within the well; and c) the coupling between a) and b) at the well screen. In addition, the b.p. itself is a boundary condition assumed to act directly on the water surface in the well and at the groundwater table. In Figure 3.2, the following region represents each part mentioned above, respectively;

a) $r_w \le r \le r_{max}$ and $0 \le z \le z_{max}$

b) $0 \le r \le r_w$ and $z_1 \le z \le z_{max}$

c) $r = r_w$ and $z_1 \le z \le z_2$

where $r$ = radial coordinate

$z$ = vertical coordinate

$r_{max}$ = maximum radial coordinate of the modeled regime

$z_{max}$ = maximum vertical coordinate of the modeled regime

$z_1$ = vertical coordinate of the bottom of well screen

$z_2$ = vertical coordinate of the top of well screen

$r_w$ = well bore radius

The model used for groundwater flows within the saturated porous medium is the case of unsteady, two-dimensional (radial-vertical), and confined flow. The governing equation for the case is:

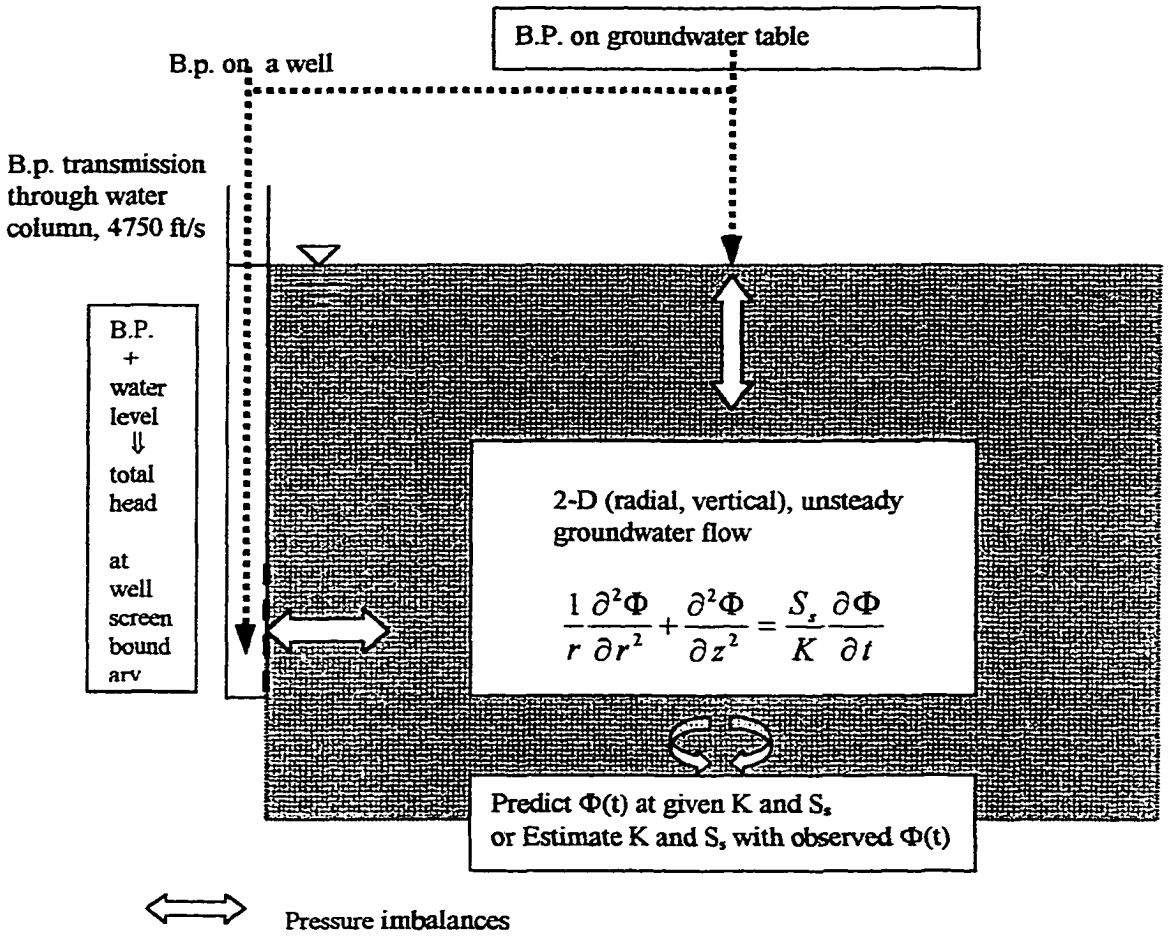


Figure 3.1. A Schematic view for the model structure.

$$\frac{1}{r}\frac{\partial}{\partial r}\left(K_r r\frac{\partial \Phi}{\partial r}\right)+\frac{\partial}{\partial z}\left(K_z\frac{\partial \Phi}{\partial z}\right)=S_s\frac{\partial \Phi}{\partial t} \tag{3-2}$$

with the boundary conditions

$$\Phi(r, z, t) = BP_0 + w_0 = \Phi_0 \quad \text{for all r and z at } t = 0 \tag{3-3}$$

$$\Phi(r, z, t) = BP(t) + w(t) \quad \text{for } r = r_w \text{ and } z_1 \le z \le z_2 \text{ at } t > 0 \tag{3-4}$$

$$\Phi(r, z, t) = BP(t) + w_0 \quad \text{for } z = z_{max} \text{ and } r \ge r_w \text{ at } t > 0 \tag{3-5}$$

$$\Phi(r, z, t) = \Phi_0 \quad \text{for } z = 0 \text{ and } r \ge r_w \text{ at } t > 0 \tag{3-6}$$

$$\Phi(r, z, t) = \Phi_0 \quad \text{for } r \to \infty \text{ and } 0 \le z \le z_{max} \text{ at } t > 0 \tag{3-7}$$

$$\lim_{r \to r_w}(2\pi r K_r \Phi\frac{\partial \Phi}{\partial r}) = 0 \quad \text{for } r = r_w \text{ and } z_2 \le z \le z_{max} \text{ at } t > 0 \tag{3-8}$$

$$\lim_{r \to r_w}(2\pi r K_r \Phi\frac{\partial \Phi}{\partial r}) = 0 \quad \text{for } r = r_w \text{ and } 0 \le z \le z_1 \text{ at } t > 0 \tag{3-9}$$

where $t$ = time

$\Phi$ = hydraulic head

$\Phi_0$ = initial hydraulic head

$K_r$ = horizontal hydraulic conductivity

$K_z$ = vertical hydraulic conductivity

$S_s$ = specific storage

$BP_0$ = initial barometric pressure

$w_0$ = initial water level

BP = barometric pressure

w = water level in the well

For the above equation, the following are assumed: a) the groundwater flow is unsteady; b) there is a radial and vertical flow; c) the porous medium is homogeneous, isotropic or anisotropic and confined (or drawdowns at the water table are negligible); d) the porous medium has an infinite aerial extent and is of uniform thickness; e) the initial potentiometric surface is uniform; and f) water is released from storage instantaneously with the decline of hydraulic head.

### 3.3 Boundary Conditions on the Well

The basic concept in the physical model for the well itself starts from the static equilibrium between inside and outside the well (Figure 3.2). The head of water in a well is treated as a column of water, with the head described by a hydrostatic pressure distribution in standing free water. The average head over the well screen, $\Phi_0$ at $t = 0$ is:

$$\Phi_0 = BP_0 + w_0 \qquad (3\text{-}10)$$

At the moment of change in atmospheric pressure at time = t,

$$BP(t) = BP_0 + \Delta BP \qquad (3\text{-}11)$$

where $\Delta BP$ = change in barometric pressure

For example, when there is an increase in b.p. ($\Delta BP > 0$), which exerts forces directly on the water within the well, an outward hydraulic gradient is established. Thus, the water level in the well will decrease and become lower than the static groundwater table around the well, and thus the water surface elevation in the well w(t) is less than $w_0$.

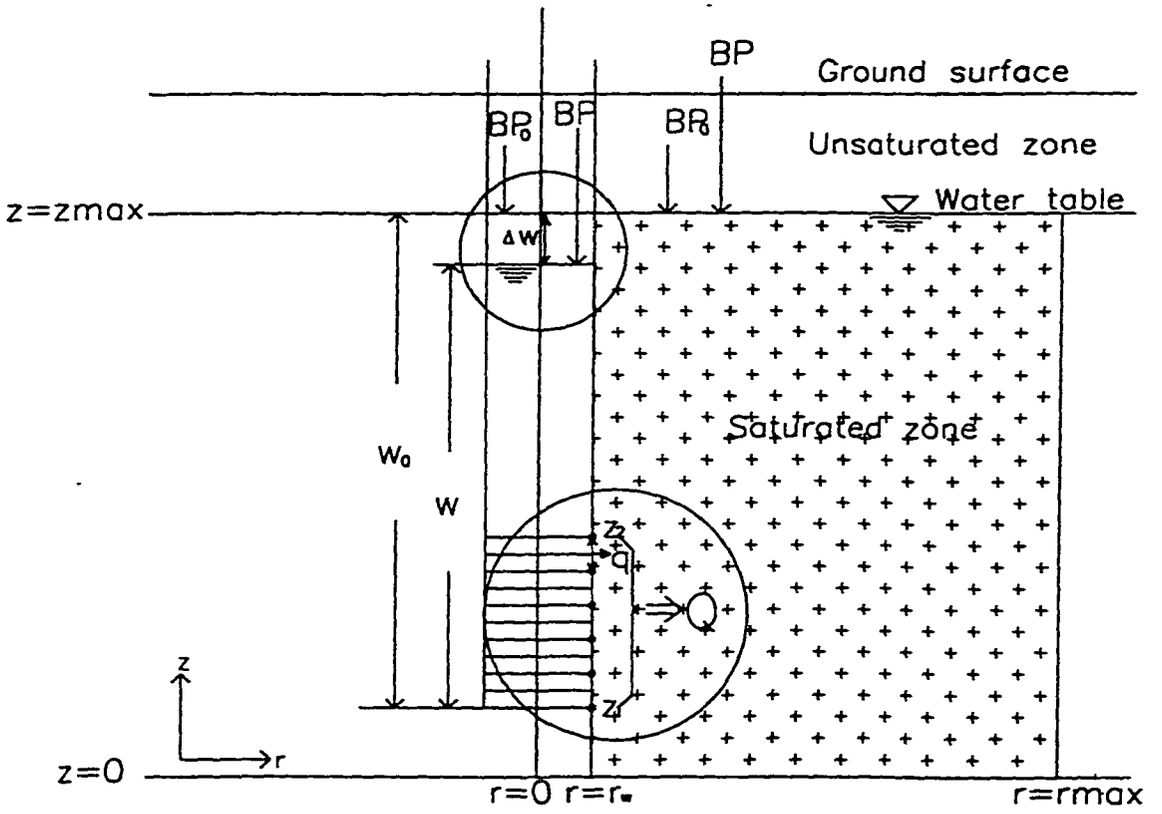


Figure 3.2. Groundwater well and saturated porous media of the physical conceptual model in this study.

When there is an decrease in b.p., the reverse phenomenon occurs. Consequently, the hydraulic head at the well screen ($r = r_w$ and $z_1 \leq z \leq z_2$) at time = t is expressed by,

$$\Phi(t) = BP(t) + w(t) \qquad (3\text{-}12)$$

Equation 3-12 says the head at the well screen boundary is the sum of the height of water above the well screen and the barometric pressure acting on the water surface in the well. The intent of the conceptual model is to predict the water level transients in the well, w(t) in the equation 3-12, responding to continuous changes in barometric pressure, BP(t).

Changes in water storage in the well casing is directly proportional to the total flux created over the screen.

$$dV = \pi r_c^2 \times dw = -Q\,dt \qquad (3\text{-}13)$$

where V = volume of water storage in the well casing

Q = well flux (flowrate) through the well screen

$r_c$ = well casing radius

Herein, rate of change of the water level, dw/dt, in the well after exertion of b.p. on the water in the well, can be expressed in the following equation.

$$\frac{dw}{dt} = -\frac{Q}{\pi r_c^2} \quad (L/T) \qquad (3\text{-}14)$$

The well and the aquifer are coupled through estimation of the flowrate (Q) through the well screen. Integration of the equation 3-14 will give the value of w(t), that serves as a partial component for boundary head for the groundwater flow in equation 3-5.

$$\Delta w = \int_{w(t)}^{w(t+\Delta t)} dw = -\int_{t}^{t+\Delta t} \frac{Q}{\pi r_c^2} dt \qquad (\Delta t << t) \qquad (3\text{-}15)$$

$$w(t+\Delta t) = w(t) + \Delta w \qquad (3\text{-}16)$$

Boundary heads for the well screen are directly affected by changes in water level, $\Delta w$, which depends on the groundwater flowrate, Q(t), around the well which affects the head.

To relate the induced groundwater flow around the well to the water level change, the flowrate over the whole length of well screen can be determined by the following relationship. Q is a function of w in equation 3-15. The flowrate Q, is coupled to the water level in the well, w.

$$Q = \int_{z_1}^{z_2} 2\pi r_w \, q\big|_{r=r_w} \, dz \qquad (3\text{-}17)$$

where q = Darcy's flux

The groundwater velocity q is given by Darcy's law.

$$q\big|_{r=r_w} = -K_r \frac{\partial \Phi}{\partial r}\Big|_{r=r_w} \qquad (3\text{-}18)$$

Thus,
$$Q = -2\pi r_w \int_{z_1}^{z_2} K_r \frac{\partial \Phi}{\partial r}\Big|_{r=r_w} dz \qquad (3\text{-}19)$$

Now, Q is a function of the first derivative of $\Phi$. The flowrate from the well and the head gradient at the well screen are associated in the above equation. Simultaneously, the flowrate directly determines the changes in water levels as mentioned. Consequently, the head gradient affects the flowrate and the flowrate anew affects the head gradient by determining the water level in the well. Finally, $\Phi(t)$, w(t) and Q(t) are implicitly related with one another. This means the determination of one of those can lead to solutions for the others through simultaneous equations 3-12, 3-15, and 3-19.

### 3.4 Boundary Condition on the Water Table

When there is a head change in the steady system as a whole, volume of water released from porous medium is dependent on specific storage of the formation through the following equation (derived form the definition formula of specific storage):

$$\overline{V} = S_s \times \forall \times \Delta\overline{\Phi} \qquad (3\text{-}20)$$

where $\overline{V}$ = volume of water released from porous medium

$S_s$ = specific storage

$\forall$ = volume of the formation

$\Delta\overline{\Phi}$ = change in hydraulic head in the system

In the test on the b.p. effects on the water table, $\Delta\overline{\Phi}$ caused by changes in ΔBP would not be great. Based on the low values in the range of $S_s$ (see Figure 2.2 in Chapter 2), volume of water released by head perturvation in the whole system due to b.p. dynamics is believed to be not significant for the water table level to be affected by changes in b.p.

The laterally average head over the water table ($r_w < r < r_{max}$ and $z = z_{max}$), $\Phi$ at $t = 0$ is:

$$\Phi_0 = w_0 + BP_0 \qquad (3\text{-}21)$$

At the moment of change in atmospheric pressure at time = t,

$$\Phi(t) = \Phi_0 + \Delta BP \qquad (3\text{-}22)$$

The fluctuation of the water table elevation due to changes in b.p. is assumed to be small and ignored. Thus, the change in b.p. in the next step is simply additive to the previous head value.

$$\Phi(t+\Delta t) = \Phi(t) + \Delta BP \qquad (3\text{-}23)$$

# CHAPTER 4. METHODS

## 4.1 Solution Method

The governing partial differential equation for groundwater flow (equation 3-2) was solved for $\Phi$ by the method of Galerkin finite-element approximation, using axis-symmetric triangular elements (Pinder and Frind, 1972; Huyakorn and Pinder, 1983). This solution method evaluates the spatial gradients over the flow domain in any direction. The finite element equations for groundwater flow are formulated by the Galerkin's weighted volume integration. Its application was carried out in deriving the numerical solution by an integral form of conservation of mass, which governs the groundwater flow within the saturated porous medium. The steps for deriving the solution in a matrix form of finite element equations are shown in the Appendix A. Naming the methodology applied, finite element method (FEM), the physical conceptual model in this study will be referred as the FEMBARO model after this point.

## 4.2 Grid Regime and Other Boundary Conditions

An example of a finite element grid used in this study is shown in Figure 4.1. The dimension of the postulated aquifer area is 800 cm (r) by 1300 cm (z). The total number of nodes and elements are 1200 and 2262, respectively. The size of a triangular element is 460 $cm^2$ (area = 0.5 x 27.59 cm x 33.33 cm). In the case of specific simulation, the size, spacing, and number of elements are somewhat changed appropriately for accuracy of results and reduction of simulation time. The finite element grid is rotated 360 degrees about the center axis within the well. Thus, the responding results can reveal three-dimensional radial and vertical groundwater flow around the well.

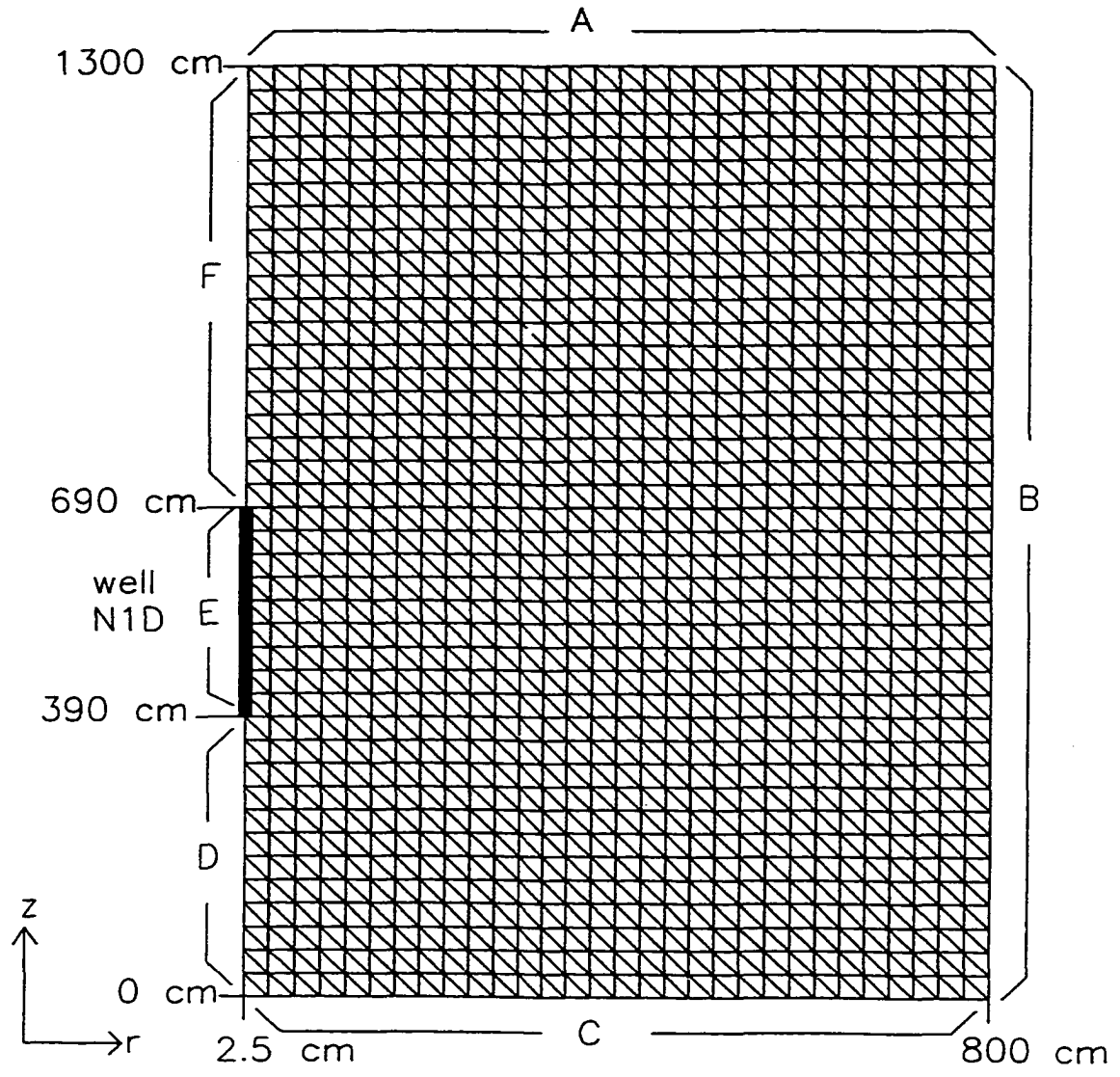


Figure 4.1. Finite element grid regime for radial and vertical groundwater flow.

To describe the groundwater flow due to b.p. changes, in detail, three types of boundary conditions are specified in this modeling. Two of those are the known-head boundaries that are directly subject to the change of atmospheric pressure. Among them, one is the well-screen and the other is the water table. Those two are represented by the band A and E in Figure 4.1. Descriptions on those boundary conditions were introduced in the previous chapter. The third condition is imposed on the rest of the margins of the grid regime, which are the bands B, C, D, and F in Figure 4.1. These boundary conditions do not affect the water level fluctuations in the well due to changes in b.p. Practically, it implies that these boundaries of the grid need to be at a distance far enough from the well so as to not influence the water level variation in the tested well over the period of simulation. In order to select the grid dimension large enough, simulations for water level changes in response to b.p. were conducted twice: once with a zero-flux boundary for the bands B and C and once using a fixed-head boundary for the bands B and C. The criterion for the selection of the grid dimension is that the estimates of barometric efficiency with two different boundary conditions differ by less than two percent. Zero flux boundary is applied for the band D and F.

### 4.3 Discretization of Continuous Changes in Barometric Pressure

A general and useful method is employed for representing the actual b.p. variations. The continuous change in b.p. is discretized into a series of step changes at a very small time interval (Figure 4.2). Barometric pressure at time = $t_i$ is:

$$BP(t_i) = BP(t_{i-1}) + \Delta BP_i \qquad (4\text{-}1)$$

$$\text{where } t_i = t_{i-1} + \Delta t \qquad (4\text{-}2)$$

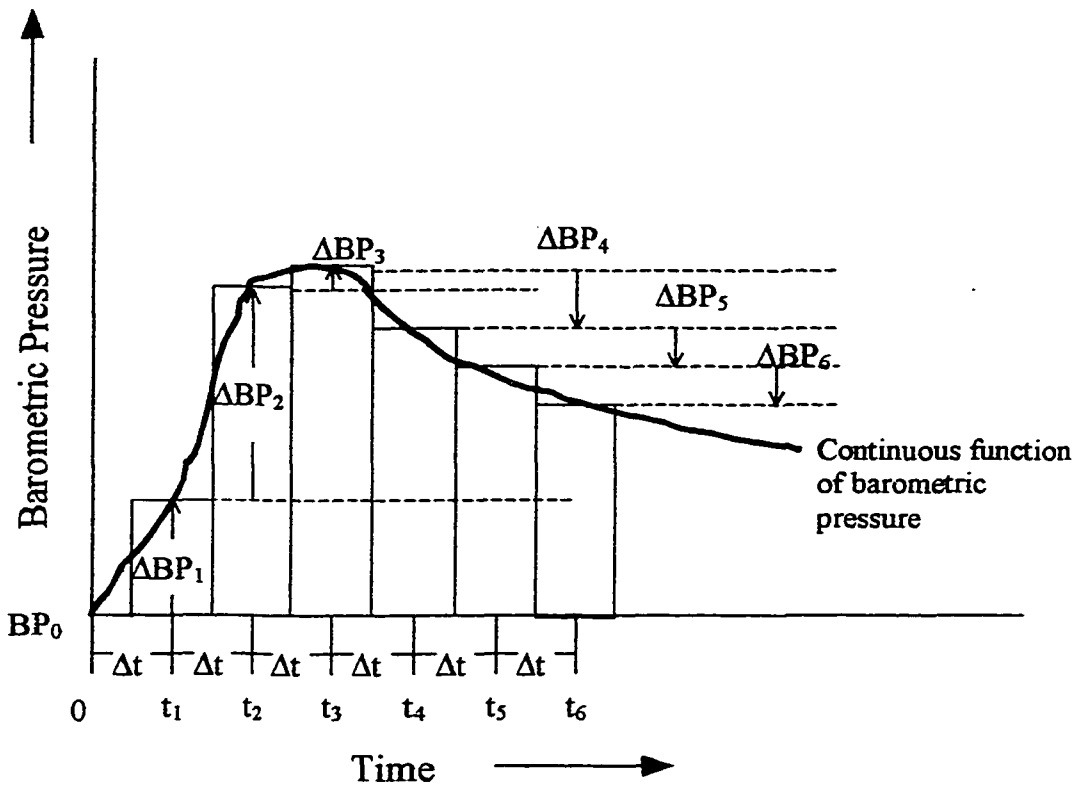


Figure 4.2. Changes in barometric pressure as a series of step changes at discrete time domain.

These step changes in b.p. are used to compute water level fluctuations in the well at each time interval. Thus, the model output of water level responding b.p. is also a discretized one.

$$w(t_i) = w(t_{i-1}) + \Delta w_i \qquad (4\text{-}3)$$

**4.4 Iteration Technique for Estimation of Well-Flux and Boundary Head**

An iterative method is used to find the Q(t) and w(t) which simultaneously satisfy the boundary condition at the well screen. When there is a change in b.p., the following boundary head, vertically averaged over the well screen, is first guessed. Therefore, flowrate over the well screen can be estimated using that boundary head through the numerical solutions for the groundwater flow in the porous medium. At the given flowrate and well casing geometry, the induced water level change in the well is easily calculated (see equation 3-13 in the Chapter 3.3). The sum of the change in b.p. and the subsequent change in water level in the well yields the estimate of boundary head. Then, this estimate is compared with the guessed boundary head. Iteration with another guess of boundary head will continue until the guessed boundary head is almost the same as the estimated head for the well screen (difference is less than 0.0001 cm_water) At last, through the repetition of mathematical iteration at every time step of the b.p. changes, the total well-flux (Q) over the screen and the water level (w) within the well are estimated, satisfying the known-head ($\Phi$) well boundary condition for the groundwater flow in the surrounding porous medium.

**4.5 Development of Program**

The flowchart for the developed computer program on the FEMBARO model is shown in Figure 4.3. The boundary conditions for the screen of well and the top of the grid scheme,

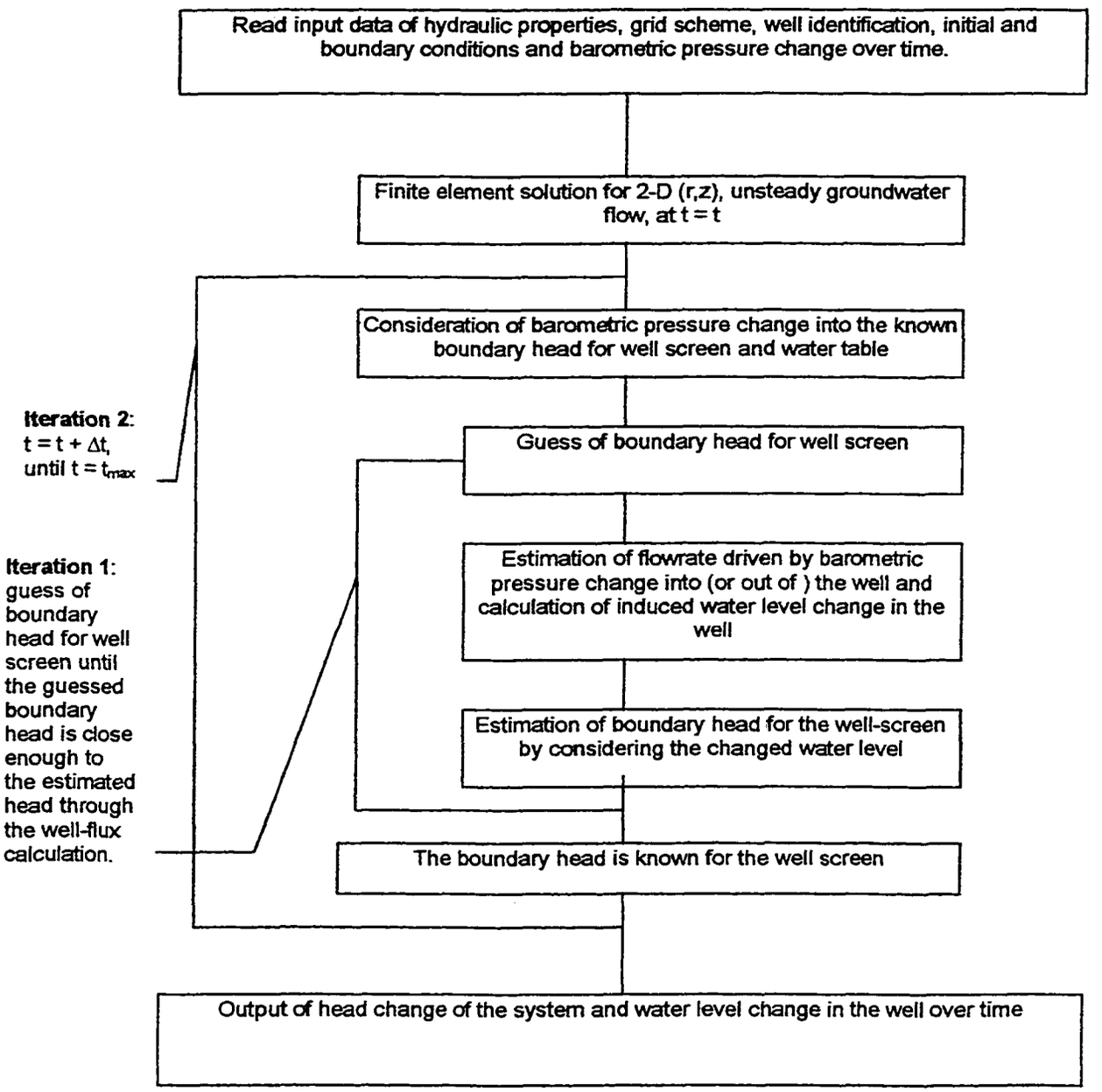


Figure 4.3. Flowchart for the simulation of the effect of barometric pressure on the groundwater level in wells.

on which b.p. changes directly exert, were most carefully considered. The Iteration 1 is for the estimation of the boundary head at the well screen, simultaneously for the well-flux and water level in the well responding to b.p. The Iteration 2 is for the change in the time steps.

### 4.6 Inverse Modeling and Estimation of Hydraulic Parameters

In simulations for actual field tests, the FEMBARO program was run repeatedly to get the best curve fitting between observed and simulated water levels in a well, using trial and error tool and visual comparison between observed and simulated hydrographs of the well. The estimates of hydraulic conductivity (K) and specific storage ($S_s$) from the hydraulic tests (slug or pumping tests) were first tried and the values of K and $S_s$ were varied gradually until the minimized deviation between observed and simulated curves was reached. The optimal values of K and $S_s$ for this criterion were assessed as hydraulic properties of the tested formation. In other words, the unknown hydraulic parameters of the tested formation are estimated, using the FEMBARO model as a simulation tool and simultaneous records of water level and b.p. as measured input data.

### 4.7 Model Evaluation Tools

Several simple statistics were chosen to evaluate model performance. The statistics include the R-square ($R^2$), and correlation coefficient (r). These summary statistics, along with graphical illustrations, are the primary means of comparison between modeled output and field observations. Formulas for the statistics and usage of those in this study are listed in the Table 4.1. The $R^2$ value, varying from 0 to 1, can be interpreted as the proportion of the variance in dependent variable attributable to the variance in independent variable. The

$R^2$ of 1 indicates that the model can completely explain the variations of the measured values. Correlation coefficient (r) was used to examine interrelation between the observed b.p. and the responding water level data.

Table 4.1. Statistics applied in model evaluation.

| Statistics | Definition Formula* | Use |
|---|---|---|
| R-square<br>(square of the Pearson product moment correlation coefficient) | $R^2 = \left[ \frac{n\sum_{i=1}^{n}(O_i S_i) - (\sum_{i=1}^{n} O_i \times \sum_{i=1}^{n} S_i)}{\sqrt{\left[n\sum_{i=1}^{n} O_i^2 - \left(\sum_{i=1}^{n} O_i\right)^2\right]\left[n\sum_{i=1}^{n} S_i^2 - \left(\sum_{i=1}^{n} S_i\right)^2\right]}} \right]^2$ | • Comparison between observed and simulated water levels in wells |
| Correlation coefficient | $r = \frac{\frac{1}{n}\sum_{i=1}^{n}(x_i - \bar{x})(y_i - \bar{y})}{\sigma_x \sigma_y}$ | • Comparison between observed b.p.(x) and total head or water levels (y). |

*$S$ and $O$ denote simulated and observed data, respectively and $\sigma$ denotes variance

# CHAPTER 5. REVISION OF MODEL FOR SLUG TESTS

## 5.1 Model for Slug Tests

Among the various techniques for the quantification of hydraulic conductivity of subsurface porous media, slug testing is probably the most popular field method. Slug test generally require less time and equipment, and are usually less costly than pumping tests. A variety of field procedures and associated methods of analysis have been developed for slug tests (Hvsorlev, 1951; Cooper et al., 1967; Bower and Rice, 1976; Nguyen and Pinder, 1984; Hyder and Butler, 1995).

In a typical slug test a certain volume of water is quickly added or removed (often called bail test) from the well. The time rate of recovery of the water level in the well to equilibrium is measured. Instead of adding water, an alternative field technique is to insert a certain volume of solid slug into the well.

Water levels in a well, which represent the hydrostatic pressure averaged over the well screen, respond to the slug impact according to the hydraulic gradient suddenly established between water in the well and the adjacent porous medium. Stabilization of the displaced water level is attained through groundwater flow across the well screen after a sufficient elapse of time. In summary, field data of slug tests include:

- the volume of water added or withdrawn
- water level in the well over time
- the well geometry (well bore and casing radius, screened length, depth of well)
- hydrogeologic setting (saturated thickness, confined or unconfined condition, penetration ratio).

As a useful tool for simulation and optimization of slug tests, this work also develops and tests a new physically based model for slug tests. The model structure is based on the physical phenomena occurring in a well and also the surrounding porous medium. Responses of a well to slug impacts can be estimated through the appropriate coupling of physical phenomena between these two parts: the well itself and the surrounding porous medium. In the model, the physical phenomena are simulated in the forms of a) water level changes in the well, b) discharge across the well screen, and c) changes in head value in the tested formation over time and space. The new model for slug tests in this study will be referred to as the FEMSLUG model.

Basically, development of the model was completed simply by modifying the boundary and initial conditions for the main model of this study, the FEMBARO model in Chapter 3. Modifications applied are

- Insertion of water-slug (at t = 0) is the only pressure impact applied on the well, instead of transient b.p. variations;
- At the well screen boundary the length of water-slug is directly added to the total head, and thus the total head is equal to the water level in the well;
- No pressure impact on the water table, i.e., the water table is treated as a constant head boundary.

The model used for groundwater flows within the saturated porous medium is unsteady, two-dimensional (radial-vertical), confined flow. The governing equation is:

$$\frac{1}{r}\frac{\partial}{\partial r}\left(K_r r\frac{\partial \Phi}{\partial r}\right)+\frac{\partial}{\partial z}\left(K_z\frac{\partial \Phi}{\partial z}\right)=S_s\frac{\partial \Phi}{\partial t} \qquad (5\text{-}1)$$

with the boundary conditions:

$$\Phi(r, z, t) = w_0 \qquad \text{for all r and z at } t = 0 \tag{5-2}$$

$$\Phi(r, z, t) = w_0 + H_0 \qquad \text{for } r = r_w \text{ at } t = 0 \tag{5-3}$$

$$\Phi(r, z, t) = w(t) \qquad \text{for } r = r_w \text{ and } z_1 \le z \le z_2 \text{ at } t > 0 \tag{5-4}$$

where $H_0$ = initial (maximum) water level displacement

The average head over the well screen, $\Phi$ at $t < 0$ is

$$\Phi = w_0 \tag{5-5}$$

At the moment of the change of head due to slug impact at for $r = r_w$ at $t = 0$

$$\Phi_0 = w_0 + H_0 \tag{5-6}$$

5-6 states that the head in the porous media at contact with the well is equal to the augmented water level in the well at the instant of slug insertion. When there is an insertion of slug ($H_0 > 0$), the water level in the well is higher than the static groundwater table around the well, and thus water surface elevation in the well, w(t), starts to fall (i.e., falling head slug tests). When there is a withdrawal of slug ($H_0 < 0$), the reverse situation occurs (i.e., rising head slug tests).

Consequently the hydraulic head at time = t is expressed as,

$$\Phi(t) = w(t) \quad \text{at} \quad r = r_w \text{ and } z_1 \le z \le z_2 \tag{5-7}$$

$$\text{where} \quad w(t) = w_0 + H(t) \tag{5-8}$$

$$\text{Thus,} \qquad \Phi(t) = w_0 + H(t) \tag{5-9}$$

The rate of change of the water level in the well, dw/dt, can be expressed in the following equation:

$$\frac{dw}{dt} = -\frac{Q}{\pi r_c^2} \tag{5-10}$$

The well and the aquifer are coupled through the estimation of hydraulic heads and flowrates,$\Phi$ and Q, over the well screen. Integration of equation 5-10 will give the well recovery data over time, w(t).

$$\Delta w = \int_{w(t)}^{w(t+\Delta t)} dw = -\int_{t}^{t+\Delta t} \frac{Q}{\pi r_c^2} dt \qquad (\Delta t << t) \qquad (5\text{-}11)$$

$$w(t+\Delta t) = w(t) + \Delta w \qquad (5\text{-}12)$$

Boundary heads for the well screen are directly affected by w(t) which depends on groundwater flowrate around the well. To relate the induced groundwater flow around the well to water level changes, the flowrate over the whole length of well screen can be determined by the following relationships:

$$Q = \int_{z_1}^{z_2} 2\pi r_w q\big|_{r=r_w} dz \qquad (5\text{-}13)$$

The groundwater flux, q, is given by Darcy's law:

$$q\big|_{r=r_w} = -K_r \frac{\partial \Phi}{\partial r}\Big|_{r=r_w} \qquad (5\text{-}14)$$

Thus,
$$Q = -2\pi r_w \int_{z_1}^{z_2} -K_r \frac{\partial \Phi}{\partial r}\Big|_{r=r_w} dz \qquad (5\text{-}15)$$

Estimation of Q and w(t) is completed through the iteration technique mentioned earlier in Chapter 4.4.

## 5.2 Superposition in Slug Tests

A slug test is performed by instantaneous insertion of a slug into a well at t = 0. The concept of the standard slug tests can be extended into a more dynamic test where additional instantaneous slug impacts are done in the well at different time intervals. A dynamic slug

test can be simulated by the FEMSLUG model. In the model, the insertion of another water-slug is simulated by adding the length of water-slug into the total head value at the well boundary, where the well is under recovery responding to the former slug impact and the head transients are being calculated at the previous time interval. This means that the principle of superposition can predict the well recovery of the dynamic slug tests. The principle of superposition says that the total water level changes at a given time is the sum of the changes caused by pressure impacts at preceding steps. Table 5.1 shows an example of the dynamic slug test. The volume of water added (or withdrawn) is converted into the length of water-slug ($l_i$) by dividing it by the cross-sectional area of the well, for consistency of units with head values. The detailed mathematics on superposition of well recovery in the slug test follow.

i) $t_1 \leq t < t_2$

$$\frac{H}{H_0} = \frac{H_1(t)}{H_0} \tag{5-16}$$

$$\text{where } H_0 = H_1(0) = l_1 \tag{5-17}$$

Table 5.1. A theoretical example of dynamic slug tests and superposition in well recovery.

| Time | Applied water-slug length | Time period | Water level displacement (or heads) transient |
|---|---|---|---|
| $t_1 = 0$ | $l_1$ | $t_1 \leq t < t_2$ | $H_1(t)$ ← Standard slug test |
| $t_2$ | $l_1+l_2$ | $t_2 \leq t < t_3$ | $H_1(t) + H_2(t)$ |
| $t_3$ | $l_1+l_2+l_3$ | $t \geq t_3$ | $H_1(t) + H_2(t) + H_3(t)$ |

ii) $t_2 \le t < t_3$

$$\frac{H}{H_0} = \frac{H_1(t) + H_2(t)}{H_0} \tag{5-18}$$

$$\text{where} \quad H_2(t) = H_1(t - t_2) \times \frac{l_2}{l_1} \tag{5-19}$$

$$\Rightarrow \frac{H}{H_0} = \frac{H_1(t)}{H_0} + \frac{H_1(t - t_1)}{H_0} \times \frac{l_2}{l_1} \tag{5-20}$$

ii) $t \ge t_3$

$$\frac{H}{H_0} = \frac{H_1(t) + H_2(t) + H_3(t)}{H_0} \tag{5-21}$$

$$\text{where} \quad H_2(t) = H_1(t - t_2) \times \frac{l_2}{l_1} \tag{5-22}$$

$$H_3(t) = H_1(t - t_3) \times \frac{l_3}{l_1} \tag{5-23}$$

$$\Rightarrow \frac{H}{H_0} = \frac{H_1(t)}{H_0} + \frac{H_1(t - t_1)}{H_0} \times \frac{l_2}{l_1} + \frac{H_1(t - t_2)}{H_0} \times \frac{l_3}{l_1} \tag{5-24}$$

### 5.3 Oscillating Slug/Bail Tests

An extreme case of dynamic slug tests can be generated with the instrumentation illustrated in Figure 5.1. When the oscillating water supply is applied in the well instead of an instantaneous slug, water level transient in the well would not be like the typical well recovery curves in slug tests. In a numerical sense, the continuously changing water supply in the well can be depicted as a series of step changes with a small time interval (Figure 5.2).

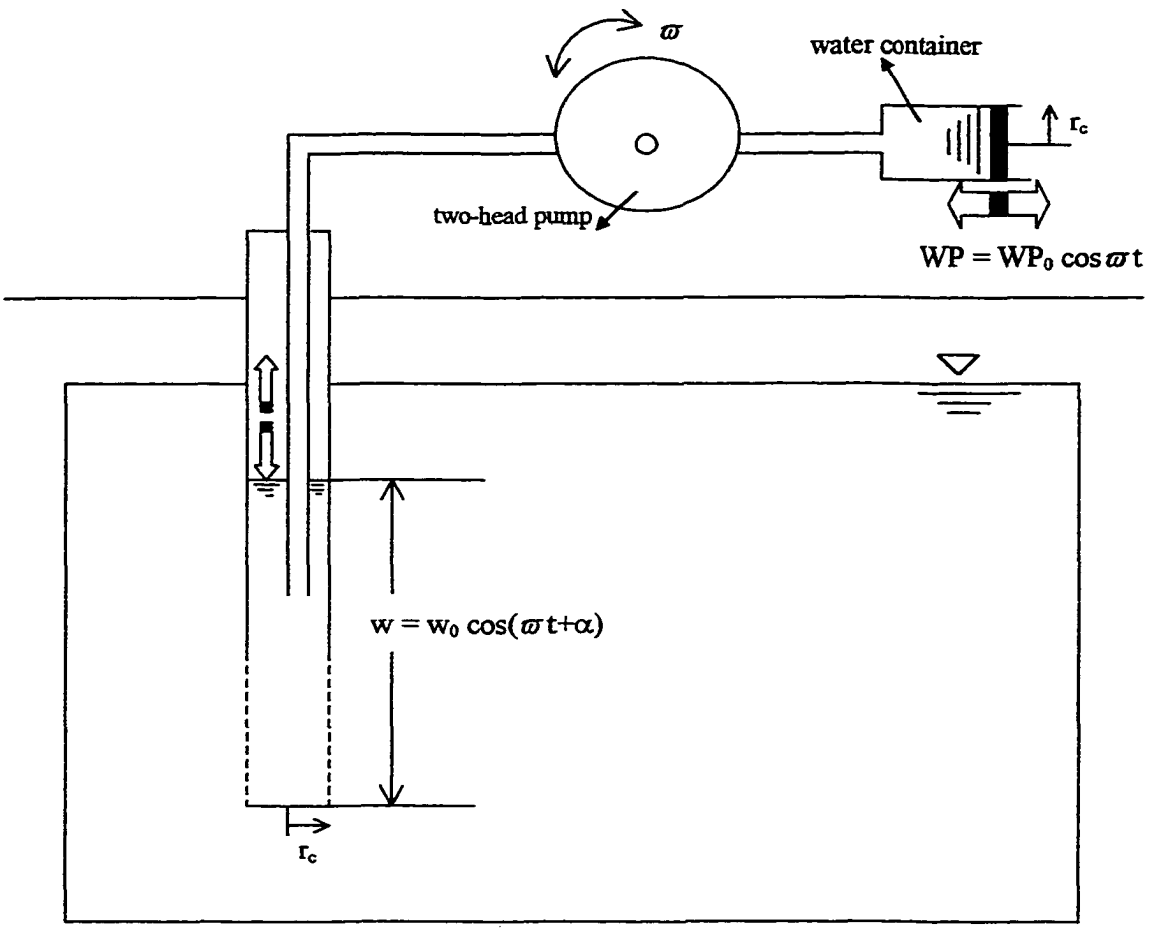


Figure 5.1. Conceptualized view for oscillating slug/bail tests

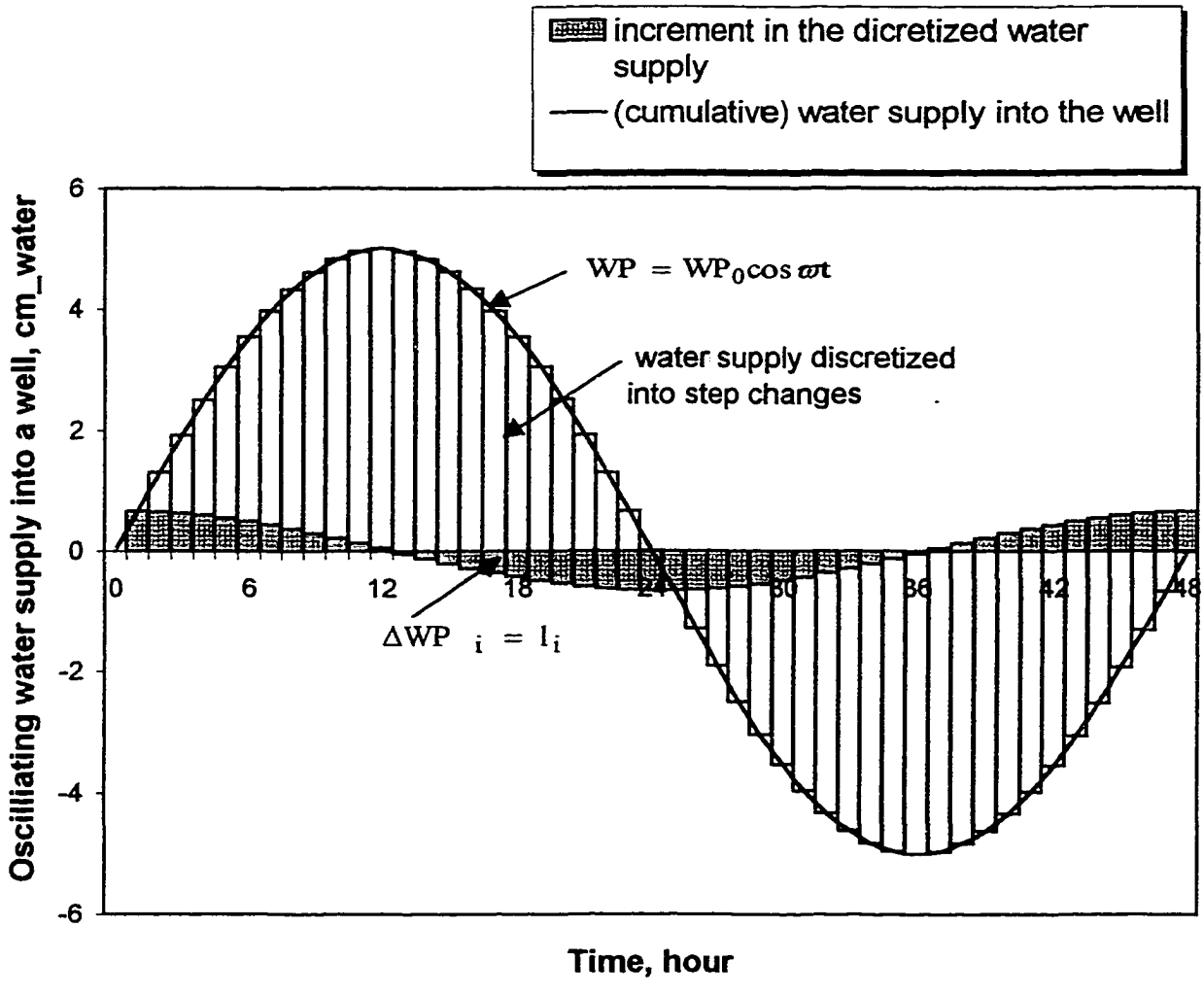


Figure 5.2. Oscilliating water supply into a well viewed as a series of sulg/bail tests.

This discrete step function represents the increment of water supplied in the well at each time interval. In other words, in the simulation of the model, the step function implicitly resembles a series of slug/bail tests; in Figure 5.2, each bar in shade represents the length of the water-slug or -bail applied into the well in order.

### 5.4 Air Pressure Variations in Wells

An alternative way for the above oscillating slug/bail tests to be conceptualized and simulated is by applying an air pressure variation in the well under sealed conditions instead of the water supply in Figure 5.1. However, unlike the water-slug tests, the method of air pressure variations on wells yields a distinct relation, in which the total head of the well is the sum of the hydraulic pressure and the air pressure. In addition, the unit of air pressure needs to be consistent with that of the pressure head in the well as the length of water. The FEMBARO model fits well to the test of air pressure variation in the well satisfying two conditions: i) continuous changes in air pressure in the well, ii) total head in the well is equal to the sum of air pressure applied and the water level in the well. In other words, the unpredictable changes in b.p. in nature can function like pressure variations applied into the well in air pressure variation tests under the condition of no b.p. exertion on the water table. For some practical instances, all changes in b.p. run out through the unsaturated zone above the water table or the confining unit in low hydraulic diffusivity. An impermeable barrier such as a clay cap existing on the top of the surface also prevent b.p. from propagating into the water table. Under such conditions, the simultaneous record of b.p and the responding water levels in the well are conceptually equivalent to the well recovery in a superimposed slug test.

For the estimation of water level transient due to dynamic and oscillating slug tests and air pressure variations in wells, step changes are incorporated using the principle of superposition in the models. Furthermore, these dynamic pressure impacts by water or air pressure on water in wells have a potential for hydraulic parameter estimation through the inverse modeling of the responding water level transient, using the FEMSLUG and FEMBARO programs.

### 5.5 Effects of Barometric Pressure on Well Recovery during Slug Tests

In slug test analysis, the effects of barometric pressure on well recovery has mostly been neglected on practical purposes. However, when the well recovery takes hours to days, changes in b.p. have the potential to affect well recovery during slug tests. As an example, Table 5.2 shows the maximum basic time-lag ($T_0$) in the Hvorslev method (1951) that correspond to different orders of K values at a given well geometry.

Table 5.2. Hydraulic conductivity and basic time-lag ($T_0$) in the Hvsorlev formulation for slug test analysis (at a given well geometry; $r_c$= 1.59 cm, $r_w$= 3.81 cm and L = 91 cm).

| K (cm/sec) | $T_0$ | K (cm/sec) | $T_0$ |
|---|---|---|---|
| 1E-01 | 0 second | 1E-07 | 5.07 days |
| 1E-02 | 4 seconds | 1E-08 | 1.69 months |
| 1E-03 | 44 seconds | 1E-09 | 1.39 years |
| 1E-04 | 7.3 minutes | 1E-10 | 13.89 years |
| 1E-05 | 1.22 hours | 1E-11 | 138.87 years |
| 1E-06 | 12.17 hours | | |

For a given well geometry, the estimate of K is dependent only on the rate of water recovery in the well. A few minutes difference between $T_0$ values can cause an order of magnitude change in K values in permeable units, whereas more than a year difference does not affect the order of magnitude of K for units with low permeabilities. The range of K that can be measured easily with a slug test ranges from about $10^{-2}$ to $10^{-9}$ cm/s. In the low permeability units ($K \leq 10^{-7}$ cm/s), the well recovery is vulnerable to variations in b.p. because of its slow response as seen in the above example. However, in the very low permeability units ($K \leq 10^{-9}$ cm/s), with months or years of recovery time, other factors such as evapotranspiration and seasonal infiltration may easily mitigate or disguise the b.p. influence on well recovery. Therefore, investigation of effects of b.p. on well recovery in slug tests in low permeability units, where the well recovery time is a period of hours to days, would be meaningful.

Simulation of slug test well response under the influence of b.p. is feasible by combining the FEMBARO and FEMSLUG models. The relation in which the total head in the well is the sum of b.p. and water level in the well is still valid as a boundary condition (see equation 3-5):

$$\Phi(t) = w(t) + BP(t) \qquad (5\text{-}25)$$

Specifically, the initial impact of the water-slug is added into the water level term (w) in the eqation 5-25, whereas the changes in b.p. are added into the air pressure term (BP) at different time intervals during the recovery. Thus, the total head in the well at time = t is

$$\Phi(t) = w_0 + H(t) + BP(t) \qquad (5\text{-}26)$$

In the above equation, H(t) is commonly utilized for construction of the well recovery curve in slug tests. Without loss of generality, the principle of superposition governs the well responses to a slug test associated with the b.p. variations.

# CHAPTER 6. MODEL APPLICATION

In this chapter, we will describe the simulations done in this study using the FEMBARO model: theoretical examples and actual field tests. The rationale for theoretical studies are first discussed, and then field sites and data collection for actual tests are described.

## 6.1 Theoretical Sensitivity Studies

In order to confirm the validity of hypotheses made in this study, two hypothetical examples, with postulated sinusoidal changes in b.p., were used to investigate the response of the well to changes in b.p. One example involved modeling the response of groundwater flow to changes in b.p. with a well and the other without a well. Comparison between the two cases will illustrate the role of the well in the response of water levels to changes in b.p. The factors controlling water level fluctuation due to changes in b.p. were examined through sensitivity studies on depth of the well screen, screened length of the well, and hydraulic properties of the screened geologic unit. The natural recharge into the water table was incorporated with b.p. effects to investigate how groundwater levels are affected for tests of a long period. In addition, the b.p. effect on slug tests was demonstrated by comparing simulated well recovery curves with assumption of constant b.p. and the other with consideration of b.p. variations during the tests. The sensitivity analyses on well geometry and slug size, as well as the hydraulic properties to the disturbed well recovery due to changes in b.p., were included in theoretical simulations. The input parameters of b.p.,

hydraulic properties, and the well assumed for most of the theoretical simulations in this study are listed in Table 6.1.

Postulated sensitivity of barometric efficiency to the depth of well screen and hydraulic properties at a given well geometry are conceptualized in Figure 6.1 (a). First, as the depth of the well increases, head loss of b.p. from the water table increases during its downward propagation. Thus, a higher hydraulic gradient between inside and outside is established at the well intake at a greater depth, leading to a higher well-flux across the screen section. Consequent a greater water level fluctuation at a deeper well leads to the relation in which barometric efficiency would increase as the depth of the well increases. At a given well screen depth below the water table, hydraulic property of the porous media could affect the magnitude of well-flux responding to changes in b.p., following the Darcy's law for groundwater flow. According to the Darcy's law, water flux at the well screen boundary is directly proportional to hydraulic conductivity of the formation. At a given barometric pressure change in the well, diffusion-type pressure propagation of it within the porous media is the determinant factor on hydraulic gradient over the screen between inside and outside of well.

Table 6.1. Postulated parameters for theoretical simulations in this study.

| | | | | |
|---|---|---|---|---|
| Barometric pressure (sinusoidal curve) | Amplitude (cm_water) | | Period (hour) | |
| | 5 or 10 | | 24 or 48 | |
| Hydraulic properties (homogeneous and isotropic condition) | K (cm/s) | | $S_s$ (1/cm) | |
| | 1E-7 | | 1E-5 | |
| Well geometry | $r_c$ (cm) | $r_w$ (cm) | L (cm) | D (m) |
| | 2.54 | 5 | 90 | 3 ~ 10 |

**(a)**

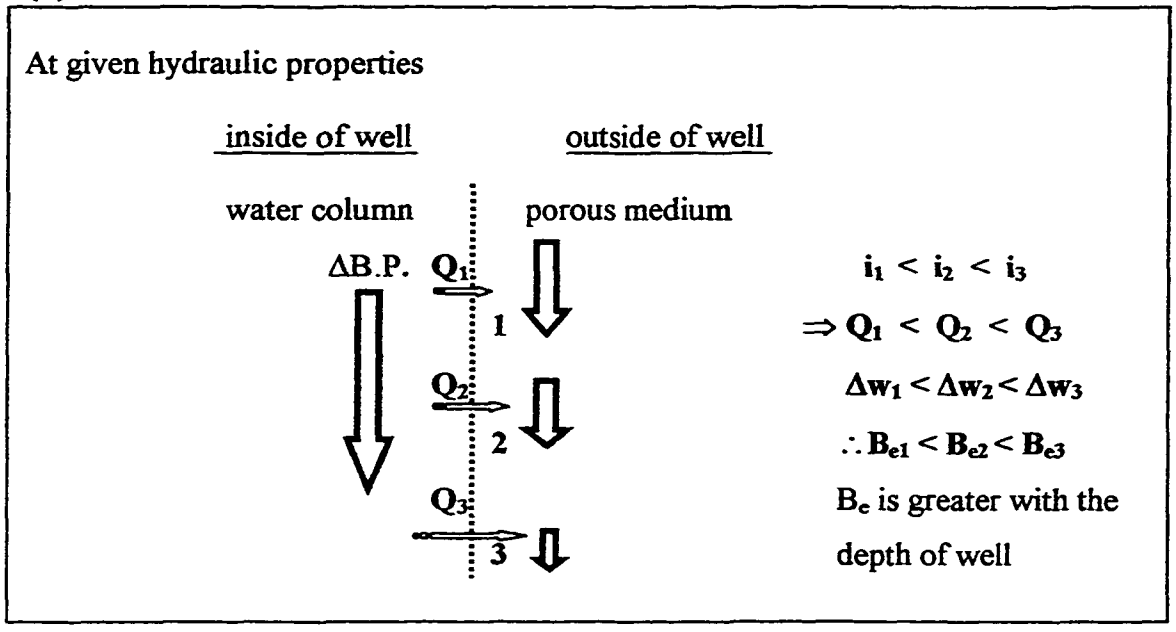


**(b)**

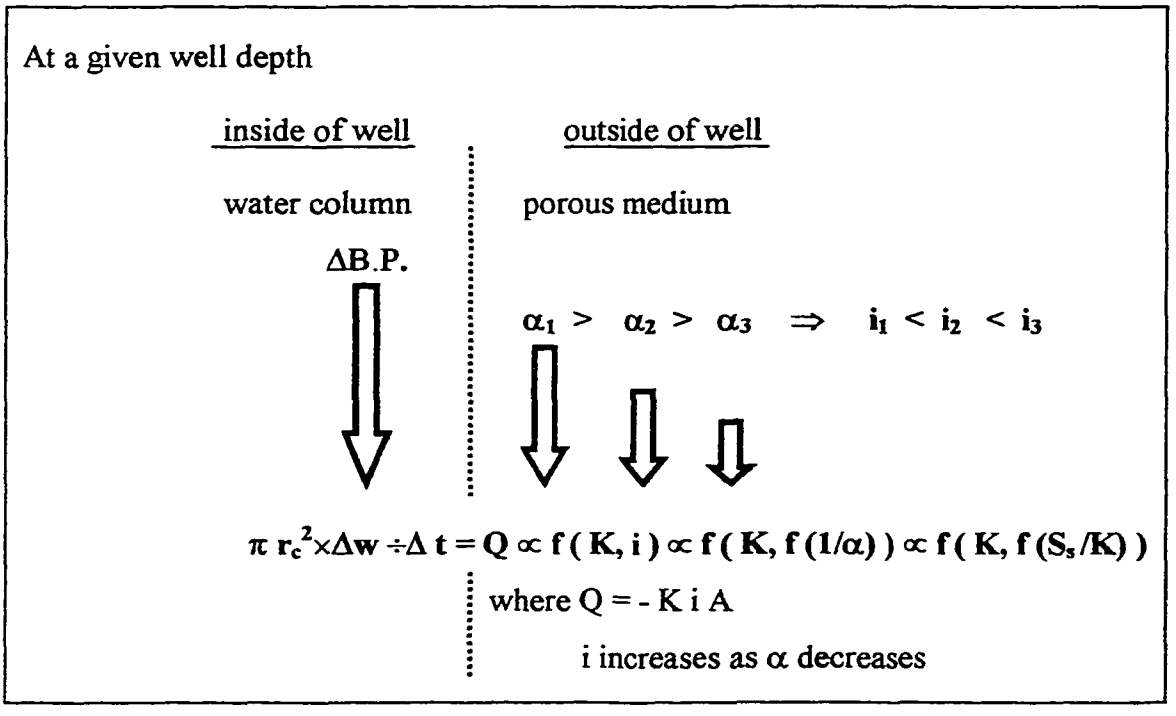


Figure 6.1. Sensitivity of barometric efficiency of a well to the depth of the well and hydraulic properties of the screened formation.

Hydraulic gradient between inside and outside of the well increases as hydraulic diffusivity of the formation decreases, where hydraulic conductivity concerns the well-flux in the inverse way to that as a coefficient in the Darcy's law. Therefore, accurate assessments of hydraulic conductivity and specific storage are necessary to explain effects of hydraulic properties on the well responses to changes in b.p.

## 6.2 Field Site and Test Descriptions

The main research site for this study is the Ames Till Hydrology Site (ATHS) at the Iowa State University Agronomy/Agricultural and Biosystem Engineering Research Farm, located 10 km west of Ames in central Iowa (Figure 6.2). Figure 6.3 is the detailed site map of the ATHS with the specific field locations for the data collected in this study.

### *6.2.1 Hydrogeology*

The ATHS site has been intensively investigated for understanding of groundwater hydrology of low permeable glacial deposits through hydraulic tests, numerical modeling of the tests, and geochemical analysis (Jones et al., 1992; Jones, 1993; Edwards and Jones, 1993; Simpkins and Parkin, 1993). The main top lithology of the site is the late Wisconsinan till from the Des Moines Lobe (Figure 6.2). It is the most recent glaciation in Iowa that had advanced into north central Iowa during the late Wisconsinan period 12,000 to 14,000 years ago (Prior, 1991). Within the late Wisconsinan till, two distinct layers, oxidized and unoxidized till, are differentiated by the color and degree of weathering. Oxidation of the Wisconsinan till is present to an average depth of 4 m and unoxidized Wisconsinan till extends from 4 m to approximately 22 m below ground surface (Lemar, 1991). The water

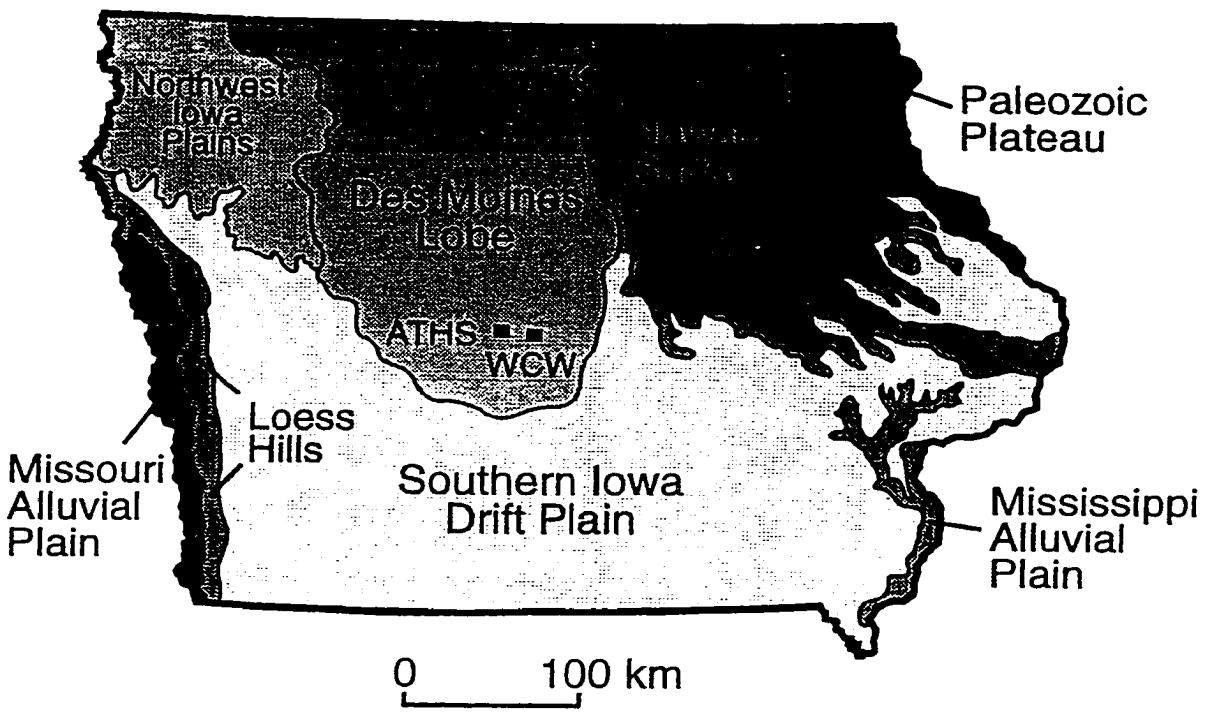


Figure 6.2. Location of the Ames Till Hydrology Site (ATHS) and landform regions in Iowa.

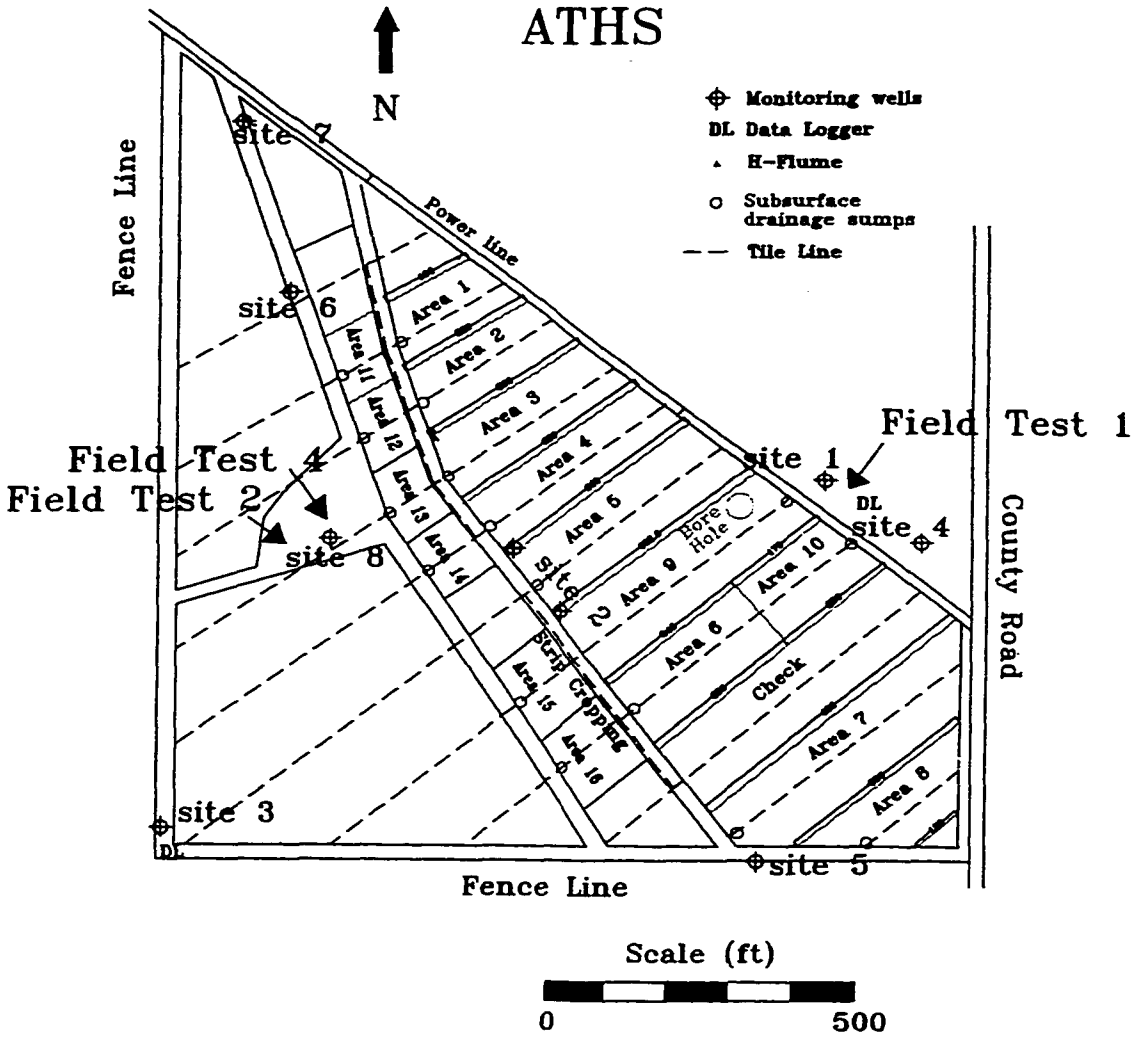


Figure 6.3. Site map of the Ames Till Hydrology Site and locations of the field tests.

table seasonally fluctuates 1 m to 3 m below the ground surface within the oxidized zone in response to precipitation and evapotranspiration. The geologic stratigraphy is discussed in more detail by Simpkins (1993).

### *6.2.2 Correlation between Barometric Pressure and Hydraulic Head Measurements*

Evidence for interaction between b.p. and well water levels was assembled from atmospheric and hydrologic data collected at the ATHS. The collected data are changes in b.p. and hydraulic head, and precipitation over a year long period from March, 1990 to February, 1991 (Figure 6.4 (a)). Precipitation was measured at the on-site weather station. Hydraulic heads were measured by pressure transducers buried at four different depths at Site 1 in the ATHS. B.p. data were obtained from National Climatic Data Center in North Carolina, which were measured at the weather station located in Des Moines, about 30 miles away from the site. The data are surely representative for b.p. changes of the ATHS except for thunderstorm periods (Hillaker, 1999). The wavings in b.p. are mainly due to the air movement in a daily period resulting from the unequivalent heating of the earth and the atmosphere by solar radiation, which is a factor driving weather changes. Summary statistics on the observed b.p. are listed in Table 6.2.

Table 6.2. Statistics for measurements of barometric pressure (cm_water) at ATHS in 1990.

| Data Period | Mean | Range | Minimum | Maximum | Median | Mode |
|---|---|---|---|---|---|---|
| One Year | 1001.65 | 37.99 | 984.50 | 1022.50 | 1001.43 | 1000.05 |
| Data Period | St. Dev. | Variation | | | | |
| One Year | 6.58 | 43.28 | | | | |

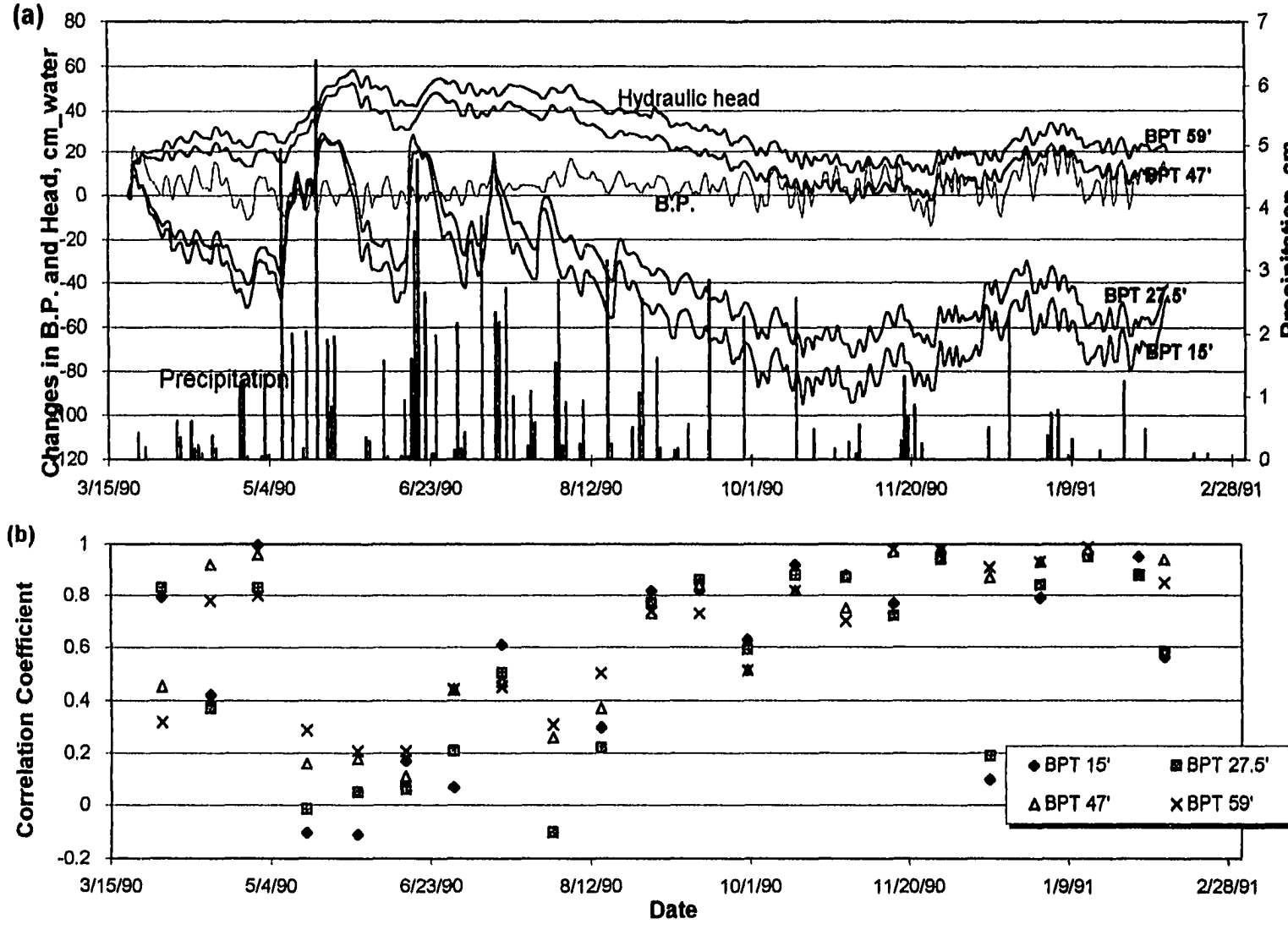


Figure 6.4. (a) Measurements of barometric pressure (B.P.), hydraulic heads, and precipitation at the ATHS and (b) Correlation between barometric pressure and hydraulic head.

If the b.p. fluctuation is presumably considered as oscillating water supply into the well, then the range of b.p., 38 cm_water, represents the range of water supply occurring in a well in terms of water-slug length ($l_i$).

Correlation coefficients between measurements of b.p. and hydraulic heads at two week intervals for annual data are plotted in Figure 6.4 (b). In addition, the lowest and highest correlation between b.p. and hydraulic heads in two different seasons, May in 1990 and January in 1991, are contrasted in Figure 6.5 (a) and (b). The numeric figures and graphical displays show that the correlation between b.p. and hydraulic head is obviously high during the seasons of late fall to winter whereas it is the lowest during spring recharge of May. The strong correlation between b.p. and head values are attributed to the minimized recharge and discharge in the late winter due to small precipitation, evapotranspiration, and infiltration into the saturated formation. To explain the trend of correlation coefficient over the year, precipitation data can be referred to. The individual peak precipitation seems to have direct effect on the hydraulic head values, especially at shallower depths of the formation. Moreover, precipitation substantially affects the correlation between b.p. and hydraulic head values. After the rainfall in May, the correlation drops drastically and then remains at low values through the summer recharge season. Correlation consistently goes up through the growing season and dry fall, from August to November. During these seasons, hydraulic heads consistently drops due to consumption of water by plants, however, there is considerable correlation of hydraulic heads with changes in b.p. This can be explained by that the discharge rate due to evapotranspiration by plant growth is somewhat moderate and constant, whereas the recharge rate after precipitation is more drastic and unpredictable.

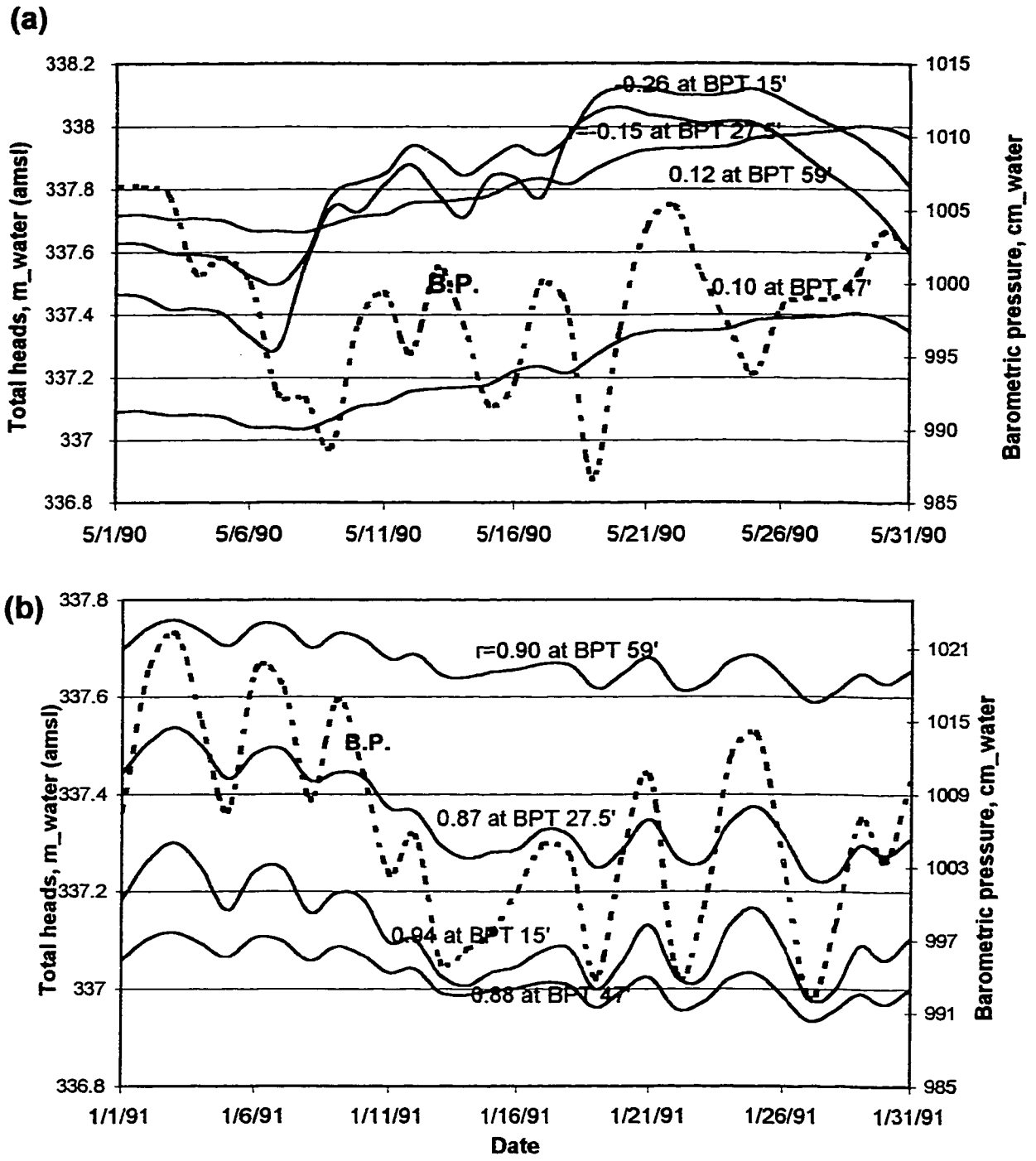


Figure 6.5. Fluctuations of total heads in the formation and correlation coefficient (r) between barometric pressure and head values in (a) spring recharge season and (b) dry winter.

The correlation keeps high values in the dry season of low precipitation and evapotranspiration, from November to February. Among the factors causing changes in hydraulic heads, the effects of barometric pressure are easily disguised by precipitation effects and thus hard to be noticeable. When recharge and discharge due to precipitation and evapotranspiration become minimized or constant, the b.p. effect on well groundwater levels are striking.

### 6.3 Collected Data and Test Sites

Application of the proposed model for actual field tests requires accurate data on well geometry, hydrogeologic setting, and simultaneous record for barograph and hydrograph. In this study, actual field observations, which show strong evidence for interaction of the b.p. and groundwater wells, are categorized into four different cases depending on their features: Field Test 1, 2, 3, and 4. Field Test 1 is for b.p. effects on total hydraulic heads within the formation without a well. Field Test 2 and 3 are about the responses of static water levels in groundwater wells to changes in b.p. Two tests were performed in two totally different lithologic units and time period; Field Test 2 were done in a glacial till unit for two days and Field Test 3 in a sandy aquifer for one month, respectively. Field Test 4 is the case in which well recovery in a slug test is disturbed by changes in b.p. Specific location for three tests, Field Test 1, 2, and 4, are all at the ATHS (Figure 6.3). Data for Field Test 3 were from another research site in New York. Description of each test in terms of the type of test, observation method for b.p. and water level elevations, dimension of the tested well, and other information is summarized in Table 6.3.

Table 6.3. Data summary for (a) Field Test 1, (b) Field Test 2, (c) Field Test 3, and (d) Field Test 4.

(a)

| | |
|---|---|
| Test Type | Head changes in the porous media due to changes in b.p. |
| Observation | 3-hour interval over one month period (Jan. 1, 1991 – Jan. 31, 1991) |
| Barometric pressure | Measured in the weather station in Des Moines, obtained from NCDC (National Climatic Data Center ) |
| Hydraulic head | Buried pressure transducers (wire vibrating ones made by GEOKON) |
| Correlation coefficient between BP(t) and $\Phi_{obs}$ (t) | 0.92 (averaged for 4 BPTs) |

| Buried pressure transducer ID | Depth (m) [a] | Screened lithologic unit |
|---|---|---|
| BPT 15'[b] | 2.6 | unox. L. Wis. till[c] |
| BPT 27.5' | 6.4 | unox. L. Wis. till |
| BPT 47' | 12.3 | unox. L. Wis. till |
| BPT 59' | 16.0 | unox. L. Wis. till |

(b)

| | |
|---|---|
| Test Type | Static water level changes in multiple observation wells due to changes in b.p. |
| Observation | 1 hour interval over 48-hour period (June 23, 1992 ~ June 25, 1992) |
| Barometric pressure | Measured in the weather station at ATHS |
| Water level | Pressure transducers |
| Correlation coefficient between BP(t) and $w_{obs}$ (t) | -0.95 (averaged for 9 wells) |

| Well ID | Depth (m) | Well casing radius (cm) | Well bore radius (cm) | Screen length (cm) | Screend lithologic unit |
|---|---|---|---|---|---|
| N1B | 3.5 | 0.95 | 5.1 | 45 | unox. l. Wis. till |
| N1C | 6.0 | 0.95 | 5.1 | 45 | unox. l. Wis. till |
| N1D | 9.7 | 0.95 | 5.1 | 90 | unox. l. Wis. till |
| N2B | 3.2 | 0.95 | 5.1 | 45 | unox. l. Wis. till |
| N2C | 5.6 | 0.95 | 5.1 | 45 | unox. l. Wis. till |
| N2D | 9.5 | 0.95 | 5.1 | 90 | unox. l. Wis. till |
| N3B | 3.2 | 0.95 | 5.1 | 45 | unox. l. Wis. till |
| N3C | 5.5 | 0.95 | 5.1 | 45 | unox. l. Wis. till |
| N3D | 9.5 | 0.95 | 5.1 | 90 | unox. l. Wis. till |

Table 6.3 continued

(c)

| | |
|---|---|
| Test Type | Water level fluctuations in a relief well within a containment system responding to changes in b.p. |
| Observation | 3-hour interval over one month period (April 20, 1993 ~ May 20, 1993) |
| Barometric pressure | Pressure transducer hung inside the riser pipe of the well (Model PTX-360) |
| Water level | Pressure transducer (Model PTX-160D) |
| Correlation coefficient between BP(t) and $w_{obs}$ (t) | -0.97 |

| Well ID | Depth (m) | Well casing radius (cm) | Well bore radius (cm) | Screen length (cm) | Screened lithologic unit |
|---|---|---|---|---|---|
| RW-1 | 9.9 | 7.62 | 12.7 | 300 | sand |
| Clay cap | Vertical thickness = 1.47 m | | K = 6.8 E-09 cm/s | | |
| Bentonite wall | Lateral thickness = 0.76 m<br>Depth from surface = 29 m | | K = 1.9E-08 cm/s | | |

(d)

| | |
|---|---|
| Test Type | Well recovery in a slug test affected by changes in b.p. |
| Observation | 2-hour interval over 7-day period in a static condition (1993)<br>and 1 hour interval over 48-hour period in a slug test (1993) |
| Barometric pressure | Measured in the weather station in Des Moines, obtained from NCDC (National Climatic Data Center ) |
| Water level | Pressure transducer |
| Correlation coefficient between BP(t) and $w_{obs}$ (t) | -0.78 ( for static water level changes) |

| Well ID | Depth (m) | Well casing radius (cm) | Well bore radius (cm) | Screen length (cm) | Screened lithologic unit |
|---|---|---|---|---|---|
| S-4W | 10.5 | 2.54 | 10.8 | 90 | unox. l. Wis. till |

[a] depth is measured from the water table to the measuring point of BPTs or mid-point of well screen.
[b] BPT15' represents the pressure transducer is buried at the depth of 15 feet from the ground surface.
[c] unox. l. Wis. till denotes the unoxidized late Wisconsinan till.

### *6.3.1 Field Test 1*

The January data in Figure 6.5 (a), showing the highest correlation of b.p and head, were selected for Field Test 1. In the test, the response of hydraulic head in the formation to b.p. variations was observed over one month using a special measurement tool, buried pressure transducers (BPTs). Figure 6.6 shows the schematic view for the BPTs in the test site. The BPTs are not in a well casing but within a borehole in hydrologic connection with the surrounding formation. Thus, measurements from the BPTs represent the total hydraulic heads in pore water in the formation. The BPTs were first installed by drilling a hole to at the desired depth. Within the about 18 cm borehole, a pressure transducer was lowered and sand filled the surrounding portion. A mixture of drill cuttings and bentonite pellets were placed above the sand making a barrier for the next pressure transducer. The same procedure continued for the next three pressure transducers. Investigations from this test will signify responses of pore water pressure in the formation to changes in b.p. and provide a comparative result to those of water levels in wells. One-dimensional diffusion-type groundwater flow model fits simulations of this test. The effects of recharge or discharge on the head responses will also be examined along with effects of b.p. in the test.

### *6.3.2 Field Test 2*

In contrast to the Field Test 1, a well is an essential part of Field Test 2 in which the fluctuation of static water level due to changes in b.p. was monitored for two days. This represents the most common case for field observations of b.p. effects on wells. The FEMBARO model fits the simulations of the test. The site of Field Test 2 is instrumented with three sets of multi-level observation wells. Figure 6.7 shows a cross-sectional view of

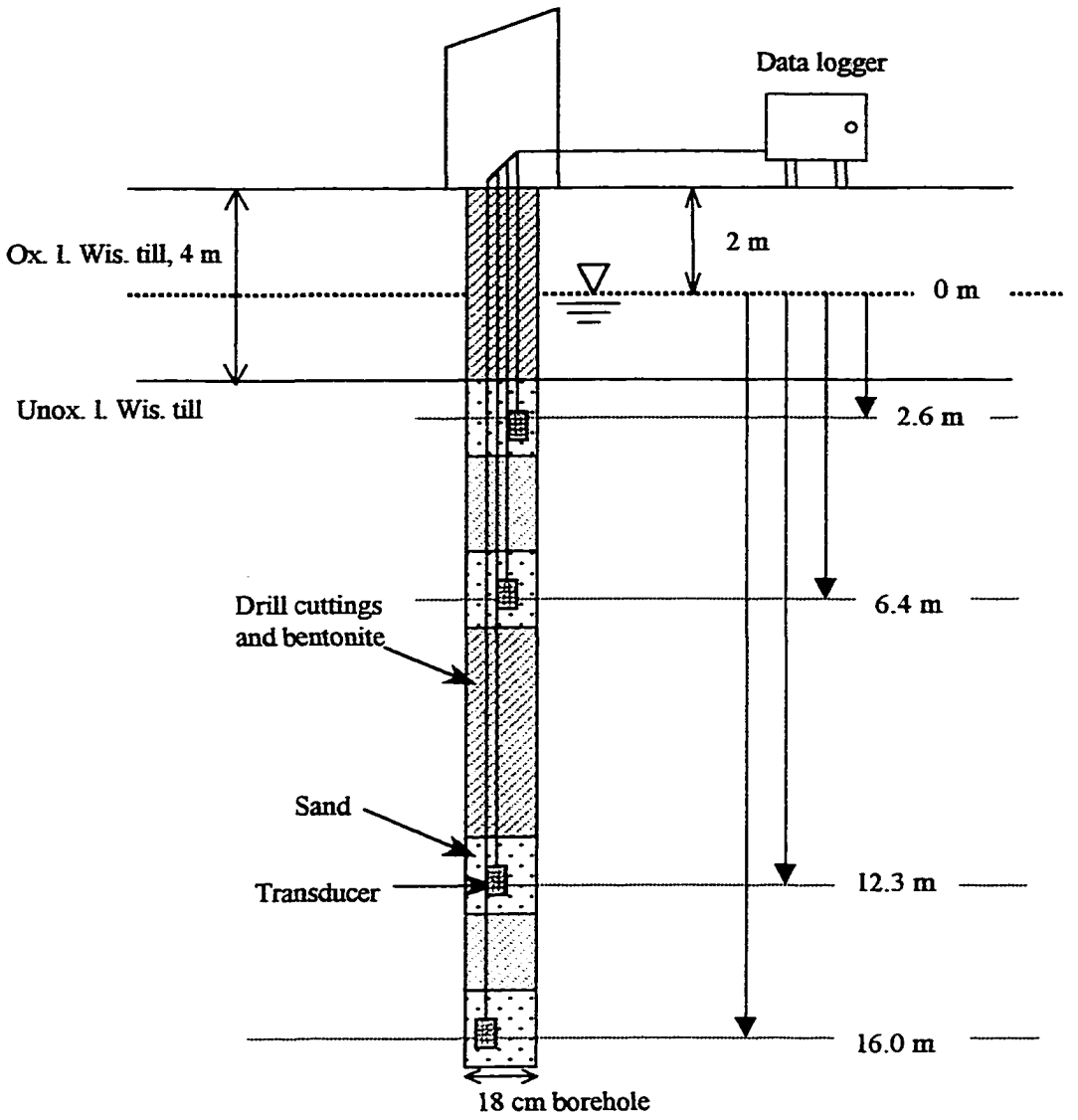


Figure 6.6. Site for Field Test 1 shown in schematic of cross-section.

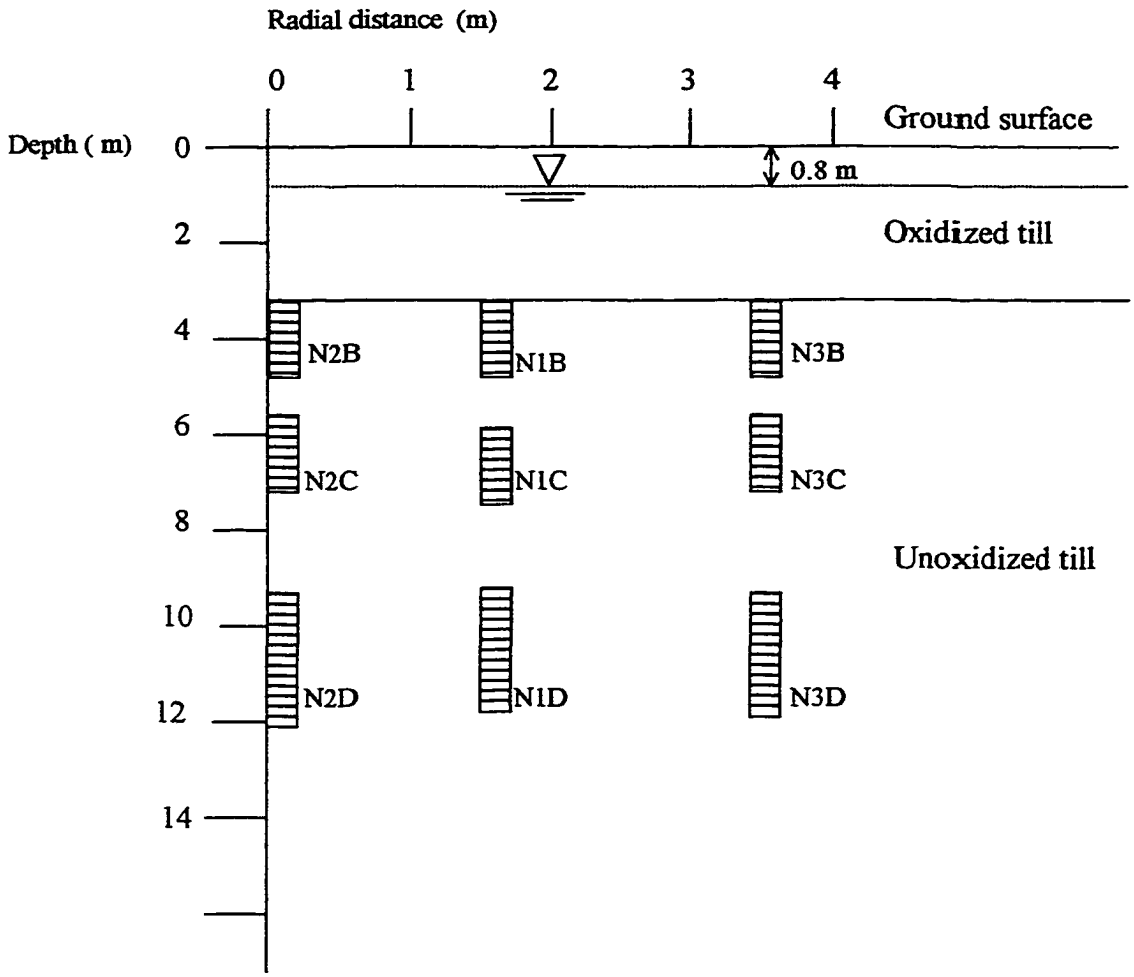


Figure 6.7. Site for Field Test 2 shown in schematic of cross-section.

well nests and observation wells in each borehole: N1, N2, and N3. Each bar represents the screened portion of each observation well. Simulations were performed for an individual well within the unoxidized zone. Capability of the FEMBARO model for estimating hydraulic parameters was evaluated in terms of its accuracy and efficiency based on the results from these simulations.

### *6.3.3 Field Test 3*

Field Test 3 is the case for b.p. effects on a groundwater well in a containment system where the well is penetrated in the very permeable sandy material in an unconfined condition. In this test, the assumption of no exertion of b.p. on the water table was applied because the top is covered with an low permeability layer in the containment system. This means that the continuous changes in b.p. probably act as a series of slug/bail tests in the well and the responding water levels can be used for analysis of the hydraulic properties of the screened geologic unit just as the well recovery curve in slug tests.

The site for Field Test 3, a containment system of a federal Superfund site for the remedy selected, is located in upstate New York. The cross-sectional view of the site is illustrated in Figure 6.8. The system consists of a clay cap on the top, soil bentonite cutoff barrier within the subsurface porous formation and a relief well. This containment system runs for an evaporation pit where liquid waste has been disposed. The bentonite wall barrier is placed through the entire thickness of an unconfined sandy aquifer at a depth of about 29 m below grade, reaching into a thick underlying glaciolacustrine clays. The cap overlies the whole evaporation pit area (1.475 hectare) and extends outward an additional 2.4 m. The size and property of the cap and the wall are listed in the Table 6.3 (c).

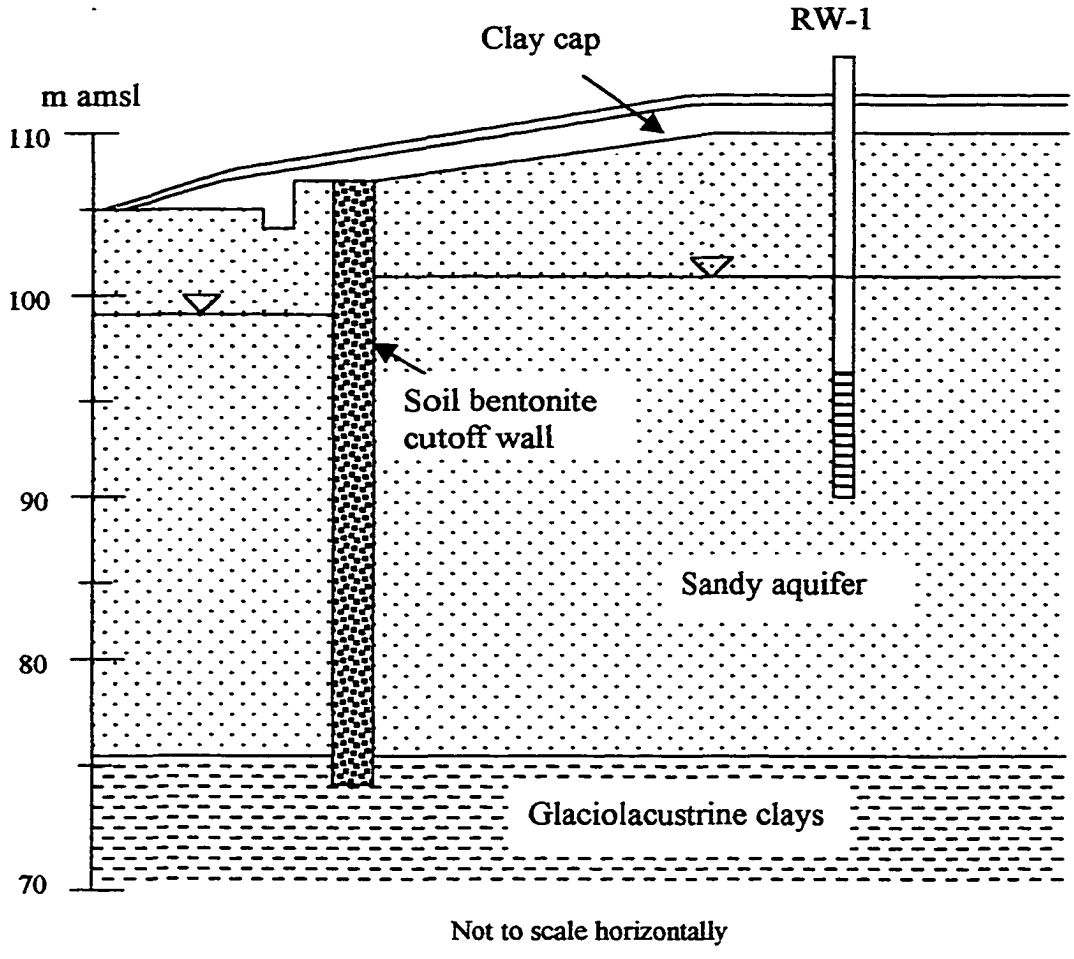


Figure 6.7. Site for Field Test 3 shown in schematic of cross-section.

### *6.3.4 Field Test 4*

As mentioned earlier, it is not easy to investigate the influence of changes in b.p. on the well recovery in actual slug tests because the degree of influence by b.p. are subject to the response time of a slug test, and the period and magnitude of changes in b.p. In Field Test 4, the effect of b.p. on well recovery in a slug test was demonstrated. Fluctuation of the transient water level was monitored during a two-day slug test with simultaneous observation of b.p. Analysis of the simultaneous records of b.p. and static water level of the tested well was also accompanied to support b.p. influence on the tested well in Field Test 4.

# CHAPTER 7. RESULTS AND DISCCUSION

## 7.1 Verification of Model

The model in this study was verified against well-known analytical solutions for typical groundwater flow problems:

- One-dimensional sinusoidal pressure propagation through the porous medium (Jacob, 1940)
- Radial flow pumping tests (Theis, 1935)
- Slug tests in a fully penetrating well with a finite well radius (Cooper et. al, 1967)

Prior to inclusion of the well in the model, a simple one-dimensional vertical flow from the water table was simulated and compared with the analytical solution (Figure 7.1). In the case without a well, changes in b.p. would propagate through a homogeneous and isotropic saturated formation in the manner of diffusion, depending on its hydraulic diffusivity. In Figure 7.2 the modeled radial groundwater flow in a constant-flowrate pumping test was verified against the Theis solution (1935). In the radial flow model, the well-flux over the screen is fixed as a constant through the entire period of the test. Thus, treatment of the pumping well as a line source in the model eliminates the iterative procedure for estimation of well-flux to satisfy Darcy's law.

Distinct features of the slug test model from the above cases are i) inclusion of the well and its geometry, and ii) approximation of well-fluxes over the screen, which are unknown transient values. A radial flow by slug impact on a fully penetrating well, simulated by the FEMSLUG model, gives precisely the same responses as the solution by Cooper et al. (Figure 7.3). The iteration technique for estimation of well-flux (see Chapter 4.4) was proven

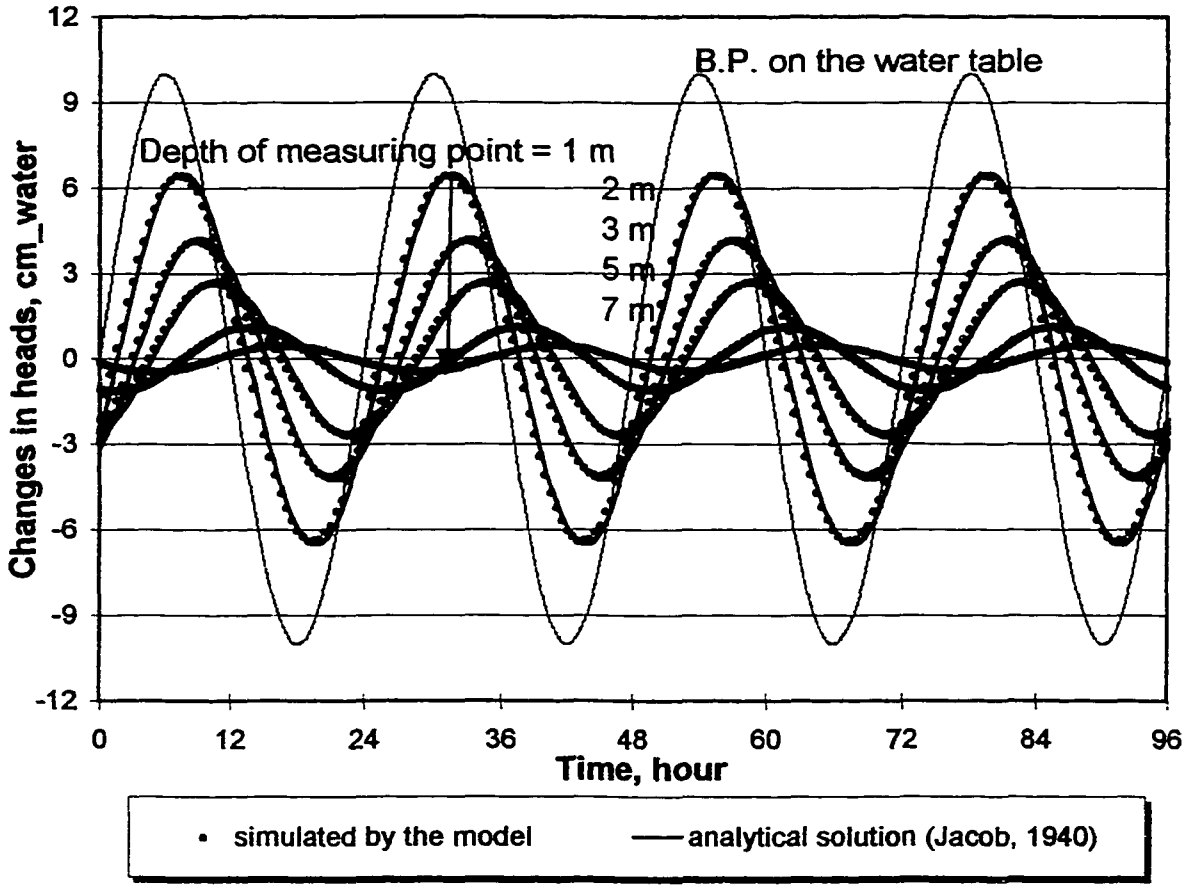


Figure 7.1. Verification of the 1-dimensional groundwater flow model against the analytical solution (assumed $D_f = 2$ cm$^2$/sec).

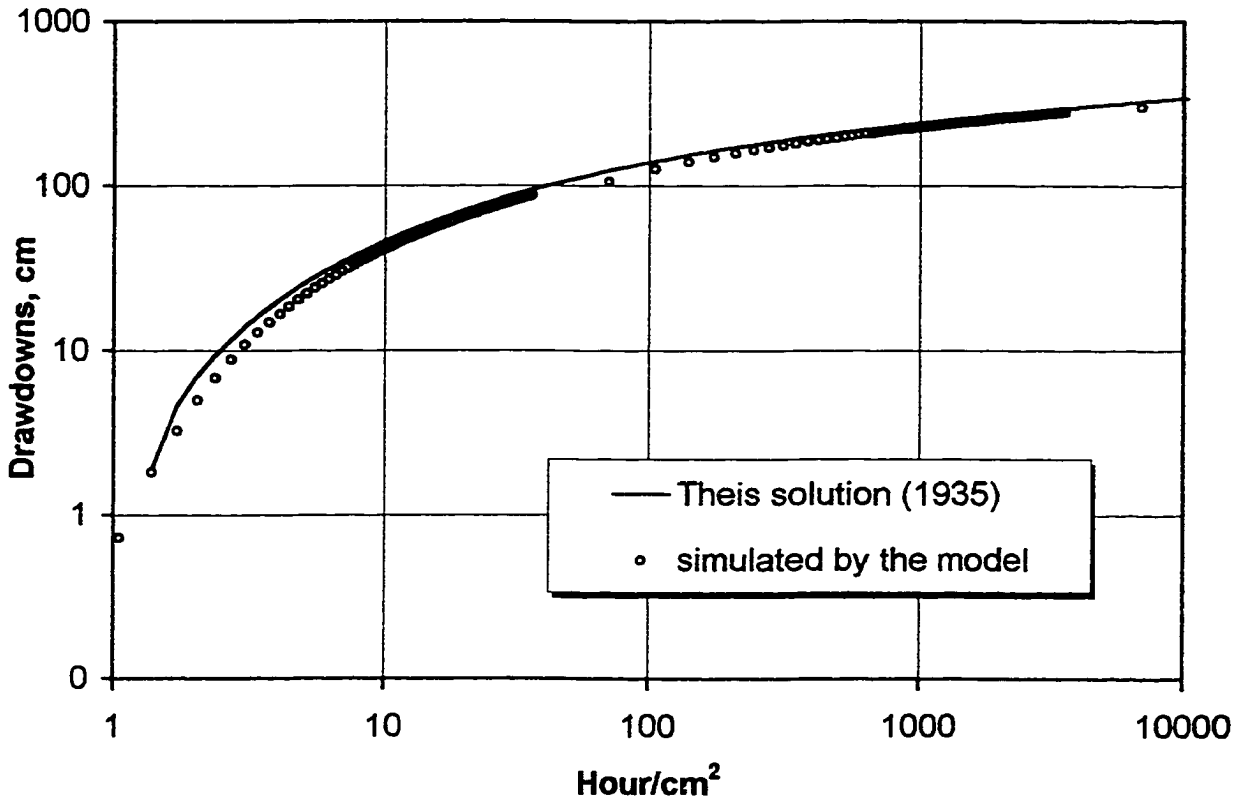


Figure 7.2. Verification of the radial groundwater flow model against the Theis solution (1935).

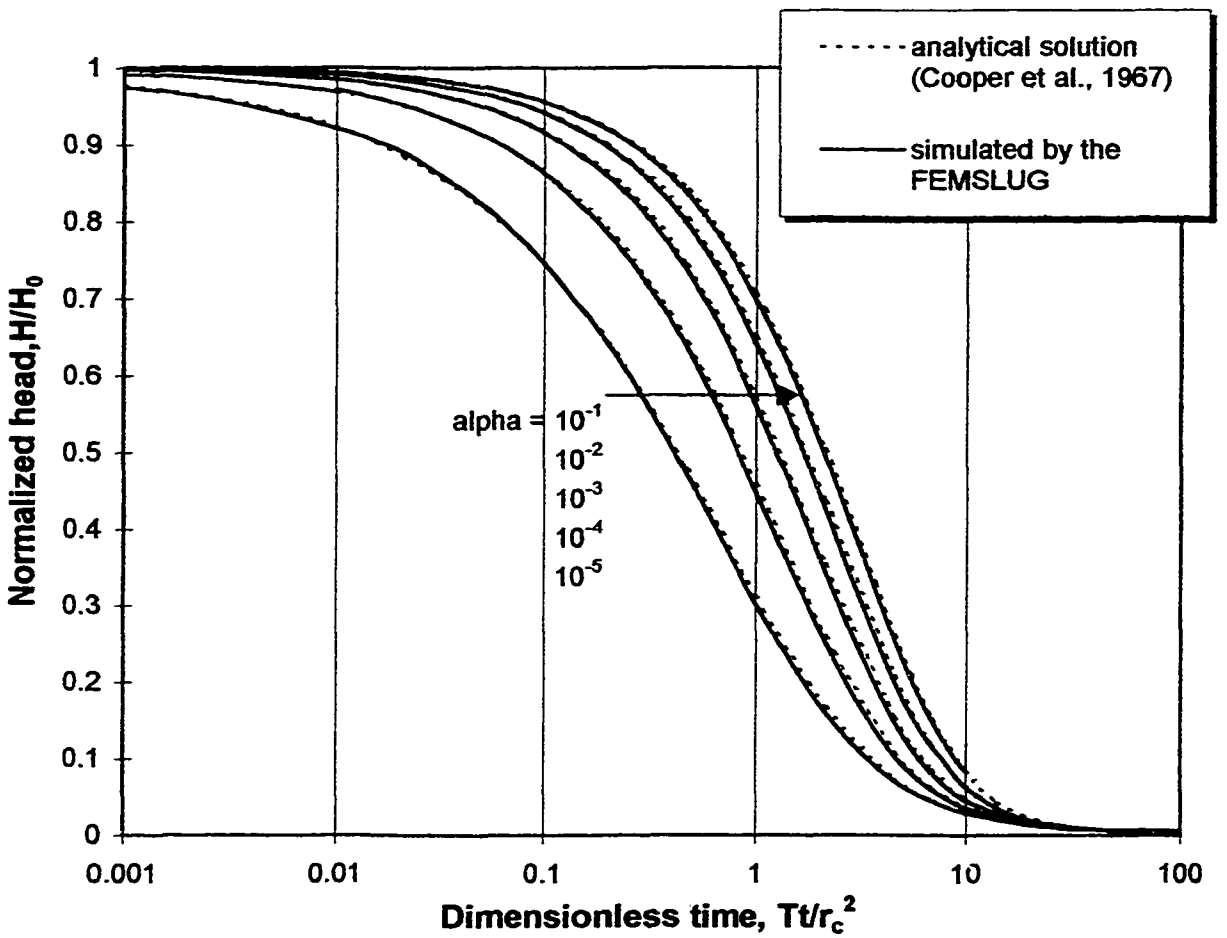


Figure 7.3. Confirmation of the FEMSLUG model against the Cooper et al.(1967) solution.

to be acceptable through this verification. Thus, the FEMSLUG model can be thought to be a numerical version of the Cooper et al. solution for radial flow. The common distinct feature of the FEMSLUG and the Cooper et al. solution from other slug test models is the concept of 'a finite diameter well' and accurate estimation of 'well-flux', instead of the assumption of a well as a line source and approximation of the flux.

The verification of the FEMSLUG to the Cooper et. al solution has a special meaning because the main model for b.p. effects on wells in this study is numerically related to the slug test model through the principle of superposition. Basically, b.p. fluctuations in the well act like a continuing series of slug impacts, whereas a slug test can be considered the simplest case of b.p. change that is given initially and kept constant over time. However, it should be noted that the one-dimensional vertical flow from the water table is associated with superimposed b.p. impacts on the well in the model for b.p. effects. The confirmation of the FEMSLUG model to the Cooper et. al solution guarantees, in a roundabout way, the validity of the FEMBARO model by confirmation of the iteration technique for the estimation of the well-flux as a useful tool in combining the changes in b.p., and the responses of the well and the surrounding porous media.

### 7.2 Superimposed Well Recovery in Slug Tests

The principle of superposition was confirmed in examples of three-step slug tests as illustrated in Figure 7.4. The simulated well recovery by the FEMSLUG and the calculated one in a spreadsheet, using the principle of superposition, match each other exactly. After insertion of the second slug, the well recovery becomes faster than in the case for the one-step

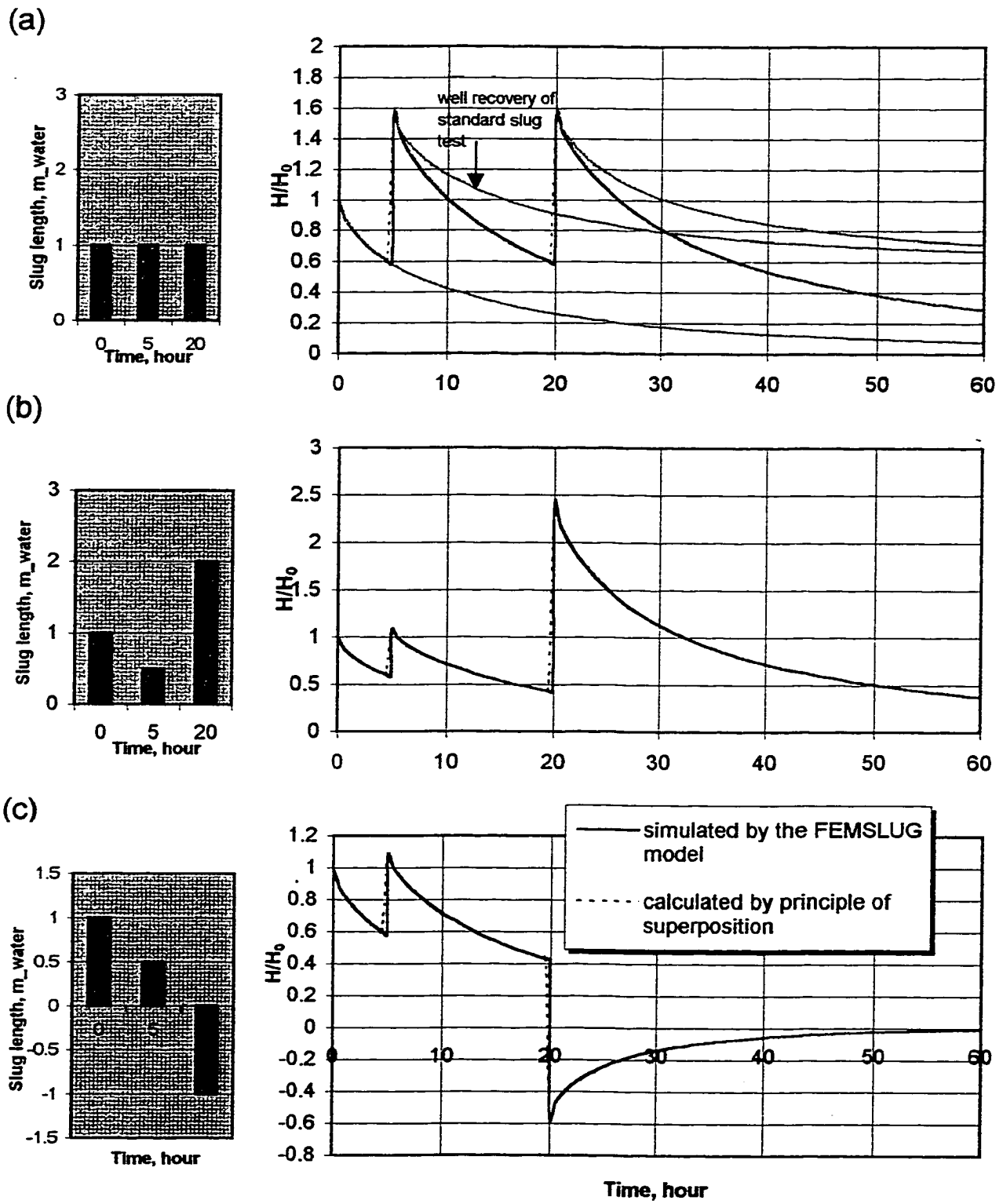


Figure 7.4. Superimposed well recovery in slug tests (a) unifrom slug input, and (b) and (c) variant slug input .

slug test. This occurs because the water level was also reclining in response to the slug impact of the preceding step (Figure 7.4 (a)). The principle of superposition is also valid in the cases of variant water slug lengths and associated bail tests, without loss of generality (Figure 7.4 (b) and (c), respectively).

### 7.3 A Series of Slug/Bail Tests and Barometric Pressure Effects on the Well

Superimposed well recovery in a series of slug/bail tests at an hour interval for two days is presented in Figure 7.5. The bar chart represents the cumulative water supply entering the well. The solid lines represent the recovery curve of the well, total head ($\Phi$) vs. time, where the total head certainly represents the water level in the well: in detail, the black lines were simulated by FEMSLUG and the gray lines calculated using the principle of superposition. The calculated one gives good approximation for the predicted value by the model.

The concept of the above series of slug/bail tests is converted into b.p. effects on the water level in the well under two assumptions: (a) the bars in Figure 7.5 represent discretized changes in b.p. and (b) no exertion of b.p. on the water table outside the well. Estimates of total head in the well (the solid line) stand for the responses of the well in the case of b.p. tests. Using the relation in which the total head is equal to the sum of the water level and b.p. in the well, the calculated water levels are plotted in Figure 7.5 (the dashed line). Water level transients in the well show the mirror image of the applied air pressure as commonly observed in field records. For the pressure changes applied in the well, either water slug or barometric pressure changes, the responding changes of total heads show the same results. However, in the b.p. tests the water level fluctuations in the well show the mirror image of the changes in

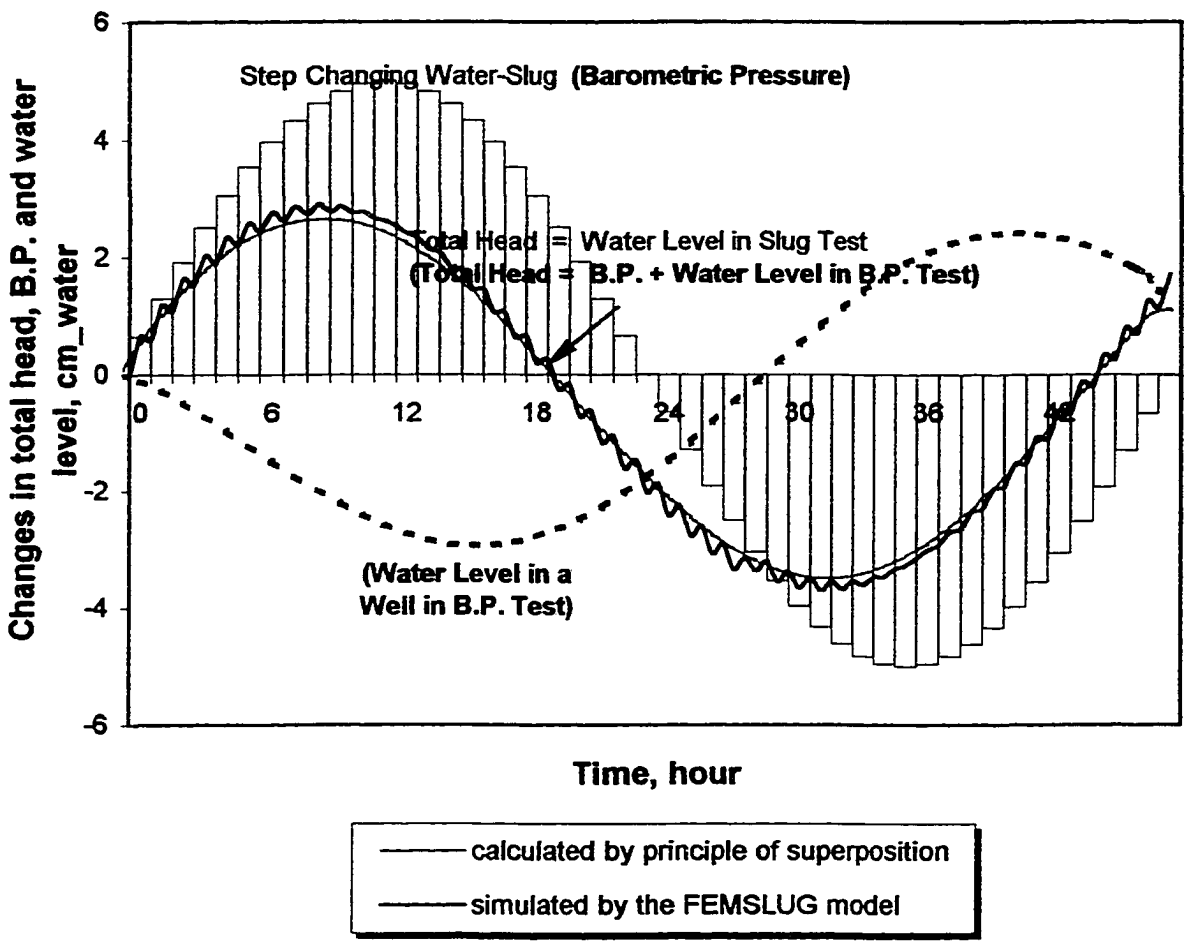


Figure 7.5. Relation between a series of slug/bail tests and effect of barometric pressure on groundwater wells.

pressure on the well, with a time lag. Water level variations to b.p. changes in a confined condition can be simulated by neglecting vertical propagation of b.p. from the water table because of the head loss of the whole b.p. through a low permeability confining unit. Even in an unconfined condition, a well far below the water table would show confined responses to b.p. because vertical head changes in the media outside the well interfere less with the well head over increasing depths of a well. The influence of b.p. on a groundwater well can be modeled in the same way well recovery of a series of slug/bail tests is solved: the principle of superposition. The numerical results of the relationship between a series of slug/bail tests and b.p. effects on a well in this study agree on the outcome from analytical trials for convolution of integral of barometric response function and use of the solutions for slug tests analysis in other studies (Furbish, 1993, Gaussman et al., 1997, and Rojastaczer, 1999).

### 7.4 Influence of Barometric Pressure on Groundwater Condition in Cases With and Without a Well

Figure 7.6 (a) displays the responses of groundwater wells to changes in b.p. in terms of two variables: changes in total head ($\Phi$) and water level (w) in wells. Head values increase as b.p. increases and decrease as b.p. decreases. However, water level changes in groundwater wells show the opposite trend: in other words, the water level declines as b.p. increases and increases as b.p. decreases. Overall, simulated changes of water level in wells exhibit the mirror images of b.p. changes with respect to factors such as dampened peaks, and a few hours of time lag. Also, the curves show that water level changes increase with an increase in

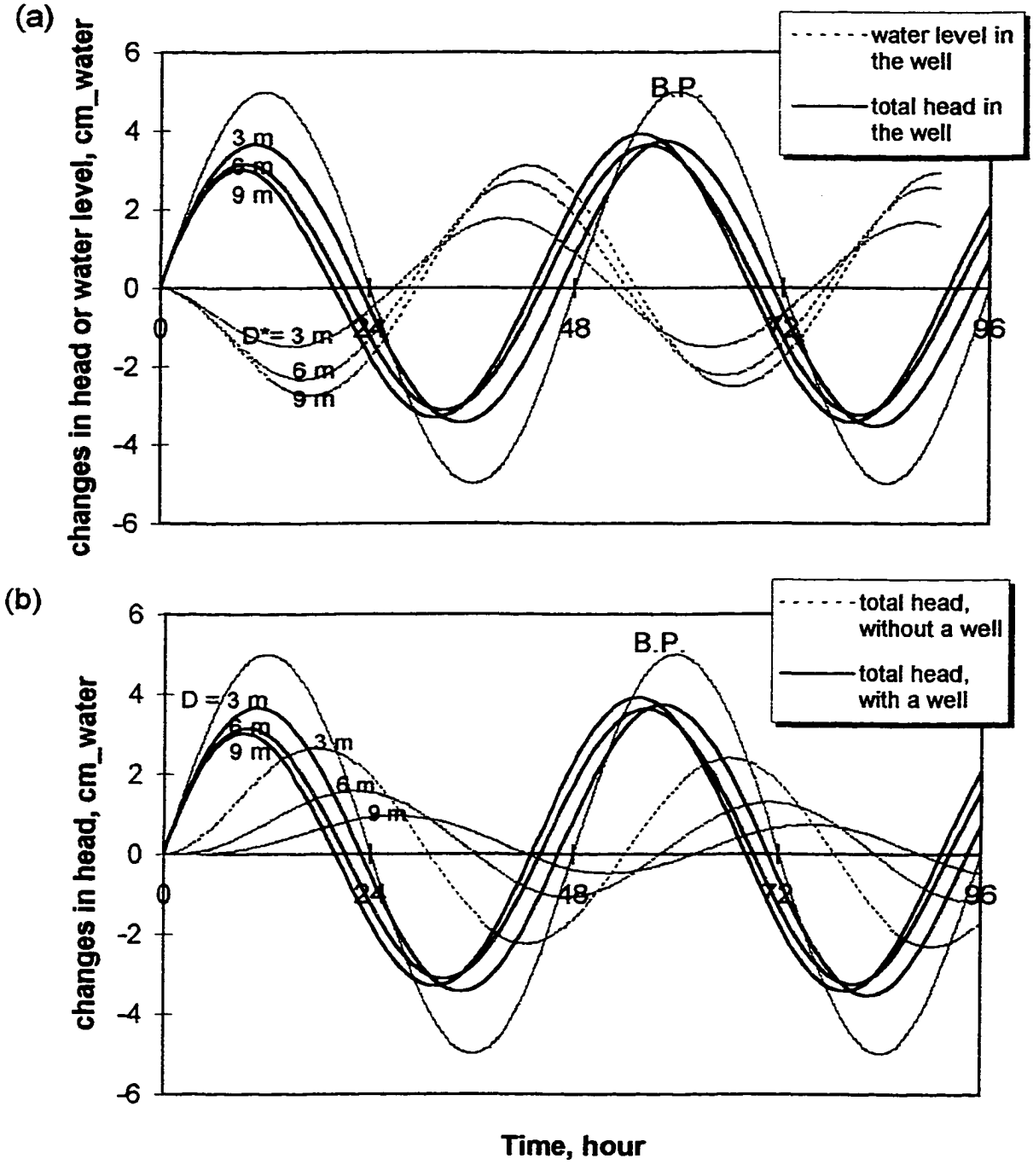


Figure 7.6. Responses of wells and porous media to barometric pressure (B.P.) (a) total heads and water levels in a well and (b) total heads in cases with and without a well. *D denotes the depth of the measuring point (or mid-point of well screen) below the water table.

the well screen depth below the water table: barometric efficiency ($B_e$) increases with increased depth of the well screen depth below the water table. This is attributed to the fact that the head loss through the formation increases with an increasing propagation depth outside of the well. Consequently, a greater hydraulic gradient around the well screen results in a greater response in the water level of the well to b.p. changes in a deeper well.

In Figure 7.6 (b), total head changes due to changes in b.p. are compared between two cases: with and without a well in the porous formation. Solid lines represent changes in the hydraulic head within the well. Dashed lines represent changes in head within the formation in the case of no well penetration. There are shorter time lags for head changes in wells than those in the formation without a well. The presence of a well within the porous medium induces a quicker response of well head changes: a well acts as a shortcut to take the changes in b.p. into the saturated porous media. In other words, the prompt propagation of pressure change in free standing water in the well and its incorporation with the gradual head changes in the porous medium bring about the fast changes of water levels and head values in the well. In the case of no well, the downward propagation of pressure change is retarded by the head loss in the porous medium.

Comparison between two groups of dashed lines in Figure 7.6 (a) and (b) signifies the role of the well itself in b.p. effects on well responses (Figure 7.7). As the depth of the measuring point increases, $B_e$ increases in the case with a well, whereas the efficiency of head changes decreases in the case of no well. Thus, those two line groups show opposite signs and the reversed trends of the response to b.p. over increasing depths.

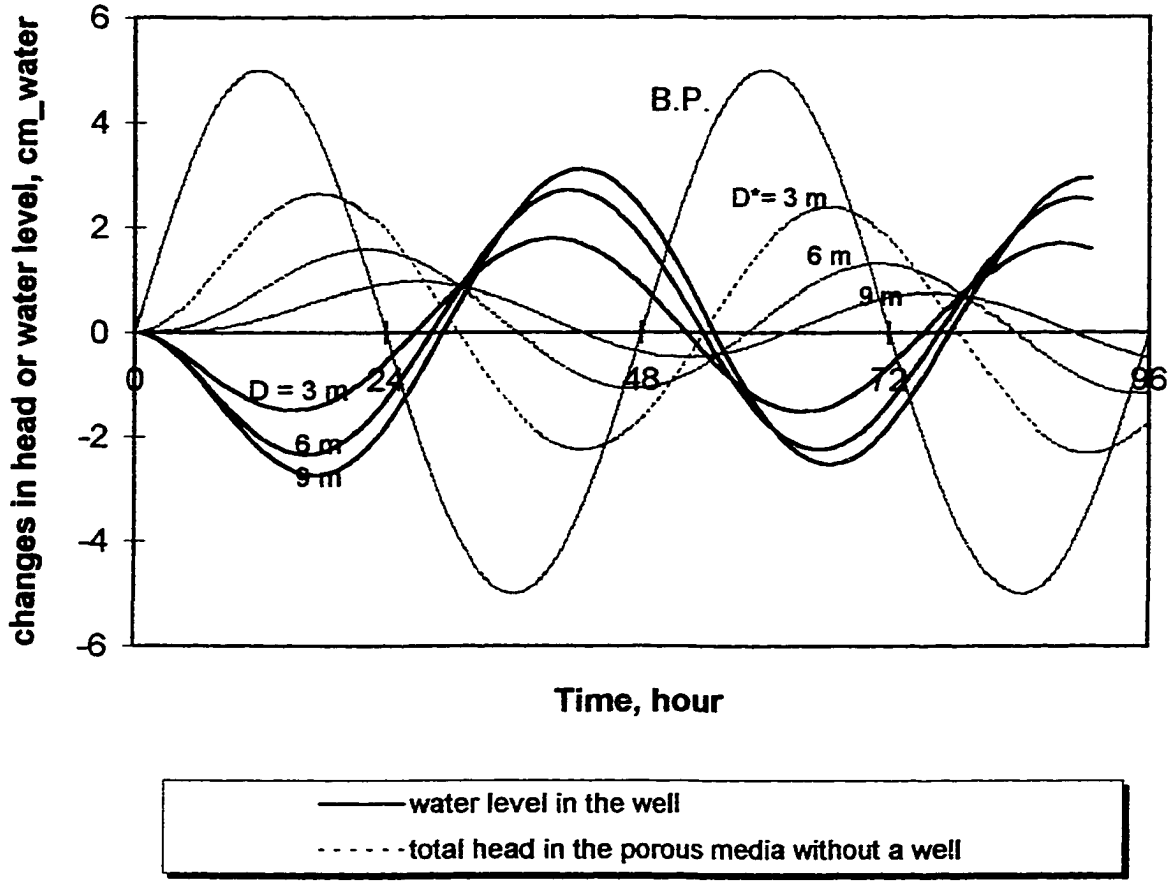


Figure 7.7. Comparison between barometric pressure (B.P.) effect on water level changes in wells and that on total heads in the case without a well. *D represents depth of measuring point (or mid-point of well screen ) below the water table.

### 7.5 Limitation of a Simple Linear Model for Estimates of Barometric Efficiency

As shown in the Figure 7.6 (a), both the total head and the water level in a well display phase shifts relative to variations in b.p. The simple linear regression between simultaneous records of b.p. and water level do not account for the phase shift factor in determination of $B_e$. Therefore, use of simple linear regression may mislead the estimates of $B_e$. Moreover, there is no agreement on the definition of $B_e$ within several text books on groundwater hydrology (e.g. Walton, 1970; Fetter, 1979). $B_e$ is defined as the relative ratio of changes in water level to changes in b.p., but in some cases, as changes in total head relative to changes in b.p. Therefore, $B_e$ of a well needs to be defined in the correct term and sign for accurate determination and its use. Estimates of $B_e$ of the well response displayed in Figure 7.6 (a) are compared under four different definitions (Table 7.1). In this study, water level data were used and corrections for phase shift were considered for determination of $B_e$ (method 1 in Table 7.1). In this case, readings of the peak to peak between b.p. and responding water level are used for approximation of $B_e$. The detailed statistical methods for estimation of $B_e$

Table 7.1. Estimates of barometric efficiency under different assumptions.

| Method | 1 | 2 | 3 | 4 |
|---|---|---|---|---|
| Definition of $B_e$ | $B_e = \frac{\Delta w}{\Delta BP}$ | $B_e = \frac{\Delta w}{\Delta BP}$ | $B_e = \frac{\Delta \Phi}{\Delta BP}$ | $B_e = \frac{\Delta \Phi}{\Delta BP}$ |
| Correction for phase sift | Yes | No | Yes | No |
| Estimate of $B_e$ | -0.60 | -0.47 | 0.63 | 0.53 |

considering the phase shift were presented thoroughly in the works by Clark (1967) and Davis and Rasmussen (1993).

### 7.6 Effect of Natural Recharge on Well Responses

In a long-term view, water levels in the well fluctuate mostly due to recharge and discharge on the water table mainly due to seasonal precipitation and evapotranspiration. Of course, the degree that it is affected by the recharge and discharge depends on the hydraulic properties of formation and intensity and duration of precipitation and evapotranspiration. Figure 7.8 illustrates how the linear recharge on the water table in a low permeable unit (assumed K = 2E-09 cm/s and $S_s$ = 1E-06 1/cm) affects the well response to changes in b.p. In a short term view, recharge does not significantly affect barometric fluctuation of the water level, even with a very high recharge rate (Figure 7.8 (a)). However, in a long-term view, the water level changes due to recharge increases extensively with time (Figure 7.8 (b)).

### 7.7 Diffusion of Changes in Barometric Pressure in the Porous Formation

In the case of no well in a porous media, changes in head values over increasing depths, with respect to b.p. changes at the water table, are displayed for three different values of hydraulic diffusivity in Figure 7.9. The graphics show that head changes gradually follow the trend in b.p. changes. An increase in b.p. leads to an increase in head values. The change in head value decreases with the depth, and a longer time lag for the dampened peak occurs at a greater depth. This is due to more head loss occurring at a greater depth during the propagation of pressure changes within the saturated porous medium. This means that

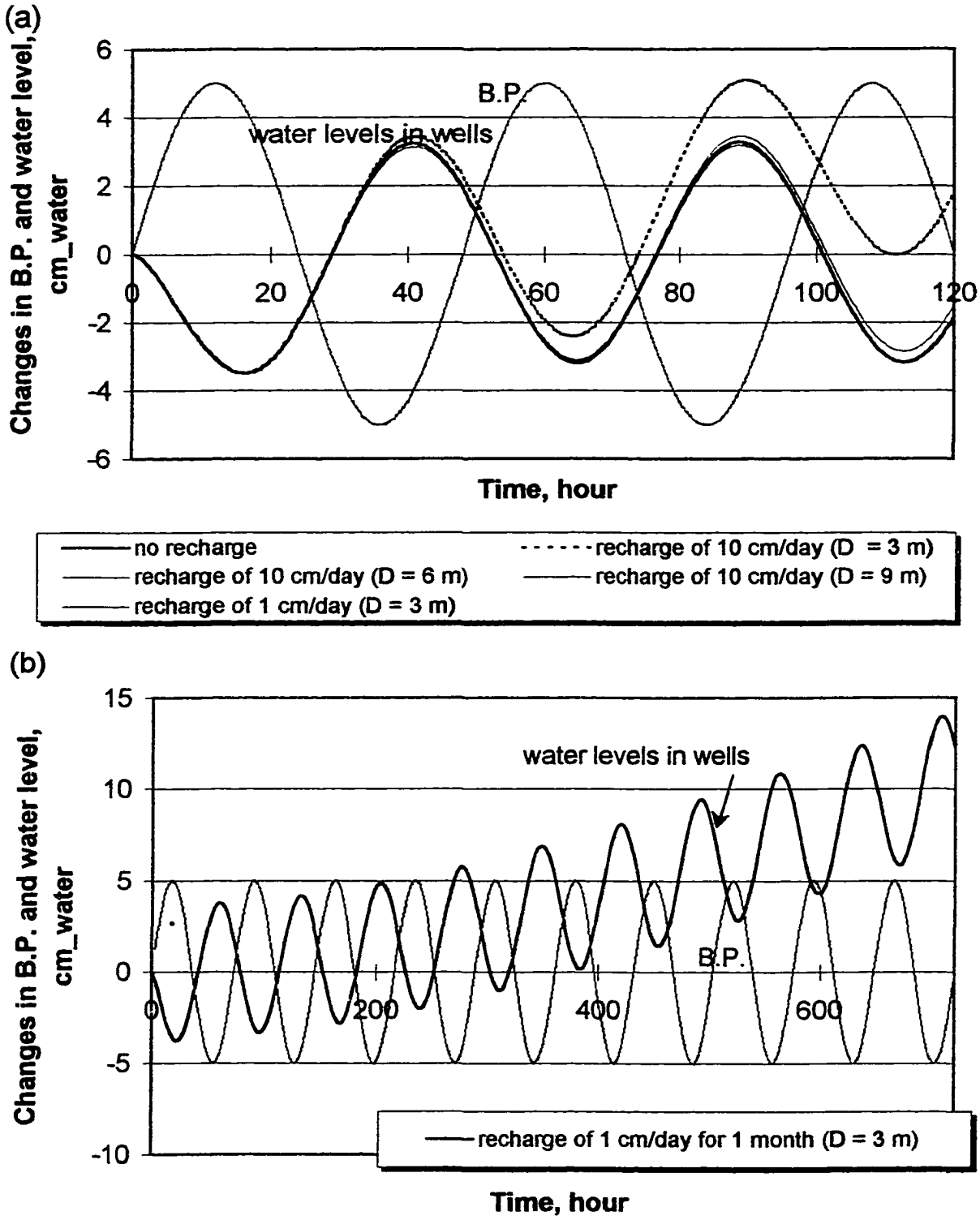


Figure 7.8. Effects of natural recharge on barometric fluctuations of water level in (a) 5 days and (b) 30 days.

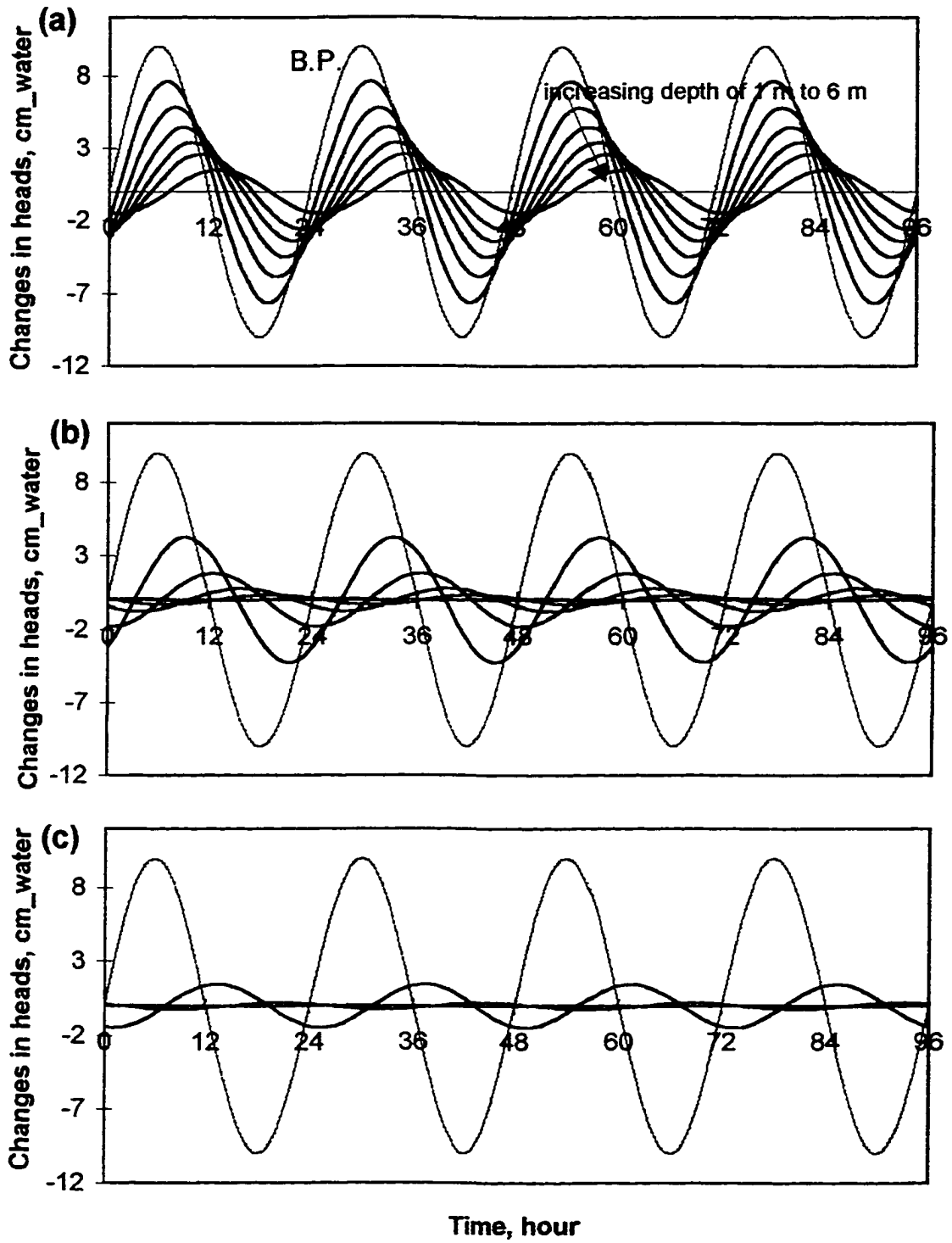


Figure 7.9. Diffusion of barometric pressure in saturated porous formation at different hydraulic diffusivities (a) 5 $cm^2/s$, (b) 0.5 $cm^2/s$, and (c) 0.1 $cm^2/s$.

sensitivity of heads in a porous media to changes in b.p. decreases as the depth of measuring point increases. Furthermore, the propagation speed and degree of head changes due to changes in b.p. decreases as hydraulic diffusivity of the formation decreases. In the formation of a lower hydraulic diffusivity, 0.1 $cm^2/s$, changes in head due to b.p. are detectable only within the top one meter from the water table (Figure 7.9 (c)). Hydraulic diffusivity of unoxidized glacial tills is about this value, based on the estimates of K and $S_s$ by the pumping tests (Jones, 1993). Herein, graphics in Figure 7.9 (c) represent, to some extent, the changes in head far outside of the well when a well exists in a low permeability media. These head transients will incorporate with head transients in the vicinity of the well leading to a change in water level fluctuations. Figure 7.9 (c) suggests that the interference of the vertical transient of b.p. from the water table with the well response is negligible in a low hydraulic diffusivity material because of the entire loss of head during b.p. propagation within the saturated porous medium outside of the well . In such a condition, the response of the well screened deeply in an unconfined condition becomes equivalent to that in a confined condition.

### *7.7.1 Simulated Field Test 1*

In the case of no well, the one-dimensional diffusion-type flow due to changes in b.p. with the associated recharge effects was examined in Field Test 1. The head variations at four different depths in the formation and applied recharge rates on the water table are presented in Figure 7.10. The estimated recharge rates on the water table are varying through the period of a month. Moreover, the estimated rates using the data from deeper buried pressure transducers (BPT 47' and BPT59') are not consistent with those from shallower ones (BPT15'

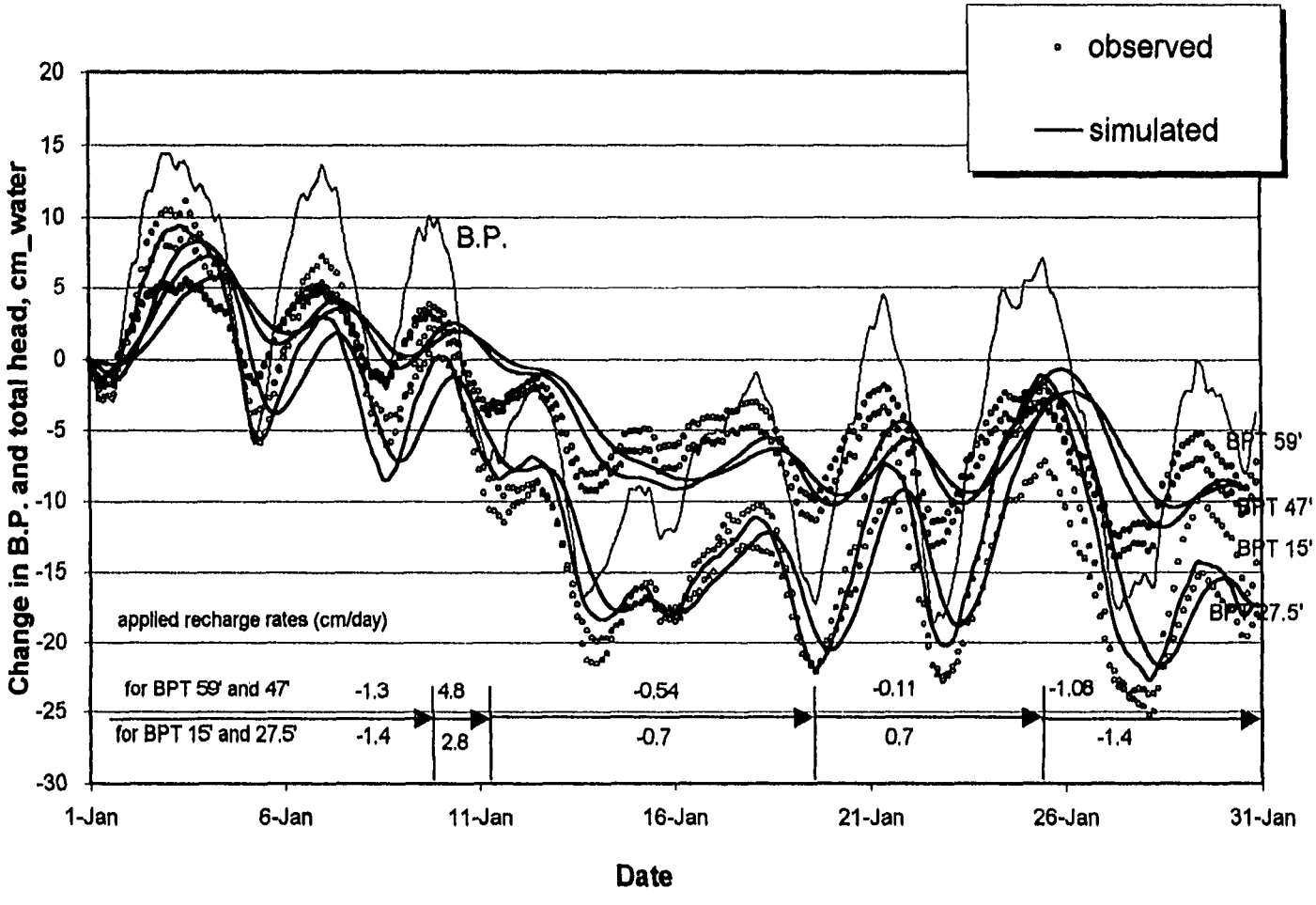


Figure 7.10. Observed and simulated total hydraulic heads responding to changes in barometric pressure (B.P.) in Field Test 1.

and BPT27.5'). The response of the deeper ones yield more moderate estimates of recharge. This difference may be due to the existing local groundflow and heterogeneity in the formation which are not considered in the simulation. Figure 7.11 illustrates the existing local hydraulic gradients below the water table which is presumed by hydraulic heads of four BPT points at the initial time. There exists an upward local groundwater flow between the BPT 27.5' and BPT 47 ', which is believed to affect the distinct head responses between the upper and lower layers in the tested unoxidized formation. Based on the result in Figure 7.10, it is also possible that there is a hydraulic discontinuity between the layers of two groups of BPTs although they are all placed in the unoxidized till units. In this point, it is more complex to estimate the hydraulic properties of formation through this simulation. Overall, comparisons between observed and simulated data indicate that, in a long term view, hydraulic head variations in the saturated formation due to changes in b.p. are explained by combined effects of diffusion of b.p., natural recharge and discharge, and existing groundwater flow.

## 7.8 **Effect of Barometric Pressure on Static Water Level in a Well**

In the results from the previous theoretical approaches using the FEMBARO model, the water level fluctuation in a groundwater well responding to changes in b.p. was clearly shown to be a phenomenon due to the presence of a well penetrated within the formation. Figure 7.12 illustrates the head configuration in the modeled groundwater regime due to changes in b.p., which directly exerts on both water in the well and the water table. The equipotential lines in Figure 7.12 illustrate that there are two main head perturbations and consequent groundwater flow due to changes in b.p.: a radial flow in the vicinity of the well and a vertical

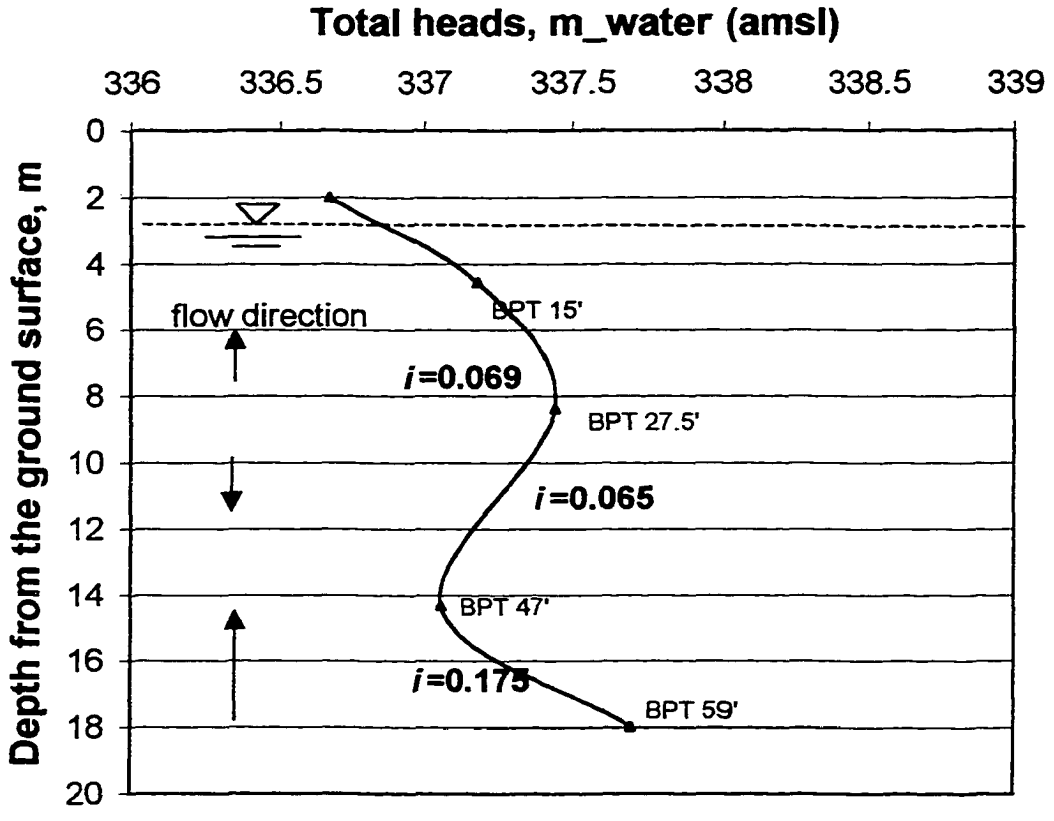


Figure 7.10. Initial head distribution within the saturated formation at the Ames Till Hydrology Site in January, 1991 (*i* denotes hydraulic gradient).

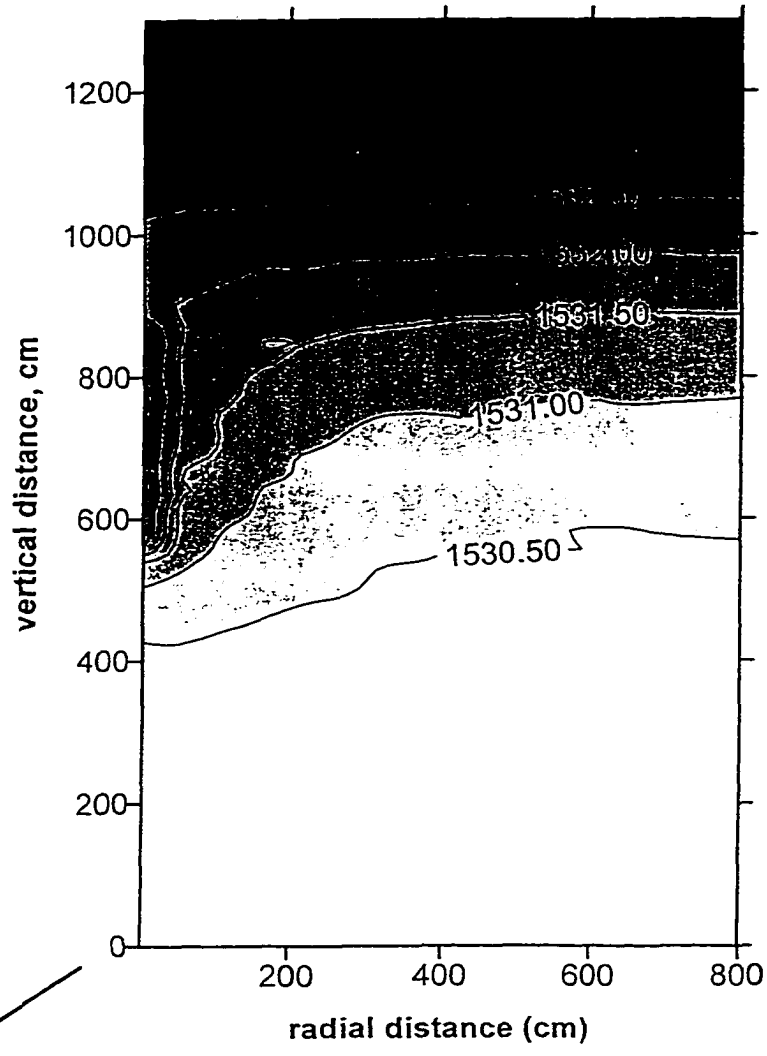


Simulation setting:

| | |
|---|---|
| Barometric pressure | Sinusoidal changes, $BP_m$ = 5 cm, T = 48 hours |
| Well | $r_c$ = 1.27 cm, L = 1.5 m, D = 6 m |
| Porous media | K = 2E-7 cm/s, $S_s$ = 5E-6 1/cm |
| Simulation time | $t_{max}$ = 100 hour, $\Delta t$ = 0.5 hour, hydraulic heads at t = 10 hour |

Figure 7.12. Equipotential lines representing groundwater flow due to changes in barometric pressure

flow from the water table. In addition, interference of the vertical flow with the radial flow from the well occurs around the well. Finally, the well-flux over the well screen created by radial and vertical flows are mainly responsible for the water level fluctuation in the well. Groundwater flow on the domain of equipotential lines in Figure 7.12 is governed by conservation of mass and Darcy's law depending on the hydraulic properties of the saturated formation. In detail, propagation of changes in head depends on the hydraulic diffusivity, whereas the pore water flux through the formation follows Darcy's law depending only on the hydraulic conductivity of the formation.

### *7.8.1 Factors Controlling Well Responses*

Results from the sensitivity analysis of barometric efficiency ($B_e$) to hydraulic parameters and the depth of the well are displayed in Figure 7.13. A larger hydraulic conductivity (K) gives a greater response in changes to b.p. within a well, i.e. a higher $B_e$ (7.13 (a)). This is due to a larger flowrate induced by a larger K value according to Darcy's law. Specific storage ($S_s$) is also a non-negligible factor, even though it is not as significant as that of K. A higher $S_s$ also gives a greater response in the well by producing a larger flowrate (Figure 7.13 (b)). At a given hydraulic diffusivity ($D_f$), $B_e$ values vary greatly, depending on both K and $S_s$ (Figure 7.13 (c)). The well-flux responding to changes in b.p. is primarily governed by K values, whereas the hydraulic gradient established over the well-screen is subject to not only lateral hydraulic diffusivity adjacent to the well but also a vertical one from the water table. It is also demonstrated in Figure 7.13 (a), (b), and (c) that $B_e$ increases with increasing depths of a well. However, this effect is limited down to a certain level of depth: for example, 6 m below the water table in the case of K = 2E-07 cm/s and $S_s$ = 5E-07 1/cm in Figure 7.13 (b).

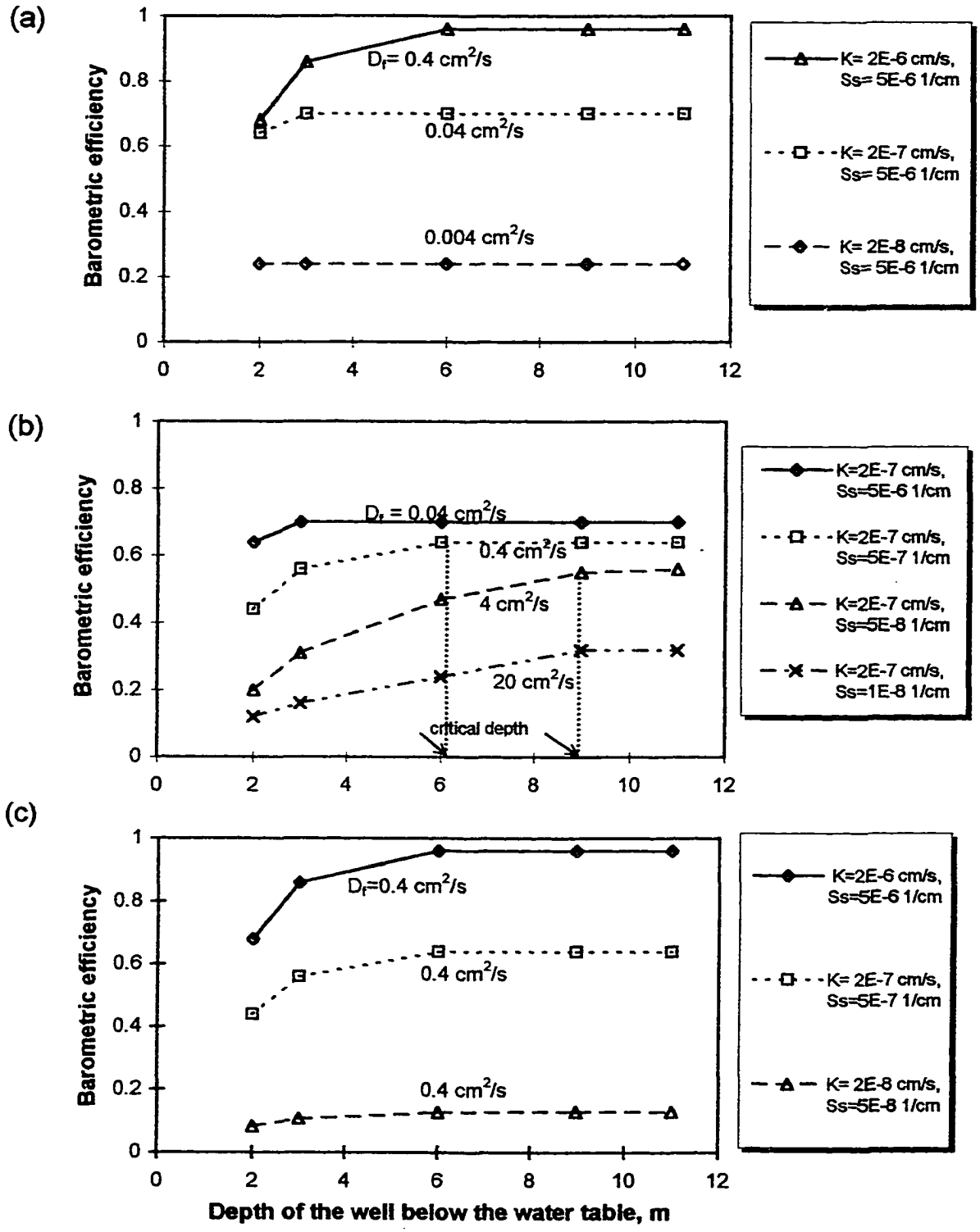


Figure 7.13. Effects of hydraulic properties and depths of well on barometric efficiency (a) hydraulic conductivity (K), (b) specific storage ($S_s$), and (c) hydraulic diffusivity ($D_f$).

Below this critical depth, $B_e$ of a well is shown to be constant and thus the depth of the well is not a factor on responses of wells to b.p. The location of the critical depth is affected by the physical and hydraulic properties of the porous medium. As $D_f$ increases, the critical depth increases: 6 m for $D_f = 0.4$ cm$^2$/s and 9 m for $D_f = 4$ cm$^2$/s in Figure 7.13 (b). In other words, the effects of well depths on the well responses to b.p. are pronounced in the material of a high $D_f$.

Figure 7.14 shows the effect of the screen length on changes in water level of a well due to b.p. fluctuations. The curves for the changes in water levels have been reversed to facilitate the visual comparison. Overall, water level changes increase with a longer screen length. Comparison of results between the top-half and the bottom-half screened well indicate that the bottom-half screened well (a deeper well) shows more water level change than the top-half screened well (a shallow well). Therefore, the depth of a well from the water table is still an important factor that affects the response of a well.

### *7.8.2 Simulated Field Test 2*

B.p. and water levels in the wells at three well nests in Field Test 2 are illustrated in Figure 7.15. The curves for the changes in water levels have been reversed to facilitate the comparison (in fact, an increase in b.p. leads to a decrease in water level). Water levels in a well fluctuate trace changes in b.p. in the opposite direction and the simulated results by the FEMBARO thoroughly explains the observed data in nine wells at three well nests. The results also show that $B_e$ increases as the depth of well increases (Figure 7.16). These distinct responses of wells at different depths support the results in the theoretical sensitivity analysis in the previous section. Figure 7.16 also displays the agreement between the observed and

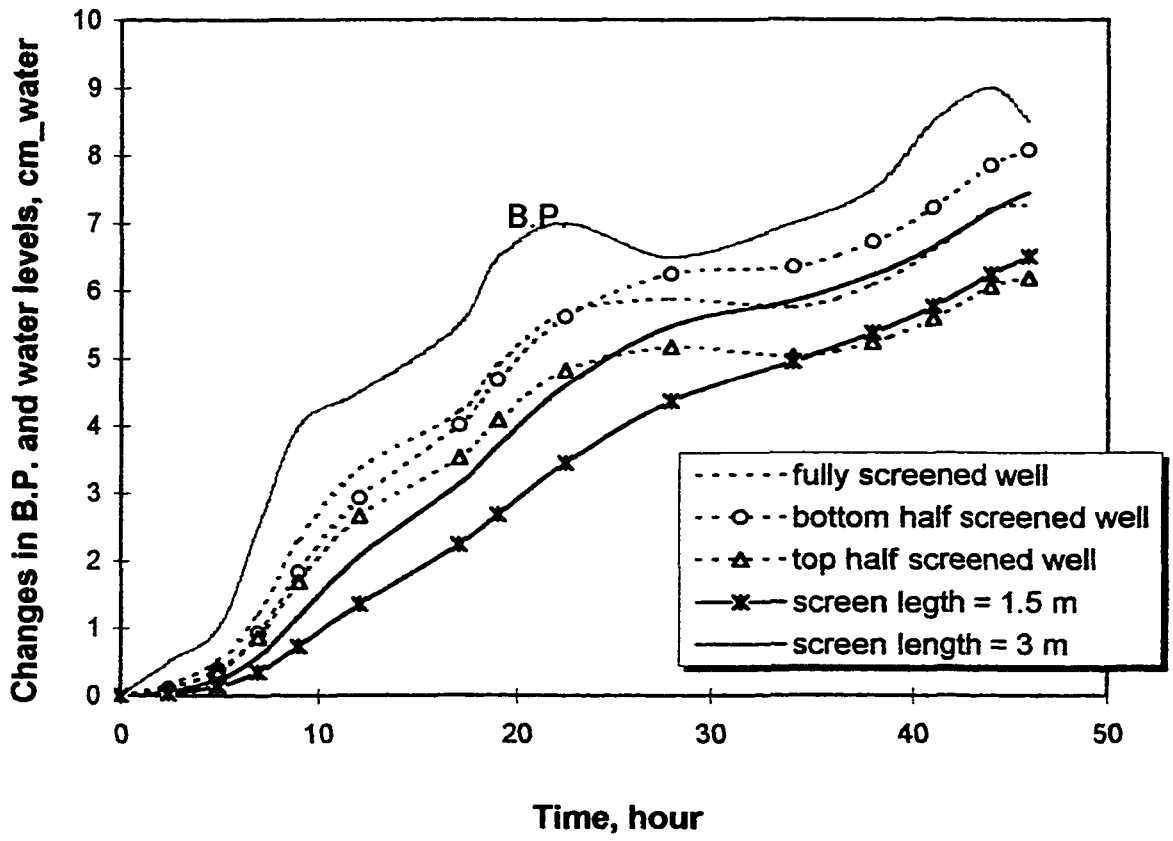


Figure 7.14. Effects of the screen length of a well on response of well to changes in barometric pressure (B.P.).

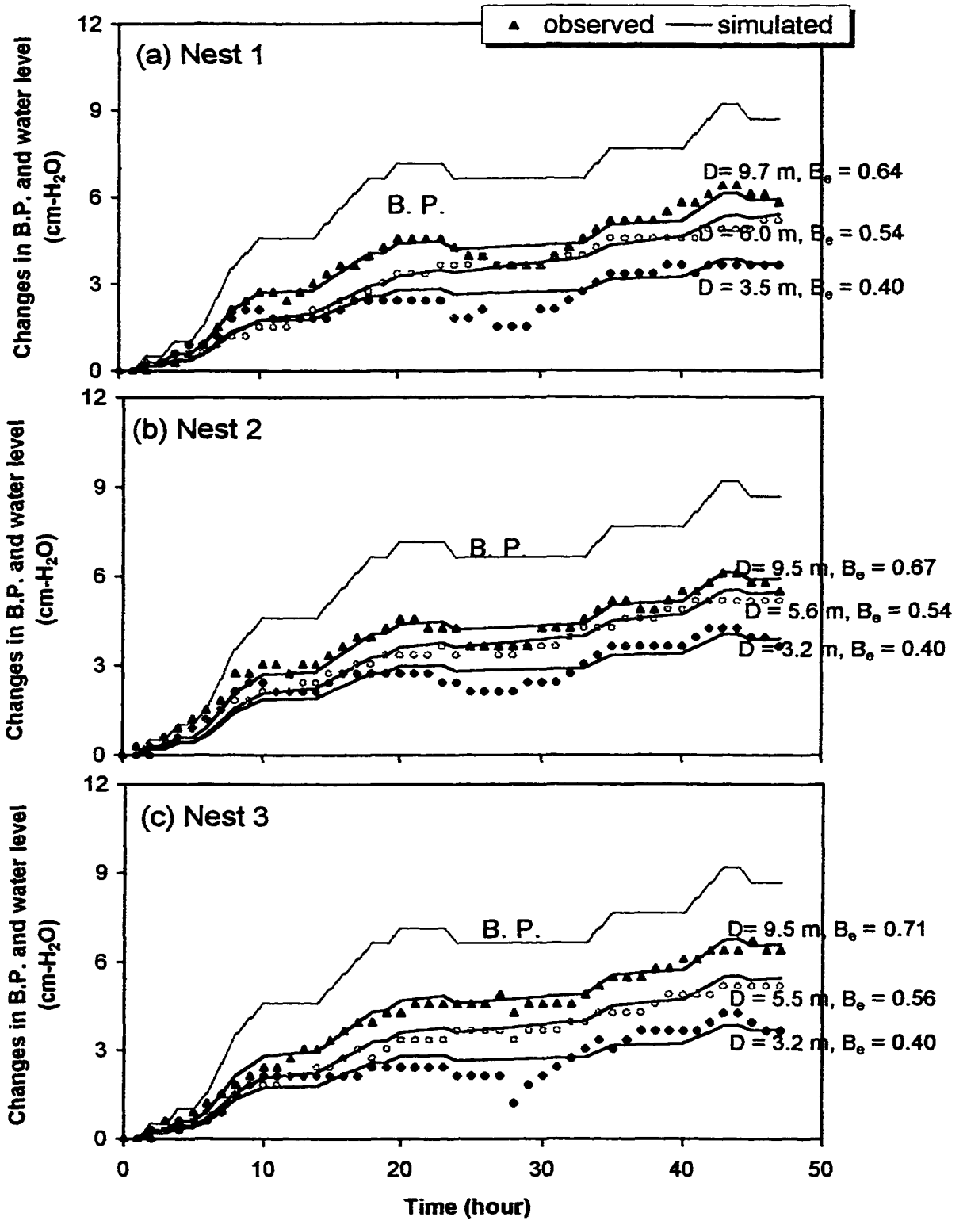


Figure 7.15. Observed and simulated water levels in wells due to changes in barometric pressure (B.P.) in Field Test 2.

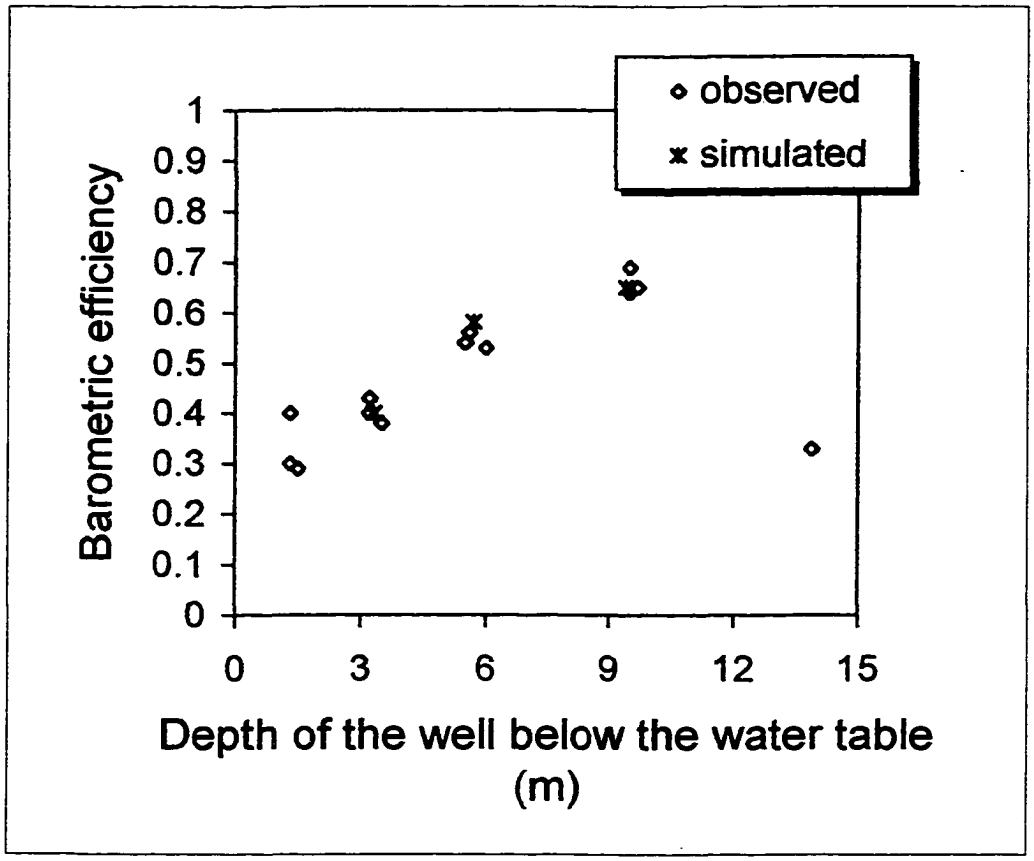


Figure 7.16. Barometric efficiency versus depth of well in Field Test 2.

simulated $B_e$ estimates. However, the screened length of N1D is greater than that of N1C and N1B. Thus, the differences in well responses between N1D and these two wells are partially due to the difference in their screen lengths. Table 7.2 contains a summary of barometric efficiency of each well and statistics for observed and simulated water levels in Field Test 2. Estimates of barometric efficiencies range from -0.29 to -0.69 and correlation coefficient between b.p. and observed water levels increases with the increasing depth of well below the water table. This trend is held consistently in all three well nests. Overall, results in Figure 7.15 and 7.16 indicate that the proposed physical model is effective in estimating the water level changes and also barometric efficiencies in wells due to the change in b.p.

In the inverse modeling for Field Test 2, the best curve fitting between observed and simulated water level data yields estimates of two hydraulic parameters: hydraulic conductivity and specific storage. Estimates of hydraulic conductivity and specific storage by the FEMBARO model are listed and compared with results from slug and pumping tests in the modeled wells (Table 7.2). Estimates by the model of b.p. effects and those by the conventional aquifer tests somewhat deviate from each other. Estimates of K by the model are about one order of magnitude less than the estimate by slug and pumping tests, whereas estimates of $S_s$ are greater than that of the pumping test by a factor of one order. Trading off between the values of two hydraulic parameters can be explained in two ways. One is the scale effect and the other is the effect of anisotrophy of the formation in a b.p. test. First, the b.p. test is believed to reflect the groundwater flow limited in the vicinity of the well because of the small range of b.p. fluctuations; the maximum b.p. is about 9.5 cm of water in Field Test 2. Thus, it tests a small scale of the formation to yield a relatively low hydraulic

Table 7.2. Estimates of $B_e$, K and $S_s$ by the FEMBARO model in Field Test 2 and comparison of values with those from other tests.

| well ID | Depth | sim. $B_e$ | obs. $B_e$ | Std. er. | $R^2$ | $K_{(FEMBARO)}$ | $K_{(Slug\ Test)}$ | $K_{(Pump\ Test)}$ | $S_{s\,(FEMBARO)}$ | $S_{s\,(Pump\ Test)}$ |
|---|---|---|---|---|---|---|---|---|---|---|
| N1B | 3.5 | -0.40 | -0.38 | 9.80E-03 | 0.84 | 4.17E-09 | 6.73E-07 | | 2.50E-05 | |
| N1C | 6.0 | -0.54 | -0.53 | 1.09E-02 | 0.91 | 3.33E-08 | 4.40E-07 | 1.20E-07 | 2.00E-05 | 2.90E-06 |
| N1D | 9.7 | -0.64 | -0.65 | 7.80E-03 | 0.97 | 1.00E-08 | 2.30E-07 | 4.30E-07 | 2.50E-05 | 3.40E-06 |
| N2B | 3.2 | -0.40 | -0.43 | 8.98E-03 | 0.88 | 4.17E-09 | 1.23E-06 | | 2.80E-05 | |
| N2C | 5.6 | -0.54 | -0.56 | 8.13E-03 | 0.94 | 2.78E-08 | 4.00E-07 | | 3.00E-05 | |
| N2D | 9.5 | -0.67 | -0.64 | 6.87E-03 | 0.97 | 1.00E-08 | 4.20E-07 | | 2.50E-05 | |
| N3B | 3.2 | -0.40 | -0.40 | 9.92E-03 | 0.86 | 4.17E-09 | 8.62E-07 | | 2.50E-05 | |
| N3C | 5.5 | -0.56 | -0.54 | 8.51E-03 | 0.94 | 3.33E-08 | 5.06E-07 | 2.80E-08 | 2.50E-05 | 5.30E-06 |
| N3D | 9.5 | -0.71 | -0.69 | 8.52E-03 | 0.96 | 2.22E-08 | 2.89E-07 | 3.10E-07 | 2.50E-05 | 1.20E-06 |
| Mean | | | | | | 1.66E-08 | 5.61E-07 | | 2.53E-05 | |
| Geo. Mean | | | | | | **1.23E-08** | **5.01E-07** | **1.45E-07** | **2.52E-05** | **2.81E-06** |

conductivity to those by other tests. Moreover, a locally high clay content or a well skin formed by smearing during installation in the vicinity of the well can also cause a low K and a high $S_s$ in the b.p. tests by reflecting the properties of a small scale of test material. Second, a pumping test mainly reflects the properties of radial flow, whereas a b.p. test does both radial and vertical components of hydraulic property in its estimation; lateral flow around the well and vertical flow form the water table by changes in b.p. are coupled for the water level fluctuation in the well as shown Figure 7.12. In glacial till units the vertical K was reported to be less than the radial K by one to three orders of magnitude (e.g. Seo, 1996). Thus, the existing low vertical K in the site of Field Test 2 is believed to be reflected in the parameter estimation by b.p. tests.

Additional analysis indicates that determination of $S_s$ in b.p. tests is credible (Figure 7.17). Well response simulated with the K and $S_s$ estimates by pumping tests do not tell the observed dynamic fluctuation of water levels (Figure 7.17 (a)). Lowering the K value helps a little to get a better fitting to observed levels, however, it does not give vivid fluctuation as observed in the well. The only way to get the observed fluctuation pattern is to increase the order of $S_s$. More detailed sensitivity analysis in a narrow range of $S_s$ in Figure 7.17 (b) indicates that a b.p. test is largely sensitive to $S_s$, as well as K.

### *7.8.3 Simulated Field Test 3*

Figure 7.18 presents the fit of simulated water levels in response to changes in b.p. to the observed data for a well in a sandy aquifer in Field Test 3. The results imply that the applied model, FEMBARO, is appropriate for describing the water level fluctuations due to changes in b.p. Because the top of the ground surface is covered by clay, the well RW-1, is the only

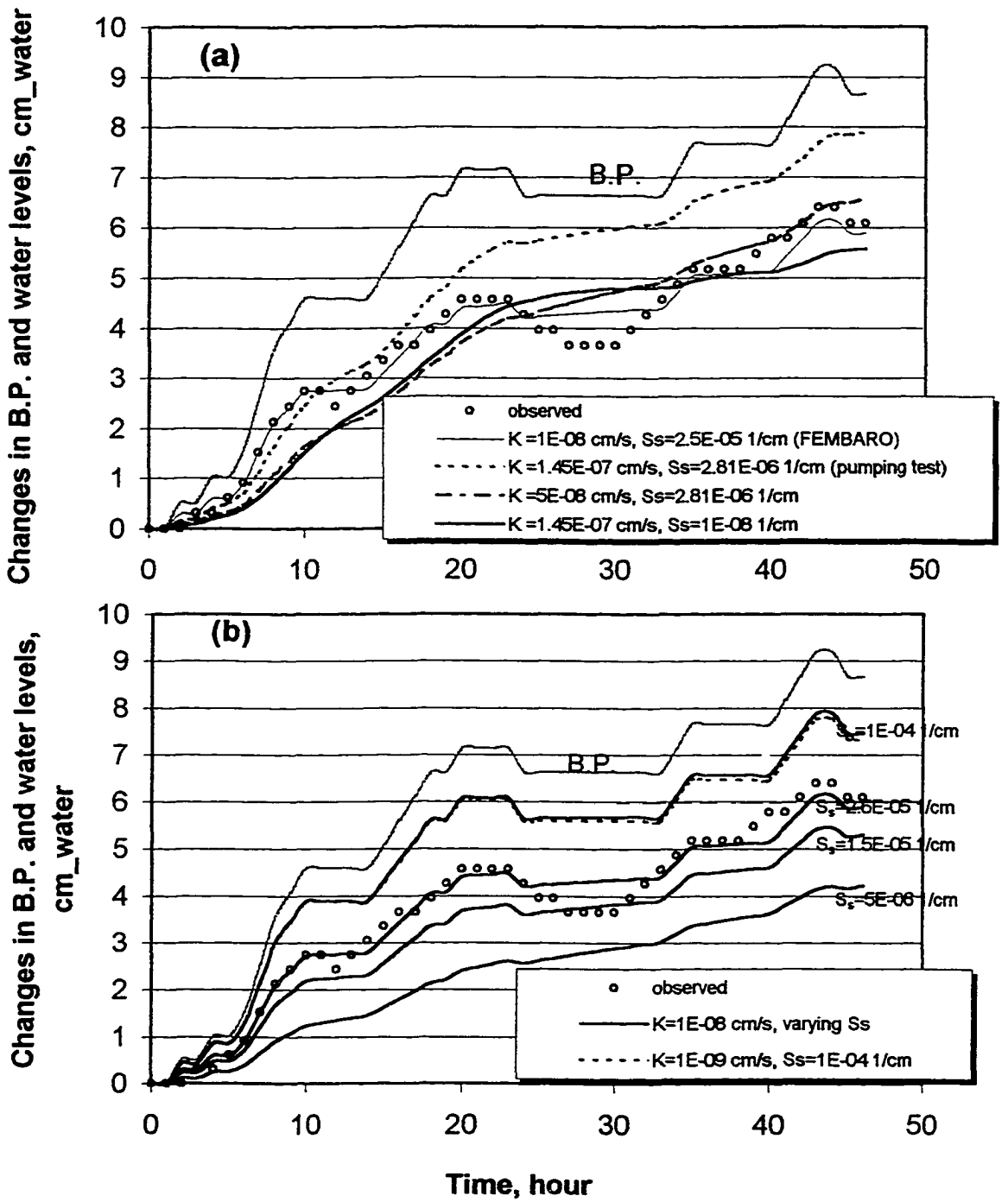


Figure 7.17. Sensitivity of barometric fluctuations of the water levels in wells to various hydrualuc conductivity (K) and specific storage (Ss) in Field Test 2 (a) use of estimates by pumping test and (b) effects of $S_s$ on fluctuation of water levls.

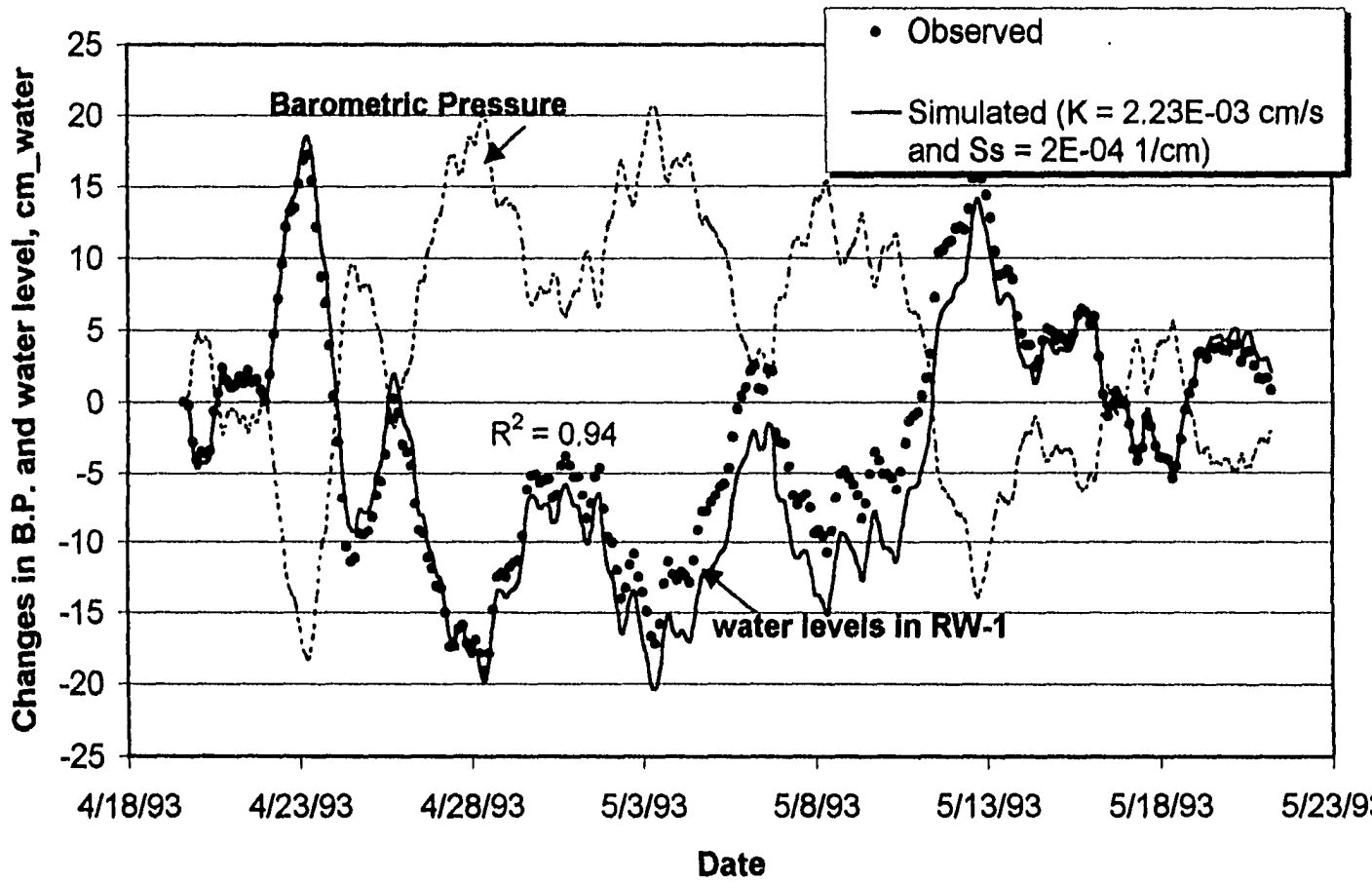


Figure 7.18. Oberved and simulated water levels in the well responding to changes in barometric pressure in Field Test 3.

route for b.p. to propagate into the subsurface regime. In other words, the water level data can be interpreted as a very dynamic well recovery curve in a series of slug/bail tests using changes in b.p. For the fit to observed data, the applied K and $S_s$ were 2.23E-03 cm/s and 0.0002 1/cm, where K is in the same order of magnitude as the known estimate by the slug tests on the well (Hare, 1998). The homogeneity of sand and no interference of the vertical flow in Field Test 3 yield the equivalent estimates in both b.p. and slug tests, reflecting only the properties of lateral flow in a large scale. Therefore, the result from Field Test 3 indicates that b.p. tests on a well within a very permeable containment system have a high potential to serve as an in-situ hydraulic test for parameter estimation.

## 7.9 Effect of Barometric Pressure on Well Recovery during Slug Tests

### *7.9.1 Theoretical Simulations*

Well recovery of a slug test can be disturbed by fluctuations in b.p. (Figure 7.19). A longer response time of a slug test in a lower permeable unit gives more time for the recovery curve to be disturbed by b.p., especially at a later time in the recovery, where it is approaching equilibrium (Figure 7.19 (a)). At a given K value, the degree of disturbance is in proportion to $S_s$ of the formation (Figure 7.19 (b)). The disturbance of well recovery by b.p. is mitigated by increasing the well casing radius, although it increases the duration of recovery (Figure 7.20 (a)). Moreover, the length of water-slug significantly affects the degree of disturbance of well recovery (Figure 7.20 (b)). As the slug length gets longer, the less the well recovery is affected by changes in b.p. The depth of well also affects the well response to b.p. during slug tests (Figure 7.21). The basic concept behind the results in Figure 7.21 is not

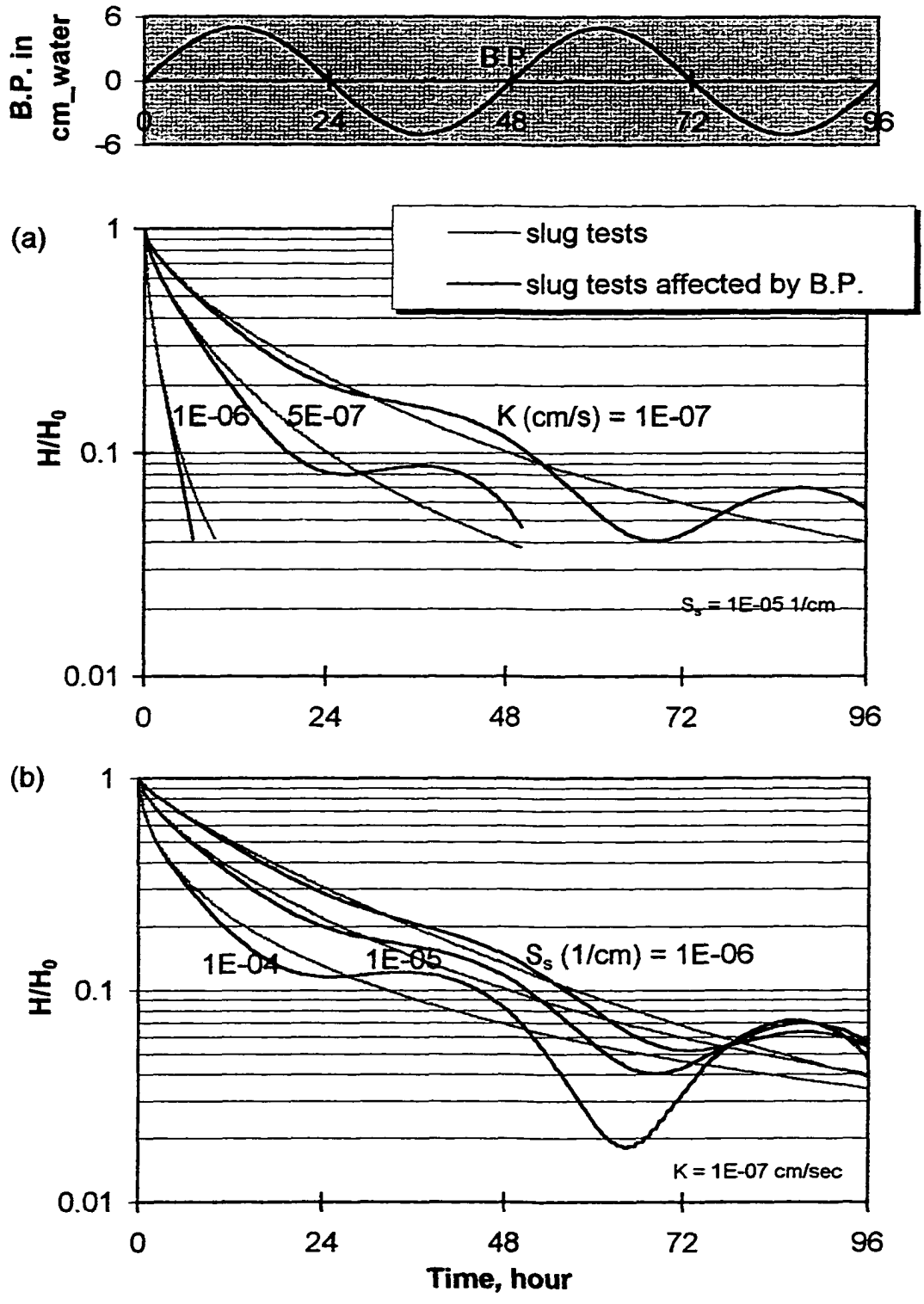


Figure 7.19. Effects of barometric pressure (B.P.) on the well recovery in slug tests at different (a) hydraulic conductivities (K) and (b) specific storages ($S_s$).

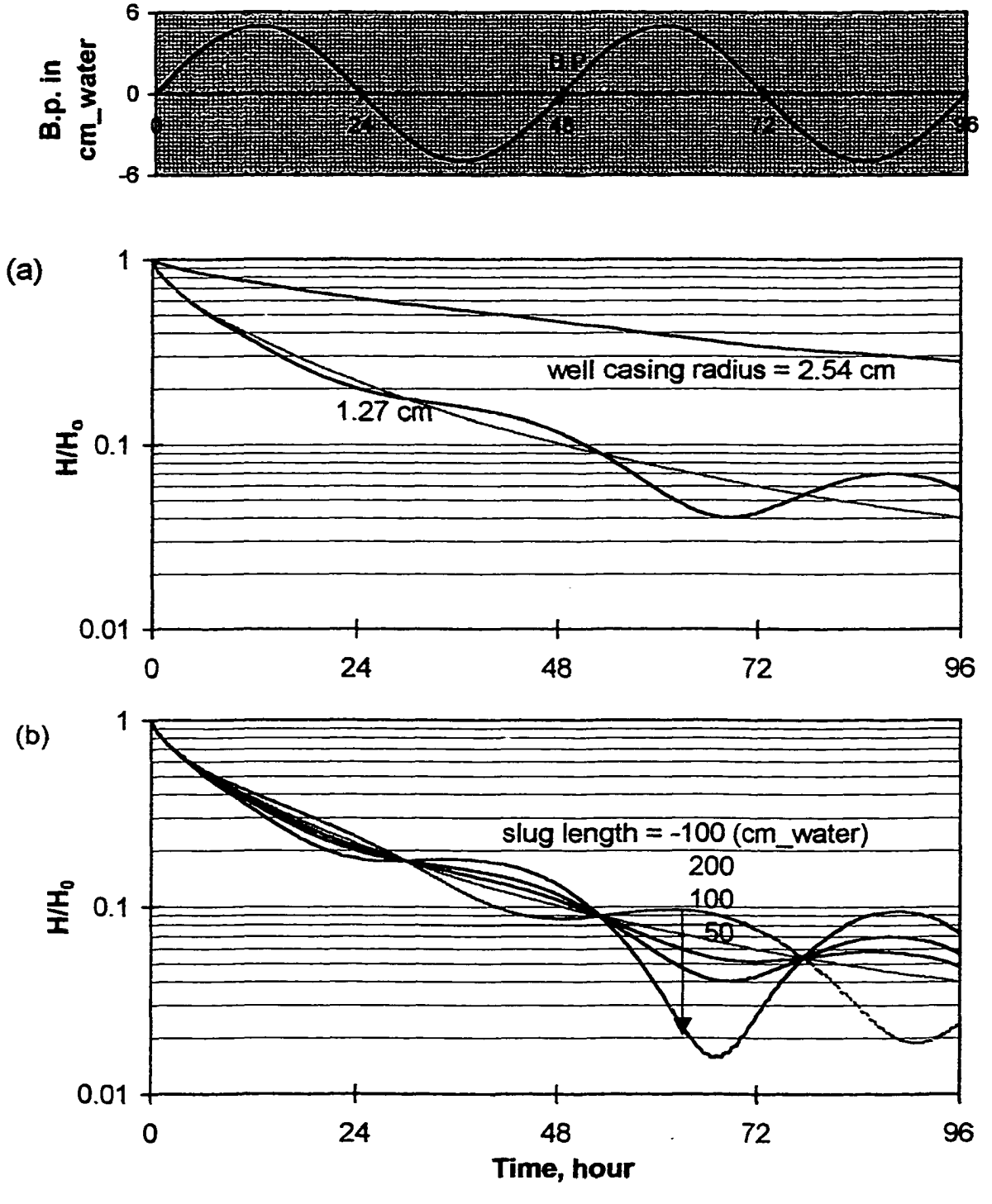


Figure 7.20. Well recovery curves in slug tests affected by changes in barometric pressure (B.P.) at different (a) well casing radii and (b) lengths of water slug.

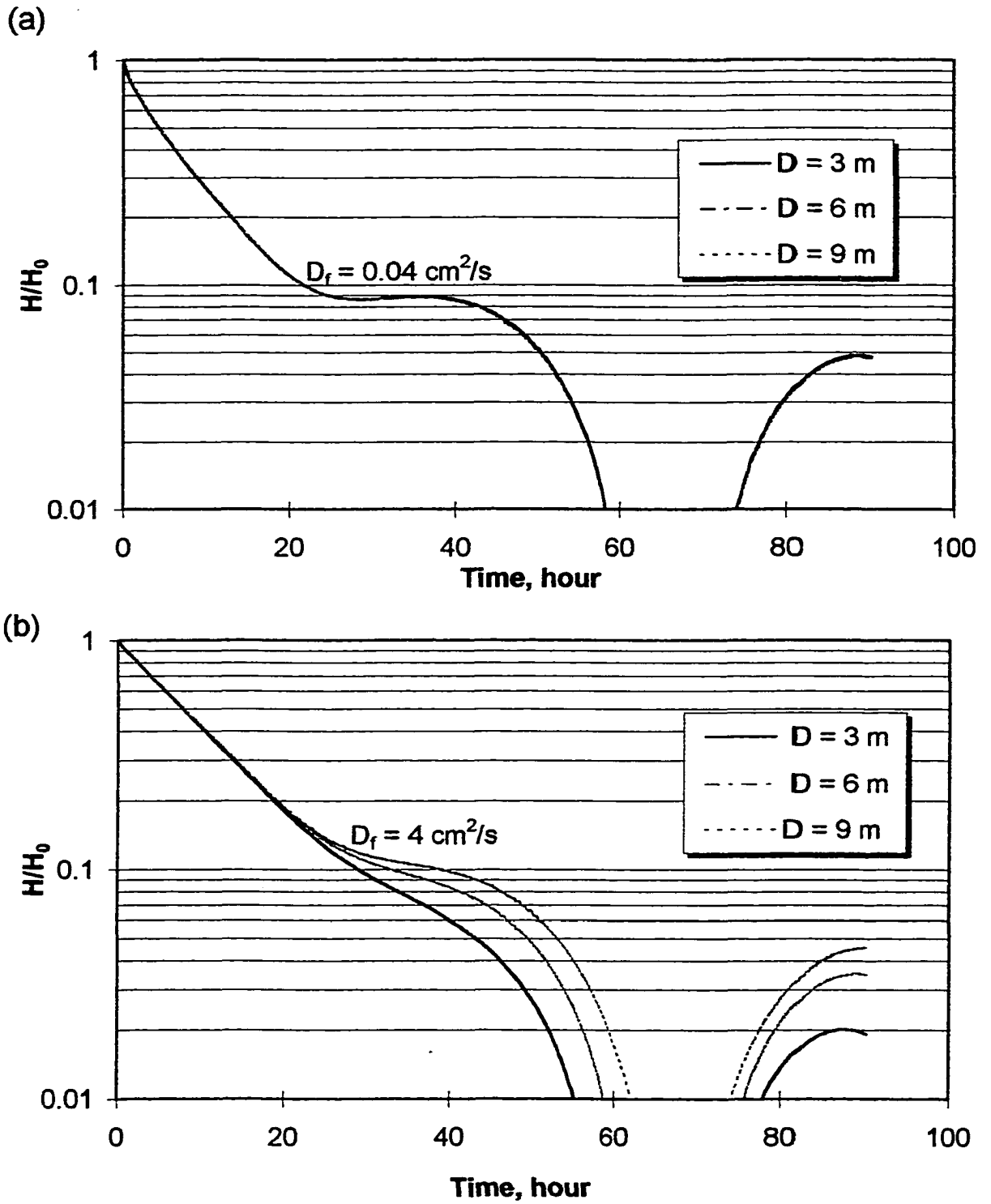


Figure 7.20. Well recovery curves affected by barometric pressure at different depths of wells (D) and hydraulic diffusivities ($D_f$): (a) $D_f = 0.04$ cm$^2$/s and (b) $D_f = 4$ cm$^2$/s.

different from those in cases in static water levels; effects of well depth in barometric fluctuations of water level is more pronounced in material of a higher hydraulic diffusivity.

As usual, the later part of the recovery data is discarded or even not collected in slug tests. For the scattered data during the later part of recovery, the average line is routinely taken in slug test analysis. A popular analytical tool, Bouwer and Rice method (Jones, 1993), was applied for estimation of K in the paired cases in Figure 7.19 and 7.20; one is the undisturbed recovery curve and the other is disturbed by b.p. The averaged percent error in K estimates between the two cases is less than two percent, which is negligible for practical purposes. Thus, in terms of final hydraulic parameter estimation in slug test analysis, it is doubtful that estimates of K would be affected by variations of b.p, even when the influence of b.p. on the recovery curve is not corrected.

### *7.9.2 Simulated Field Test 4*

In Figure 7.22, the simulated and the observed water level data in Field Test 4 were fitted along with the estimated hydraulic parameters. Comparison between simulated lines with and without correction of discharge effects (solid and dashed lines, respectively) signifies how discharge of water from the water table affects water level fluctuation in association with b.p. effects. The simulated curve without the applied discharge on the water table does not tell the declining trend of water level although it shows the mirror image of b.p. fluctuation. In the simulation for the best curve fitting to the observed data, increasing discharge rates over time is probably due to enhanced evapotranspiration during plant growing season. Hydraulic parameters estimated by the model are K = 1.0E-07 cm/s and $S_s$ = 2E-03 1/cm, whereas K = 9.6E-07 cm/s by slug tests analysis on the well (Hvsorev (1951) method was applied).

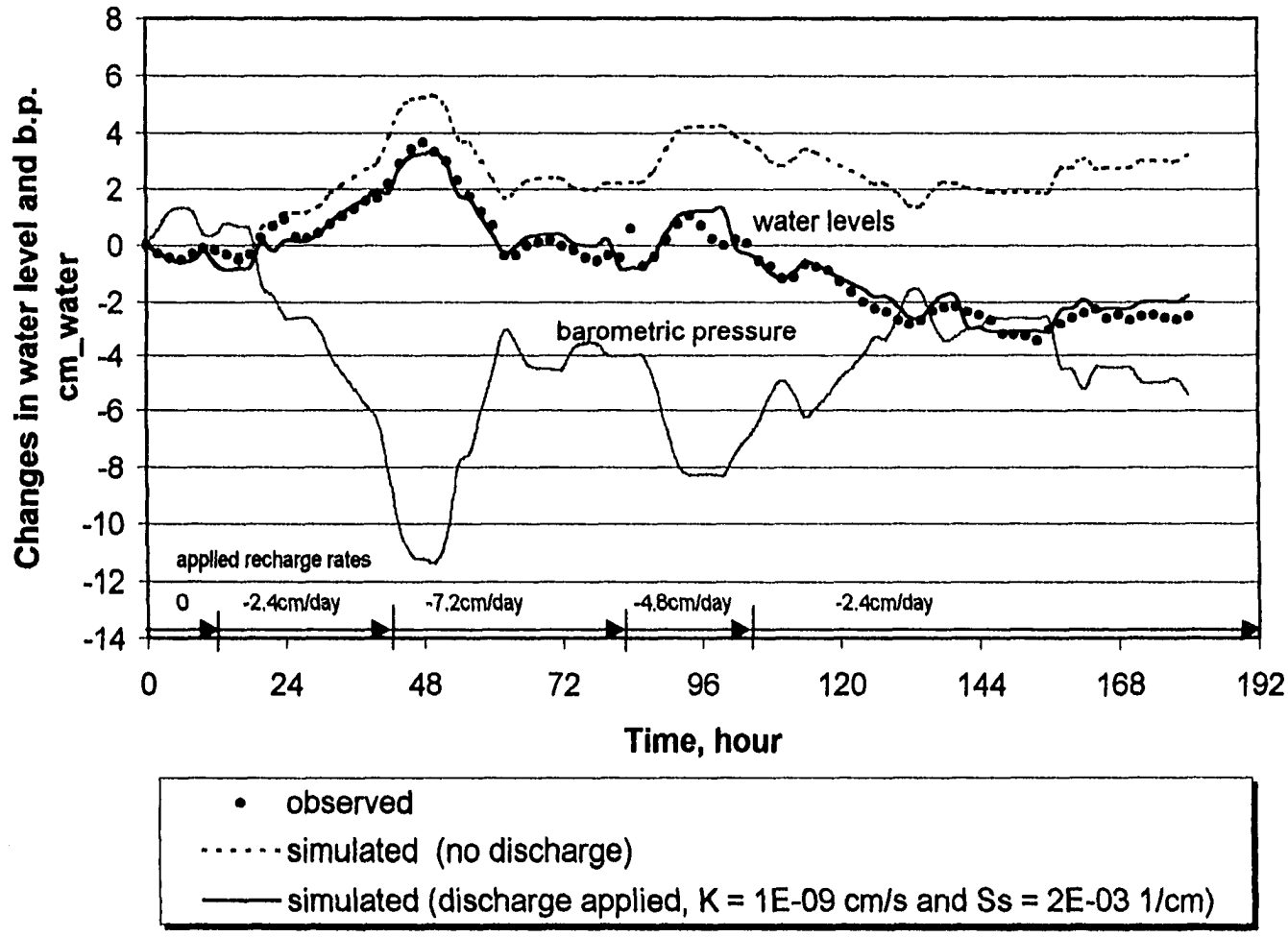


Figure 7.22. Oberved and simulated water levels in the well responding to changes in barometric pressure in Field Test 4.

In Hvsorev slug test analysis, $S_s$ is assumed to be zero but not in b.p. tests in this study. It is well known that K can be overestimated, neglecting storage factors in slug test analysis (Chirlin, 1989; Butler et al, 1990, and Demir and Narashmhan, 1994). Estimation of both K and $S_s$ is an advantage of b.p. test analysis and may explain some of the deviation of K from the estimate by slug tests. Disturbance in the final equilibrium of the well recovery in a slug test at the same well was simulated by the model (Figure 7.23). B.p. influences the water level in the well under recovery in the same way as in the static water level case; increase in b.p. leads to a decrease in water level and vice versa. However, the disturbance is quite limited to the final equilibrium of the test.

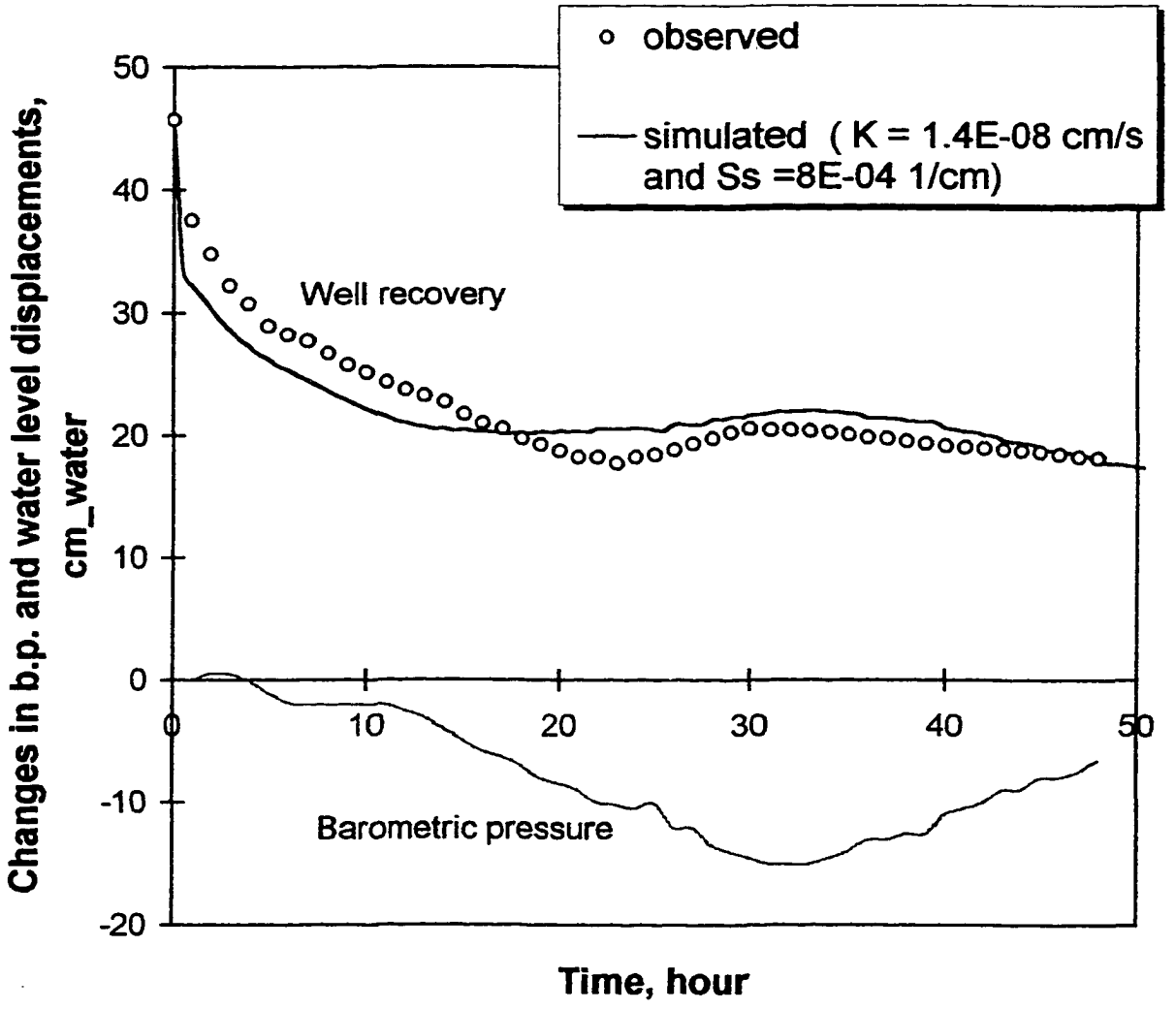


Figure 7.23. Well recovery in a slug test influenced by changes in barometric pressure in Field Test 4.

# CHAPTER 8. CONCLUSIONS

## 8.1 Summary

Naturally, barometric pressure continuously changes in the atmosphere, and groundwater within the saturated porous media of the subsurface responds to that change, which may be reflected by water level changes in wells. A physically based conceptual model for the influence of changes in b.p. on groundwater level in wells was developed and tested. Both barometric pressure and a well are essential parts in the model structure, as well as the governing theories (Darcy's law and conservation of mass) for groundwater flow in saturated porous media. The important relationship adopted in the model is that the total hydraulic head in the well is not equal to the water level, but is the sum of the water level and barometric pressure. Adopting the traditional differential equation and the related well physics as a boundary condition for groundwater flow influenced by changes in b.p. was validated through theoretical analysis and four actual field studies. Simulations by the proposed model require accurate mathematical definitions of the well and hydraulic properties of the porous medium. Due to the unknown hydraulic properties of the tested formation in some actual field situations, the suggested model can be solved inversely using measured well water level and b.p. data to obtain estimates of hydraulic parameters. Using the benefit of the similarity and the relation between b.p. effects and slug tests on a well, a new slug test model is also developed and its applicability for superposition in slug tests are demonstrated. The results from the applications of the models indicate that:

- Groundwater flow and consequent water level fluctuations in a well induced by b.p. variations can be analyzed by means of a two-dimensional and unsteady flow model, with the well itself as an incorporated boundary condition.
- Based on the principle of superposition, the effect of b.p. on a well is, in a numerical sense, equivalent to a series of slug/bail tests with simultaneous exertion of b.p. on the water table.
- In the case of no well within the porous medium, the effect of b.p. changes on head values at different depths exhibits the opposite sign and trend to that on the water level changes in the case of having a well. These results imply that the well itself has a significant role in controlling the b.p. effect on water level variations. The observed data from wells and buried pressure transducers within porous media at different depths clearly support the theoretical results.
- As the depth of well increases, the corresponding water level change increases proportionally as they reflect changes in b.p. In other words, barometric efficiency improves with the depth of well.
- At a given depth and geometry of a well, the magnitude of water level fluctuations due to changes in b.p. is greater when the surrounding porous medium is more 'conductible' (a higher hydraulic conductivity) and has more 'storage' (a higher specific storage).
- The simple linear model without adjustment of time lagging leads to erroneous estimates of $B_e$.

- In the long term, natural recharge and discharge on the water table gradually affects water levels in addition to barometrical water level variations. During an early spring, heavy rainfall, and summer growing seasons, the correlation between b.p. and groundwater pore pressure is low, whereas the correlation is maximized in November to January for the research site of this study.
- The changes in b.p. and responding water level data can serve as an in-situ hydraulic test for evaluation of hydraulic parameters such as hydraulic conductivity and specific storage. Estimation of specific storage of the formation is a benefit of the b.p. tests. However, the two estimates reflect the properties on a small scale of the tested formation, relative to those by slug and pumping tests.
- B.p. effects are not limited only to the wells in a confined condition. If a well is screened at a level below the water table in an unconfined condition of low permeability units, the water level behaves like that of a confined. The man-made environment for a well, a clay cap in a containment system, maximizes the well response in an unconfined condition to changes in b.p. by preventing the diffusion of b.p. from the ground surface.
- The final equilibrium of the well recovery of a slug test in a low permeability unit has only a slight chance to be affected by changes in b.p. However, estimates of K are not significantly biased by b.p. fluctuations because the later response data are usually ignored. Moreover, averaging over the disturbed portion eliminates the possibility for slug test analysis to be affected by b.p. On a practical basis, an increase in the slug

length is the best way to mitigate the possible interference of b.p. variations with well recovery during slug tests.

**8.2 Final Remarks**

In this study, the importance of varying b.p. in terms of a groundwater well, was pointed out by including both b.p. and a well as possible sources of pore pressure changes in a groundwater flow model. In conclusion, the proposed physical model is effective in describing the water level fluctuation in a well responding to changes in b.p. The model has advantages for obtaining estimated values of differences in water levels in the well, well fluxes, and hydraulic heads in the formation, specifically, responding to changes in b.p. Findings in this study, to some extent, contradicts the concepts in the classical previous works; barometric efficiencies of wells vary a great deal, depending not only on the elastic properties of the formation, but also on the transmissible property, the well casing radius, the screened length, and the depth of the well. This means that the well itself is responsible for water level fluctuation, which usually mirrors the image of varying b.p. The observed various responses of groundwater condition to b.p. fluctuations in wells and in porous media at different field situations were appropriately explained by applying the model. Overall, the influence of b.p. on wells should not be ignored for correct cognition of groundwater level in wells.

# APPENDIX A: GOVERING EQUATION FOR 2-D UNSTEADY GROUNDWATER FLOW AND ITS SOLUTION BY GLERKIN METHOD

**1. Governing equation for two dimensional, unsteady state, radial-vertical flow**

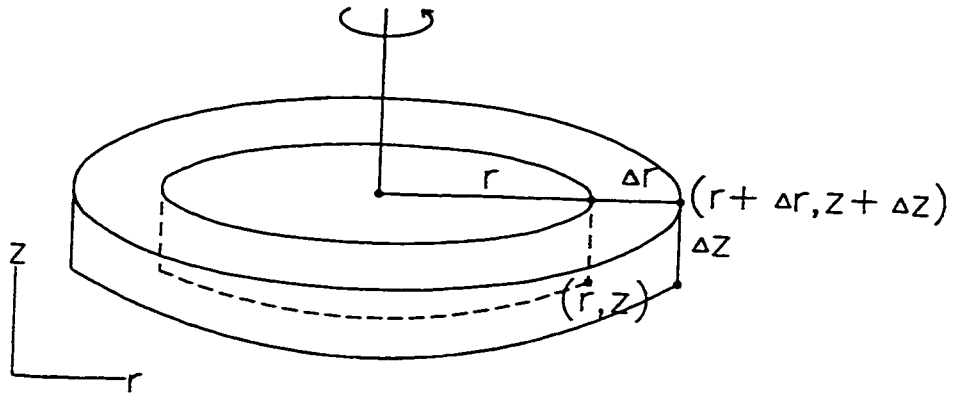


1) Change in storage during Δt within the volume of $2\pi r\Delta r\Delta z$:

$$S_0 \times 2\pi r\Delta r\Delta z \times [\Phi(t+\Delta t)-\Phi(t)] \tag{1}$$

2) Inflow - Outflow for radial component during Δt within depth of Δz:

$$[q(r)\times 2\pi r\Delta z - q(r+\Delta r)\times 2\pi(r+\Delta r)\Delta z]\times \Delta t \cong [q(r)-q(r+\Delta r)]\times 2\pi r\Delta z\Delta t \tag{2}$$

3) Inflow - Outflow for vertical component during Δt within width of Δr:

$$[q(z)-q(z+\Delta z)]\times 2\pi r\Delta r\Delta t \tag{3}$$

$\therefore$ Eq. (2) + Eq. (3) = Eq. (1)

4) Inflow - Outflow = Change in storage

$$\Rightarrow [[q(r)-q(r+\Delta r)]\times 2\pi r\Delta z\Delta t + [q(z)-q(z+\Delta z)]\times 2\pi r\Delta r\Delta t]$$

$$= S_0 \times 2\pi r\Delta r\Delta z \times [\Phi(t+\Delta t)-\Phi(t)] \tag{4}$$

divided by (Δt·Δz·Δr)

$$2\pi r\frac{q(r)-q(r+\Delta r)}{\Delta r} + 2\pi r\frac{q(z)-q(z+\Delta z)}{\Delta z} = S_0 \times 2\pi r \times \frac{\Phi(t+\Delta t)-\Phi(t)}{\Delta t} \tag{5}$$

$$-\frac{\partial q(r)}{\partial r} - 2\pi r\frac{\partial q(z)}{\partial z} = S_0 2\pi r\frac{\partial \Phi}{\partial t} \tag{6}$$

$$q(r) = -K_r 2\pi r\frac{\partial \Phi}{\partial r} \quad \text{and} \quad q(z) = -K_z\frac{\partial \Phi}{\partial z}$$

$$\Rightarrow \frac{\partial}{\partial r}\left(K_r 2\pi r\frac{\partial \Phi}{\partial r}\right) + 2\pi r\frac{\partial}{\partial z}\left(K_z\frac{\partial \Phi}{\partial z}\right) = S_0 2\pi r\frac{\partial \Phi}{\partial t} \tag{7}$$

Thus the governing equation is followed as

$$\frac{1}{r}\frac{\partial}{\partial r}(K_r r\frac{\partial \Phi}{\partial r})+\frac{\partial}{\partial z}\left(K_z\frac{\partial \Phi}{\partial z}\right)=S_0\frac{\partial \Phi}{\partial t} \quad (8)$$

$$\frac{1}{r}\frac{\partial}{\partial r}(K_r r\frac{\partial \Phi}{\partial r})+\frac{\partial}{\partial z}\left(K_z\frac{\partial \Phi}{\partial z}\right)-S_0\frac{\partial \Phi}{\partial t}=0 \quad (9)$$

where (r, z) = radial and vertical location

t = time

$K_r$ = horizontal hydraulic conductivity

$K_z$ = vertical hydraulic conductivity

$S_0$ = storativity

$\Phi$ = hydraulic head.

**2. The elements**

For the Galerkin finite element method, the simplest element, the triangle, is used. A linear triangular element is defined by three nodes (i, j, k), which are labeled in a counter-clockwise direction.

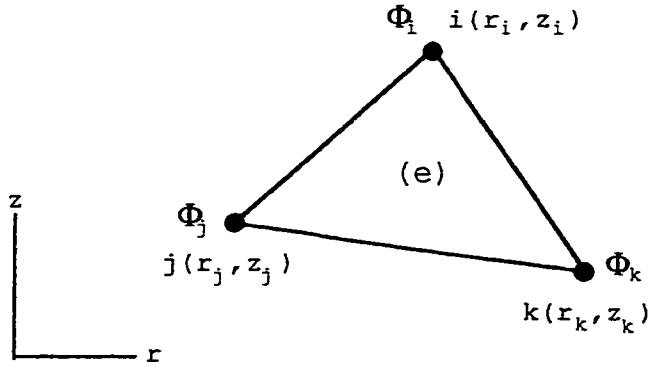


The head is interpolated linearly over the element, depending on the head values at the nodes.

$$\Phi(r, z) = N_i(r,z)\,\Phi_i + N_j(r,z)\,\Phi_j + N_k(r,z)\,\Phi_k \quad (10)$$

where $N_i$, $N_j$, $N_k$ are basis functions

$$N_i(r,z) = 1/2A^e \times [(r_j z_k - r_k z_j) + (z_j - z_k)r + (r_k - r_j)z] \quad (11)$$

$$N_j(r,z) = 1/2A^e \times [(r_k z_i - r_i z_k) + (z_k - z_i)r + (r_i - r_k)z] \quad (12)$$

$$N_k(r,z) = 1/2A^e \times [(r_iz_j - r_jz_i) + (z_i - z_j)r + (r_j - r_i)z] \quad (13)$$

$A^e$ is the area of the element,

$$2A^e = (r_iz_j - r_jz_i) + (r_kz_i - r_iz_k) + (r_jz_k - r_kz_j) \quad (14)$$

At the node locations, the value of the basis function for that node is equal to 1 and it is equal to 0 at the other nodes.

$$N_i(r_i, z_i) = 1,\ N_i(r_j, z_j) = 0,\ N_i(r_k, z_k) = 0$$

$$N_j(r_i, z_i) = 0,\ N_j(r_j, z_j) = 1,\ N_j(r_k, z_k) = 0$$

$$N_k(r_i, z_i) = 0,\ N_k(r_j, z_j) = 0,\ N_k(r_k, z_k) = 1$$

**3. The Galerkin's finite element method**

Application of the weighted residual method to the governing equation (9) produces n equations in the form of:

$$\iint_{A^e} w_i \left[ \frac{1}{r}\frac{\partial}{\partial r}\left( K_r r \frac{\partial \Phi}{\partial r} \right) + \frac{\partial}{\partial z}\left( K_z \frac{\partial \Phi}{\partial z} \right) - S_0 \frac{\partial \Phi}{\partial z} \right] 2\pi r dr dz = 0 \qquad i = 1, 2, 3, \ldots\ldots n$$

(15)

where $W_i$: the weighting function for node i

$W_i = N_i$ in the Galerkin method

$\Phi$: the approximation given by the Eq. (10)

$$\Phi(r, z) = N_1\Phi_1 + N_2\Phi_2 + \ldots\ldots + N_n\Phi_n \quad (16)$$

**4. The element equation in a matrix form**

For an arbitrary element, each node has the three element equations using the Galerkin method.

$$\iint_{A^e} N_i \left[ \frac{1}{r}\frac{\partial}{\partial r}\left( K_r r \frac{\partial \Phi}{\partial r} \right) + \frac{\partial}{\partial z}\left( K_z \frac{\partial \Phi}{\partial z} \right) - S_0 \frac{\partial \Phi}{\partial z} \right] 2\pi r dr dz = 0 \quad (17)$$

$$\iint_{A^e} N_j \left[ \frac{1}{r}\frac{\partial}{\partial r}\left( K_r r \frac{\partial \Phi}{\partial r} \right) + \frac{\partial}{\partial z}\left( K_z \frac{\partial \Phi}{\partial z} \right) - S_0 \frac{\partial \Phi}{\partial z} \right] 2\pi r dr dz = 0 \quad (18)$$

$$\iint_{A^e} N_k \left[ \frac{1}{r}\frac{\partial}{\partial r}\left( K_r r \frac{\partial \Phi}{\partial r} \right) + \frac{\partial}{\partial z}\left( K_z \frac{\partial \Phi}{\partial z} \right) - S_0 \frac{\partial \Phi}{\partial z} \right] 2\pi r dr dz = 0 \tag{19}$$

$$\rightarrow \quad \iint_{A^e} N_i \left[ \frac{\partial}{\partial r}\left( K_r 2\pi r \frac{\partial \Phi}{\partial r} \right) + 2\pi r \frac{\partial}{\partial z}\left( K_z \frac{\partial \Phi}{\partial z} \right) - S_0 2\pi r \frac{\partial \Phi}{\partial z} \right] dr dz = 0 \tag{20}$$

$$\iint_{A^e} N_j \left[ \frac{\partial}{\partial r}\left( K_r 2\pi r \frac{\partial \Phi}{\partial r} \right) + 2\pi r \frac{\partial}{\partial z}\left( K_z \frac{\partial \Phi}{\partial z} \right) - S_0 2\pi r \frac{\partial \Phi}{\partial z} \right] dr dz = 0 \tag{21}$$

$$\iint_{A^e} N_k \left[ \frac{\partial}{\partial r}\left( K_r 2\pi r \frac{\partial \Phi}{\partial r} \right) + 2\pi r \frac{\partial}{\partial z}\left( K_z \frac{\partial \Phi}{\partial z} \right) - S_0 2\pi r \frac{\partial \Phi}{\partial z} \right] dr dz = 0 \tag{22}$$

For Eq. (20)

$$\iint_{A^e} N_i \frac{\partial}{\partial r}\left( K_r 2\pi r \frac{\partial \Phi}{\partial r} \right) dr dz + \iint_{A^e} N_i 2\pi r \frac{\partial}{\partial z}\left( K_z \frac{\partial \Phi}{\partial z} \right) dr dz + \iint_{A^e} N_i S_0 2\pi r \left( \frac{\partial \Phi}{\partial t} \right) dr dz = 0$$

.....(23)

By the Gauss-Green theorem

$$\int_A \beta \frac{\partial p_r}{\partial r} dA = \int_C \beta P_r n_r \, dC - \int_A \frac{\partial \beta}{\partial r} P_r \, dA \quad (24) \qquad \int_A \beta \frac{\partial p_z}{\partial z} dA = \int_C \beta P_z n_z \, dC - \int_A \frac{\partial \beta}{\partial z} P_z \, dA \quad (25)$$

Letting $\beta = N_i, P_r = K_r 2\pi r \frac{\partial \Phi}{\partial r}$ *and* $\beta = N_i, P_z = 2\pi r \frac{\partial}{\partial z}(K_z \frac{\partial \Phi}{\partial z})$

Eq. (23) turns into

$$\rightarrow \quad \int_C N_i \left( K_r 2\pi r \frac{\partial \Phi}{\partial r} \right) n_r dC - \int_A \frac{\partial N_i}{\partial r} \left( K_r 2\pi r \frac{\partial \Phi}{\partial r} \right) dA$$

$$+ \int_C N_i \left( K_z 2\pi r \frac{\partial \Phi}{\partial z} \right) n_z dC - \int_A \frac{\partial N_i}{\partial z} \left( K_z 2\pi r \frac{\partial \Phi}{\partial z} \right) dA$$

$$- \iint_{A^e} N_i S_0 2\pi r \left[ N_i \frac{\partial \Phi_i}{\partial t} + N_j \frac{\partial \Phi_j}{\partial t} + N_k \frac{\partial \Phi_k}{\partial t} \right] dA = 0 \tag{26}$$

where C is the boundary of the element

The boundary integrals in Eq. (26) can be combined into one as following:

$$\int_C N_i\left(K_r 2\pi r\frac{\partial\Phi}{\partial r}\right)n_r dC+\int_C N_i\left(K_z 2\pi r\frac{\partial\Phi}{\partial z}\right)n_z dC=\int_C N_i q_n dC \tag{27}$$

where $q_n$ is the flow normal to the boundary

Same procedures are applied to Eq. (21) and Eq. (22) and thus Eqs. (20) ~ (22) turn into

$$\int_{C^e} N_i q_n dC=\int_{A^e}\frac{\partial N_i}{\partial r}\left(K_r 2\pi r\frac{\partial\Phi}{\partial r}\right)dA+\int_{A^e}\frac{\partial N_i}{\partial z}\left(K_z 2\pi r\frac{\partial\Phi}{\partial z}\right)dA$$
$$+\iint_{A^e} N_i S_0 2\pi r\left[N_i\frac{\partial\Phi_i}{\partial t}+N_j\frac{\partial\Phi_j}{\partial t}+N_k\frac{\partial\Phi_k}{\partial t}\right]dA \tag{28}$$

$$\int_{C^e} N_j q_n dC=\int_{A^e}\frac{\partial N_j}{\partial r}\left(K_r 2\pi r\frac{\partial\Phi}{\partial r}\right)dA+\int_{A^e}\frac{\partial N_j}{\partial z}\left(K_z 2\pi r\frac{\partial\Phi}{\partial z}\right)dA$$
$$+\iint_{A^e} N_j S_0 2\pi r\left[N_i\frac{\partial\Phi_i}{\partial t}+N_j\frac{\partial\Phi_j}{\partial t}+N_k\frac{\partial\Phi_k}{\partial t}\right]dA \tag{29}$$

$$\int_{C^e} N_k q_n dC=\int_{A^e}\frac{\partial N_k}{\partial r}\left(K_r 2\pi r\frac{\partial\Phi}{\partial r}\right)dA+\int_{A^e}\frac{\partial N_k}{\partial z}\left(K_z 2\pi r\frac{\partial\Phi}{\partial z}\right)dA$$
$$+\iint_{A^e} N_k S_0 2\pi r\left[N_i\frac{\partial\Phi_i}{\partial t}+N_j\frac{\partial\Phi_j}{\partial t}+N_k\frac{\partial\Phi_k}{\partial t}\right]dA \tag{30}$$

For the first term in right side of the equation (28), using the following relationships

$$\frac{\partial N_i}{\partial r}=\frac{\partial}{\partial r}\left\{\frac{1}{2A^e}\left[\left(r_j z_k-r_k z_j\right)+\left(z_j-z_k\right)r+\left(r_k-r_j\right)z\right]\right\}=\frac{\left(z_j-z_k\right)}{2A^e}=\frac{a_r}{2A^e} \tag{31}$$

$$\frac{\partial N_j}{\partial r}=\frac{\partial}{\partial r}\left\{\frac{1}{2A^e}\left[\left(r_k z_i-r_i z_k\right)+\left(z_k-z_i\right)r+\left(r_i-r_k\right)z\right]\right\}=\frac{\left(z_k-z_i\right)}{2A^e}=\frac{b_r}{2A^e} \tag{32}$$

$$\frac{\partial N_k}{\partial r}=\frac{\partial}{\partial r}\left\{\frac{1}{2A^e}\left[\left(r_i z_j-r_j z_i\right)+\left(z_i-z_j\right)r+\left(r_j-r_i\right)z\right]\right\}=\frac{\left(z_i-z_j\right)}{2A^e}=\frac{c_r}{2A^e} \tag{33}$$

$$\frac{\partial\Phi}{\partial r}=\frac{\partial}{\partial r}\left(N_i\Phi_i+N_j\Phi_j+N_k\Phi_k\right)=\Phi_i\frac{\partial N_i}{\partial r}+\Phi_j\frac{\partial N_j}{\partial r}+\Phi_k\frac{\partial N_k}{\partial r} \tag{34}$$

where $\Phi_i$, $\Phi_j$, and $\Phi_k$ are independent of r and z

$$r=r_i N_i+r_j N_j+r_k N_k \tag{35}$$

and $N_i$, $N_j$, $N_k = f(r, z)$

Integration of the first term is followed:

$$\rightarrow \quad \int_{A^e} \frac{\partial N_i}{\partial r}\left(K_r 2\pi r \frac{\partial \Phi}{\partial r}\right) dA = \int_{A^e} \frac{\partial N_i}{\partial r} K_r 2\pi r [\Phi_i \frac{\partial N_i}{\partial r} + \Phi_j \frac{\partial N_j}{\partial r} + \Phi_k \frac{\partial N_k}{\partial r}] dr dz$$

$$= \int_{A^e} \frac{\partial N_i}{\partial r} K_r 2\pi \left(r_i N_i + r_j N_j + r_k N_k\right) [\Phi_i \frac{\partial N_i}{\partial r} + \Phi_j \frac{\partial N_j}{\partial r} + \Phi_k \frac{\partial N_k}{\partial r}] dr dz$$

$$= \frac{\partial N_i}{\partial r} K_r 2\pi [\Phi_i \frac{\partial N_i}{\partial r} + \Phi_j \frac{\partial N_j}{\partial r} + \Phi_k \frac{\partial N_k}{\partial r}] \int_{A^e} \left(r_i N_i + r_j N_j + r_k N_k\right) dr dz$$

$$= \frac{\partial N_i}{\partial r} K_r 2\pi [\Phi_i \frac{\partial N_i}{\partial r} + \Phi_j \frac{\partial N_j}{\partial r} + \Phi_k \frac{\partial N_k}{\partial r}] (r_i \int_{A^e} N_i dr\, dz + r_j \int_{A^e} N_j dr\, dz + r_k \int_{A^e} N_k dr\, dz)$$

$$= \frac{\partial N_i}{\partial r} K_r 2\pi [\Phi_i \frac{\partial N_i}{\partial r} + \Phi_j \frac{\partial N_j}{\partial r} + \Phi_k \frac{\partial N_k}{\partial r}] (r_i \frac{1}{3!} 2A^e + r_j \frac{1}{3!} 2A^e + r_k \frac{1}{3!} 2A^e)$$

$$= K_r 2\pi \frac{2A^e}{3!} (r_i + r_j + r_k) \frac{\partial N_i}{\partial r} [\Phi_i \frac{\partial N_i}{\partial r} + \Phi_j \frac{\partial N_j}{\partial r} + \Phi_k \frac{\partial N_k}{\partial r}]$$

$$= 2\pi A^e K_r \frac{(r_i + r_j + r_k)}{3} \frac{\partial N_i}{\partial r} [\Phi_i \frac{\partial N_i}{\partial r} + \Phi_j \frac{\partial N_j}{\partial r} + \Phi_k \frac{\partial N_k}{\partial r}]$$

$$= 2\pi A^e K_r \frac{(r_i + r_j + r_k)}{3} [\frac{\partial N_i}{\partial r}\frac{\partial N_i}{\partial r} + \frac{\partial N_i}{\partial r}\frac{\partial N_j}{\partial r} + \frac{\partial N_i}{\partial r}\frac{\partial N_k}{\partial r}] \begin{bmatrix} \Phi_i \\ \Phi_j \\ \Phi_k \end{bmatrix} \qquad (36)$$

For the second term in right side of equation (28), using the following relationships

$$\frac{\partial N_i}{\partial z} = \frac{\partial}{\partial z}\left\{\frac{1}{2A^e}\left[\left(r_j z_k - r_k z_j\right) + \left(z_j - z_k\right) r + \left(r_k - r_j\right) z\right]\right\} = \frac{\left(r_k - r_j\right)}{2A^e} = \frac{a_z}{2A^e} \qquad (37)$$

$$\frac{\partial N_j}{\partial z} = \frac{\partial}{\partial z}\left\{\frac{1}{2A^e}\left[\left(r_k z_i - r_i z_k\right) + \left(z_k - z_i\right) r + \left(r_i - r_k\right) z\right]\right\} = \frac{\left(r_i - r_k\right)}{2A^e} = \frac{b_z}{2A^e} \qquad (38)$$

$$\frac{\partial N_k}{\partial z} = \frac{\partial}{\partial z}\left\{\frac{1}{2A^e}\left[\left(r_i z_j - r_j z_i\right) + \left(z_i - z_j\right) r + \left(r_j - r_i\right) z\right]\right\} = \frac{\left(r_j - r_i\right)}{2A^e} = \frac{c_z}{2A^e} \qquad (39)$$

$$\frac{\partial \Phi}{\partial r} = \frac{\partial}{\partial r}\left(N_i \Phi_i + N_j \Phi_j + N_k \Phi_k\right) = \Phi_i \frac{\partial N_i}{\partial r} + \Phi_j \frac{\partial N_j}{\partial r} + \Phi_k \frac{\partial N_k}{\partial r} \qquad (40)$$

Integration of the second term is followed:

$$\rightarrow \quad \int_{A^e} \frac{\partial N_i}{\partial z}\left(K_z 2\pi r \frac{\partial \Phi}{\partial z}\right) dA = \int_{A^e} \frac{\partial N_i}{\partial z} K_z 2\pi r [\Phi_i \frac{\partial N_i}{\partial z} + \Phi_j \frac{\partial N_j}{\partial z} + \Phi_k \frac{\partial N_k}{\partial z}] dr dz$$

$$= \int_{A^e} \frac{\partial N_i}{\partial z} K_z 2\pi \left(r_i N_i + r_j N_j + r_k N_k\right) [\Phi_i \frac{\partial N_i}{\partial z} + \Phi_j \frac{\partial N_j}{\partial z} + \Phi_k \frac{\partial N_k}{\partial z}] dr dz$$

$$= \frac{\partial N_i}{\partial z} K_z 2\pi [\Phi_i \frac{\partial N_i}{\partial z} + \Phi_j \frac{\partial N_j}{\partial z} + \Phi_k \frac{\partial N_k}{\partial z}] \int_{A^e} \left(r_i N_i + r_j N_j + r_k N_k\right) dr dz$$

$$= \frac{\partial N_i}{\partial z} K_z 2\pi [\Phi_i \frac{\partial N_i}{\partial z} + \Phi_j \frac{\partial N_j}{\partial z} + \Phi_k \frac{\partial N_k}{\partial z}] (r_i \int_{A^e} N_i dr\, dz + r_j \int_{A^e} N_j dr\, dz + r_k \int_{A^e} N_k dr\, dz)$$

$$= \frac{\partial N_i}{\partial z} K_z 2\pi [\Phi_i \frac{\partial N_i}{\partial z} + \Phi_j \frac{\partial N_j}{\partial z} + \Phi_k \frac{\partial N_k}{\partial z}] (r_i \frac{1}{3!} 2A^e + r_j \frac{1}{3!} 2A^e + r_k \frac{1}{3!} 2A^e)$$

$$= K_z 2\pi \frac{2A^e}{3!} (r_i + r_j + r_k) \frac{\partial N_i}{\partial z} [\Phi_i \frac{\partial N_i}{\partial z} + \Phi_j \frac{\partial N_j}{\partial z} + \Phi_k \frac{\partial N_k}{\partial z}]$$

$$= 2\pi A^e K_z \frac{(r_i + r_j + r_k)}{3} [\frac{\partial N_i}{\partial z}\frac{\partial N_i}{\partial z} + \frac{\partial N_i}{\partial z}\frac{\partial N_j}{\partial z} + \frac{\partial N_i}{\partial z}\frac{\partial N_k}{\partial z}] \begin{bmatrix} \Phi_i \\ \Phi_j \\ \Phi_k \end{bmatrix} \qquad (41)$$

For the third term in right side of the equation (28)

$$\iint_{A^e} N_i S_0 2\pi r \left[N_i \frac{\partial \Phi_i}{\partial t} + N_j \frac{\partial \Phi_j}{\partial t} + N_k \frac{\partial \Phi_k}{\partial t}\right] dA$$

$$= 2\pi S_0 \iint_{A^e} N_i (r_i N_i + r_j N_j + r_k N_k) \left[N_i \frac{\partial \Phi_i}{\partial t} + N_j \frac{\partial \Phi_j}{\partial t} + N_k \frac{\partial \Phi_k}{\partial t}\right] dA$$

$$= 2\pi S_0 \iint_{A^e} \{(r_i \frac{\partial \Phi_i}{\partial t} N_i^3 + r_i \frac{\partial \Phi_j}{\partial t} N_i^2 N_j + r_i \frac{\partial \Phi_k}{\partial t} N_i^2 N_k)$$

$$+ (r_j \frac{\partial \Phi_i}{\partial t} N_i^2 N_j + r_j \frac{\partial \Phi_j}{\partial t} N_i N_j^2 + r_j \frac{\partial \Phi_k}{\partial t} N_i N_j N_k) + (r_k \frac{\partial \Phi_i}{\partial t} N_i^2 N_k + r_k \frac{\partial \Phi_j}{\partial t} N_i N_j N_k + r_k \frac{\partial \Phi_k}{\partial t} N_i N_k^2)\} a$$

$$= 2\pi S_0 \{(r_i \frac{\partial \Phi_i}{\partial t} \frac{3!}{5!} 2A^e + r_i \frac{\partial \Phi_j}{\partial t} \frac{2!}{5!} 2A^e + r_i \frac{\partial \Phi_k}{\partial t} \frac{2!}{5!} 2A^e) + (r_j \frac{\partial \Phi_i}{\partial t} \frac{2!}{5!} 2A^e + r_j \frac{\partial \Phi_j}{\partial t} \frac{2!}{5!} 2A^e + r_j \frac{\partial \Phi_k}{\partial t} \frac{1}{5!} 2A^e)$$

$$= 2\pi S_0\{(\frac{A^e}{10}r_i + \frac{A^e}{30}r_j + \frac{A^e}{30}r_k)\frac{\partial \Phi_i}{\partial t} + (\frac{A^e}{30}r_i + \frac{A^e}{30}r_j + \frac{A^e}{60}r_k)\frac{\partial \Phi_j}{\partial t} + (\frac{A^e}{30}r_i + \frac{A^e}{60}r_j + \frac{A^e}{30}r_k)\frac{\partial \Phi_k}{\partial t}\}$$

$$= \pi S_0 A^e\{(\frac{1}{5}r_i + \frac{1}{15}r_j + \frac{1}{15}r_k)\frac{\partial \Phi_i}{\partial t} + (\frac{1}{15}r_i + \frac{1}{15}r_j + \frac{1}{30}r_k)\frac{\partial \Phi_j}{\partial t} + (\frac{1}{15}r_i + \frac{1}{30}r_j + \frac{1}{15}r_k)\frac{\partial \Phi_k}{\partial t}\}$$

$$= \frac{\pi S_0 A^e}{30}[(6r_i + 2r_j + 2r_k),(2r_i + 2r_j + r_k),(2r_i + r_j + 2r_k)]\begin{bmatrix}\frac{\partial \Phi_i}{\partial t}\\ \frac{\partial \Phi_j}{\partial t}\\ \frac{\partial \Phi_k}{\partial t}\end{bmatrix} \quad \text{.....(42)}$$

Same procedures for Eqs. (29) and (30) result in followings

For Eq. (29)

$$\int_{A^e}\frac{\partial N_j}{\partial r}\left(K_r 2\pi r\frac{\partial \Phi}{\partial r}\right)dA =$$

$$2\pi A^e K_r\frac{(r_i + r_j + r_k)}{3}[\frac{\partial N_j}{\partial r}\frac{\partial N_i}{\partial r} + \frac{\partial N_j}{\partial r}\frac{\partial N_j}{\partial r} + \frac{\partial N_j}{\partial r}\frac{\partial N_k}{\partial r}]\begin{bmatrix}\Phi_i\\ \Phi_j\\ \Phi_k\end{bmatrix}$$

.....(43)

$$\int_{A^e}\frac{\partial N_j}{\partial z}\left(K_z 2\pi r\frac{\partial \Phi}{\partial z}\right)dA =$$

$$2\pi A^e K_z\frac{(r_i + r_j + r_k)}{3}[\frac{\partial N_j}{\partial z}\frac{\partial N_i}{\partial z} + \frac{\partial N_j}{\partial z}\frac{\partial N_j}{\partial z} + \frac{\partial N_j}{\partial z}\frac{\partial N_k}{\partial z}]\begin{bmatrix}\Phi_i\\ \Phi_j\\ \Phi_k\end{bmatrix}$$

.....(44)

$$\iint_{A^e} N_i S_0 2\pi r\left[N_i\frac{\partial \Phi_i}{\partial t} + N_j\frac{\partial \Phi_j}{\partial t} + N_k\frac{\partial \Phi_k}{\partial t}\right]dA$$

$$= \frac{\pi S_0 A^e}{30}[(2r_i + 2r_j + r_k),(2r_i + 6r_j + 2r_k),(r_i + 2r_j + 2r_k)]\begin{bmatrix}\frac{\partial \Phi_i}{\partial t}\\ \frac{\partial \Phi_j}{\partial t}\\ \frac{\partial \Phi_k}{\partial t}\end{bmatrix} \quad \text{.....(45)}$$

For Eq. (30)

$$\int_{A^e} \frac{\partial N_k}{\partial r}\left(K_r 2\pi r \frac{\partial \Phi}{\partial r}\right) dA =$$

$$2\pi A^e K_r \frac{(r_i + r_j + r_k)}{3}\left[\frac{\partial N_k}{\partial r}\frac{\partial N_i}{\partial r} + \frac{\partial N_k}{\partial r}\frac{\partial N_j}{\partial r} + \frac{\partial N_k}{\partial r}\frac{\partial N_k}{\partial r}\right]\begin{bmatrix}\Phi_i \\ \Phi_j \\ \Phi_k\end{bmatrix}$$

.....(46)

$$\int_{A^e} \frac{\partial N_k}{\partial z}\left(K_z 2\pi r \frac{\partial \Phi}{\partial z}\right) dA =$$

$$2\pi A^e K_z \frac{(r_i + r_j + r_k)}{3}\left[\frac{\partial N_k}{\partial z}\frac{\partial N_i}{\partial z} + \frac{\partial N_k}{\partial z}\frac{\partial N_j}{\partial z} + \frac{\partial N_k}{\partial z}\frac{\partial N_k}{\partial z}\right]\begin{bmatrix}\Phi_i \\ \Phi_j \\ \Phi_k\end{bmatrix}$$

.....(47)

$$\iint_{A^e} N_k S_0 2\pi r\left[N_i \frac{\partial \Phi_i}{\partial t} + N_j \frac{\partial \Phi_j}{\partial t} + N_k \frac{\partial \Phi_k}{\partial t}\right] dA$$

$$= \frac{\pi S_0 A^e}{30}\left[(2r_i + r_j + 2r_k),(r_i + 2r_j + 2r_k),(2r_i + 2r_j + 6r_k)\right]\begin{bmatrix}\frac{\partial \Phi_i}{\partial t} \\ \frac{\partial \Phi_j}{\partial t} \\ \frac{\partial \Phi_k}{\partial t}\end{bmatrix} \quad \text{.....(48)}$$

**The element equations for an arbitrary element in matrix form**

$$2\pi A^e \frac{(r_i + r_j + r_k)}{3} \begin{bmatrix} K_r \frac{\partial N_i}{\partial r}\frac{\partial N_i}{\partial r} + K_z \frac{\partial N_i}{\partial z}\frac{\partial N_i}{\partial z}, & K_r \frac{\partial N_i}{\partial r}\frac{\partial N_j}{\partial r} + K_z \frac{\partial N_i}{\partial z}\frac{\partial N_j}{\partial z}, & K_r \frac{\partial N_i}{\partial r}\frac{\partial N_k}{\partial r} + K_z \frac{\partial N_i}{\partial z}\frac{\partial N_k}{\partial z} \\ K_r \frac{\partial N_j}{\partial r}\frac{\partial N_i}{\partial r} + K_z \frac{\partial N_j}{\partial z}\frac{\partial N_i}{\partial z}, & K_r \frac{\partial N_j}{\partial r}\frac{\partial N_j}{\partial r} + K_z \frac{\partial N_j}{\partial z}\frac{\partial N_j}{\partial z}, & K_r \frac{\partial N_j}{\partial r}\frac{\partial N_k}{\partial r} + K_z \frac{\partial N_j}{\partial z}\frac{\partial N_k}{\partial z} \\ K_r \frac{\partial N_k}{\partial r}\frac{\partial N_i}{\partial r} + K_z \frac{\partial N_k}{\partial z}\frac{\partial N_i}{\partial z}, & K_r \frac{\partial N_k}{\partial r}\frac{\partial N_j}{\partial r} + K_z \frac{\partial N_k}{\partial z}\frac{\partial N_j}{\partial z}, & K_r \frac{\partial N_k}{\partial r}\frac{\partial N_k}{\partial r} + K_z \frac{\partial N_k}{\partial z}\frac{\partial N_k}{\partial z} \end{bmatrix} \begin{bmatrix} \Phi_i \\ \Phi_j \\ \Phi_k \end{bmatrix} \quad \text{.....(49)}$$

$$+ \frac{\pi S_0 A^e}{30} \begin{bmatrix} 6r_i + 2r_j + 2r_k, & 2r_i + 2r_j + r_k, & 2r_i + r_j + 2r_k \\ 2r_i + 2r_j + r_k, & 2r_i + 6r_j + 2r_k, & r_i + 2r_j + 2r_k \\ 2r_i + r_j + 2r_k, & r_i + 2r_j + 2r_k, & 2r_i + 2r_j + 6r_k \end{bmatrix} \begin{bmatrix} \frac{\partial \Phi_i}{\partial t} \\ \frac{\partial \Phi_j}{\partial t} \\ \frac{\partial \Phi_k}{\partial t} \end{bmatrix} = \begin{bmatrix} \int_{c^e} N_i q_n dC \\ \int_{c^e} N_j q_n dC \\ \int_{c^e} N_k q_n dC \end{bmatrix}$$

$$2\pi A^e \frac{(r_i + r_j + r_k)}{3} \begin{bmatrix} K_r a_r^2 + K_z a_z^2, & K_r a_r b_r + K_z a_z b_z, & K_r a_r c_r + K_z a_z c_z, \\ K_r b_r a_r + K_z b_z a_z, & K_r b_r^2 + K_z b_z^2, & K_r b_r c_r + K_z b_z c_z, \\ K_r c_r a_r + K_z c_z a_z, & K_r c_r a_r + K_z c_z b_z, & K_r c_r^2 + K_z c_z^2, \end{bmatrix} \begin{bmatrix} \Phi_i \\ \Phi_j \\ \Phi_k \end{bmatrix}$$

$$+ \frac{\pi S_0 A^e}{30} \begin{bmatrix} 6r_i + 2r_j + 2r_k, & 2r_i + 2r_j + r_k, & 2r_i + r_j + 2r_k \\ 2r_i + 2r_j + r_k, & 2r_i + 6r_j + 2r_k, & r_i + 2r_j + 2r_k \\ 2r_i + r_j + 2r_k, & r_i + 2r_j + 2r_k, & 2r_i + 2r_j + 6r_k \end{bmatrix} \begin{bmatrix} \frac{\partial \Phi_i}{\partial t} \\ \frac{\partial \Phi_j}{\partial t} \\ \frac{\partial \Phi_k}{\partial t} \end{bmatrix} = \begin{bmatrix} \int_{c^e} N_i q_n dC \\ \int_{c^e} N_j q_n dC \\ \int_{c^e} N_k q_n dC \end{bmatrix} \quad \text{.....(50)}$$

where $a_r = z_j - z_k$, $a_z = r_k - r_j$, $b_r = z_k - z_i$, $b_z = r_i - r_k$, $c_r = z_i - z_j$, $c_z = r_j - r_i$

$$\frac{\pi}{2A^e}\bar{r}\begin{bmatrix} & M & \end{bmatrix}\begin{bmatrix}\Phi_i\\ \Phi_j\\ \Phi_k\end{bmatrix} + \frac{\pi S_0 A^e}{30}\begin{bmatrix} & N & \end{bmatrix}\begin{bmatrix}\frac{\partial \Phi_i}{\partial t}\\ \frac{\partial \Phi_j}{\partial t}\\ \frac{\partial \Phi_k}{\partial t}\end{bmatrix} = \begin{bmatrix}\int_{C^e} N_i q_n dC\\ \int_{C^e} N_i q_n dC\\ \int_{C^e} N_k q_n dC\end{bmatrix} \quad \text{.....(51)}$$

where $\bar{r} = \frac{r_i + r_j + r_k}{3}$

$$M = \begin{bmatrix} K_r a_r^2 + K_z a_z^2 & K_r a_r b_r + K_z a_z b_z & K_r a_r c_r + K_z a_z c_z \\ K_r b_r a_r + K_z b_z a_z & K_r b_r^2 + K_r b_z^2 & K_r b_r c_r + K_z b_z c_z \\ K_r c_r a_r + K_z c_z a_z & K_r c_r b_r + K_z c_z b_z & K_r c_r^2 + K_r c_z^2 \end{bmatrix} \quad \text{and} \quad N = \begin{bmatrix} 6r_i + 2r_j + 2r_k & 2r_i + 2r_j + r_k & 2r_i + r_j + 2r_k \\ 2r_i + 2r_j + r_k & 2r_i + 6r_j + 2r_k & r_i + 2r_j + 2r_k \\ 2r_i + r_j + 2r_k & r_i + 2r_j + 2r_k & 2r_i + 2r_j + 6r_k \end{bmatrix}$$

.....(52) and (53)

**Time consideration in fully implicit method**

$$\frac{\pi}{2A^e}\bar{r}\begin{bmatrix} & M & \end{bmatrix}\begin{bmatrix}\Phi_i(t+\Delta t)\\ \Phi_j(t+\Delta t)\\ \Phi_k(t+\Delta t)\end{bmatrix}+\frac{\pi S_0 A^e}{30\Delta t}\begin{bmatrix} & N & \end{bmatrix}\begin{bmatrix}\Phi_i(t+\Delta t)-\Phi(t)\\ \Phi_j(t+\Delta t)-\Phi(t)\\ \Phi_k(t+\Delta t)-\Phi(t)\end{bmatrix}=\begin{bmatrix}0\\0\\0\end{bmatrix}$$

.....(54)

$$\frac{\pi}{2A^e}\bar{r}\begin{bmatrix} & M & \end{bmatrix}\begin{bmatrix}\Phi_i(t+\Delta t)\\ \Phi_j(t+\Delta t)\\ \Phi_k(t+\Delta t)\end{bmatrix}+\frac{\pi S_0 A^e}{30\Delta t}\begin{bmatrix} & N & \end{bmatrix}\begin{bmatrix}\Phi_i(t+\Delta t)\\ \Phi_j(t+\Delta t)\\ \Phi_k(t+\Delta t)\end{bmatrix}=\frac{\pi S_0 A^e}{30\Delta t}\begin{bmatrix} & N & \end{bmatrix}\begin{bmatrix}\Phi_i(t)\\ \Phi_j(t)\\ \Phi_k(t)\end{bmatrix}$$

.....(55)

$$\Rightarrow \quad [K^{(e)} + C^{(e)}]\,\Phi^{(e)}(t+\Delta t) = C(e)\,\Phi^{(e)}(t) \tag{56}$$

$$A^{(e)}\,\Phi^{(e)}(t+\Delta t) = C^{(e)}\,\Phi^{(e)}(t) \tag{57}$$

$$A\Phi = b \tag{58}$$

$$A^e = \begin{bmatrix} con1(K_r a_r^2 + K_z a_z^2) & con1(K_r a_r b_r + K_z a_z b_z) & con1(K_r a_r c_r + K_z a_z c_z) \\ +con2(6r_i + 2r_j + 2r_k), & +con2(2r_i + 2r_j + r_k), & +con2(2r_i + r_j + 2r_k) \\ con1(K_r b_r a_r + K_z b_z a_z) & con1(K_r b_r^2 + K_z b_z^2) & con1(K_r b_r c_r + K_z b_z c_z) \\ +con2(2r_i + 2r_j + r_k)), & +con2(2r_i + 6r_j + 2r_k), & +con2(r_i + 2r_j + 2r_k) \\ con1(K_r c_r a_r + K_z c_z a_z) & con1(K_r c_r b_r + K_z c_z b_z) & con1(K_r c_r^2 + K_z c_z^2) \\ +con2(2r_i + r_j + 2r_k), & +con2(r_i + 2r_j + 2r_k), & +con2(2r_i + 2r_j + 6r_k) \end{bmatrix}$$

.....(59)

$$C^e = \begin{bmatrix} con2(6r_i + 2r_j + 2r_k) & con2(2r_i + 2r_j + r_k) & con2(2r_i + r_j + 2r_k) \\ con2(2r_i + 2r_j + r_k) & con2(2r_i + 6r_j + 2r_k) & con2(r_i + 2r_j + 2r_k) \\ con2(2r_i + r_j + 2r_k) & con2(r_i + 2r_j + 2r_k) & con2(2r_i + 2r_j + 6r_k) \end{bmatrix}$$

.....(60)

*where* $con1 = \dfrac{\pi}{2A^e}\dfrac{r_i + r_j + r_k}{3}$ *and* $con2 = \dfrac{\pi S_0 A^e}{30\Delta t}$

**Global matrix assembly**

The size of global matrix is n by n, where n is total number of node. The global matrix assembly for node i is total of the $N_i$ contributions from each element that includes node i. As each element is evaluated the coefficients are located into the proper position in the global matrix. The global matrix location (row, column) of the coefficient in integrated element matrix (Eq. (54)) is shown :

$$\begin{bmatrix} (rowi,coli) & (rowi,colj) & (rowi,colk) \\ (rowj,coli) & (rowj,colj) & (rowj,colk) \\ (rowk,coli) & (rowk,coli) & (rowk,colk) \end{bmatrix}$$

The matrices A and C are obtained by adding the contributions from all the elements the node is a part of . For example of an arbitrary element contributions of (row i ,col j):

$$A(rowi,colj) = A(rowi,colj) + con1(K_r b_r a_r + K_z b_z a_z) + con2(2r_i + 2r_i + r_i)$$

$$C(rowi,colj) = C(rowi,colj) + con2(2r_i + 2r_i + r_i)$$

# APPENDIX B: BASIC PROGRAM FOR 2-D, UNSTEADY, RADIAL AND VERTICAL , AND CONFINED GROUNDWATER FLOW WITH CONSIDERATION OF BAROMETRIC PRESSURE EFFECTS

```
Attribute VB_Name = "fembaro3"
Option Explicit


Public Sub barometric()
'2-23-97
'Program "fembaro3.bas" created by Hyejoung Han Seo
      '  Civil Engineering
      '  194 Town Engineering
      '  Iowa State University
      '  Ames, Iowa 50011
      ' Copyright 1997 Hyejoung Han Seo

'.....TWO DIMENSIONAL UNSTEADY GROUNDWATER PROGRAM.....
'.....FINITE ELEMENT METHOD.....
'.....APPLICATION FOR BAROMETRIC PRESSURE EFFECT.....


Dim filein As String, fileout As String, title As String
Dim interit As Integer
femmain.text3.Text = femmain.txtFilein.Text

filein = femmain.txtFilein.Text
Open filein For Input As #1
fileout = femmain.Text2.Text
Open fileout For Output As #2
Line Input #1, title
Print #2, title
Line Input #1, title
Print #2, title

Dim nnode As Integer, nelem As Integer
Input #1, nelem, nnode
Print #2, nelem, nnode
ReDim nodei(nelem) As Integer, nodej(nelem) As Integer, nodek(nelem) As Integer
ReDim hydr(nelem) As Double, hydz(nelem) As Double, stor(nelem) As Double
ReDim rloc(nnode) As Double, zloc(nnode) As Double
Dim m As Integer, n As Integer
Dim ne As Integer, nnum As Integer
Line Input #1, title
'Print #2, title

'read in node number, elem number, r-loc, z-loc, hyd-r, hyd-z, and stor

   For m = 1 To nelem
   Input #1, ne, nodei(ne), nodej(ne), nodek(ne), hydr(ne), hydz(ne), stor(ne)
   'Print #2, ne, nodei(ne), nodej(ne), nodek(ne), hydr(ne), hydz(ne), stor(ne)
   Next m

Line Input #1, title
'Print #2, title

   For m = 1 To nnode
   Input #1, nnum, rloc(nnum), zloc(nnum)
   'Print #2, nnum, rloc(nnum), zloc(nnum)
   Next m

' read well-screen boundary condition
Dim numqbh As Integer
```

```
Line Input #1, title
Print #2, title
Input #1, numqbh
Print #2, numqbh
ReDim qhnode(numqbh) As Integer, iqbhead(numqbh) As Double
Line Input #1, title
Print #2, title
   For m = 1 To numqbh
   Input #1, qhnode(m), iqbhead(m)
   Print #2, qhnode(m), iqbhead(m)
   Next m

' read top known-head boundary condition
Dim numtbh As Integer
Line Input #1, title
Print #2, title
Input #1, numtbh
Print #2, numtbh
ReDim thnode(numtbh) As Integer, itbhead(numtbh) As Double
Line Input #1, title
Print #2, title
   For m = 1 To numtbh
   Input #1, thnode(m), itbhead(m)
   Print #2, thnode(m), itbhead(m)
   Next m

'read initial head
ReDim ihead(nnum) As Double
Line Input #1, title
'Print #2, title
   For m = 1 To nnode
   Input #1, nnum, ihead(nnum)
   'Print #2, nnum, ihead(nnum)
   Next m

'read delta t and maximum time
Dim delt As Double, tmax As Double
Line Input #1, title
Print #2, title
Input #1, delt, tmax
Print #2, delt, tmax

'read specific time interval for printing
Dim nprt As Integer, prtnum As Integer
Line Input #1, title
'Print #2, title
Input #1, nprt
'Print #2, nprt
Line Input #1, title
'Print #2, title
ReDim Interval(nprt) As Single
   For m = 1 To nprt
   Input #1, prtnum, Interval(prtnum)
   'Print #2, prtnum, Interval(prtnum)
   Next m

' read specific time interval for B.P. change and delta B.P.
Dim nbp As Integer, bpnum As Integer
Line Input #1, title
Print #2, title
```

```
Input #1, nbp
Print #2, nbp
Line Input #1, title
Print #2, title
ReDim bpintv(nbp) As Single, delbp(nbp) As Double
   For m = 1 To nbp
   Input #1, bpnum, bpintv(bpnum), delbp(bpnum)
   Print #2, bpnum, bpintv(bpnum), delbp(bpnum)
   Next m

'read well-casing radius
Dim rc As Double
Line Input #1, title
Print #2, title
Input #1, rc
Print #2, rc

Close #1


'computation of the bandwidth
Dim i As Integer, j As Integer, k As Integer
Dim iband As Integer, iband1 As Integer, iband2 As Integer
Dim isum1 As Integer, isum2 As Integer, isum3 As Integer
Dim imax As Integer, icount As Integer

      iband = 0

      For m = 1 To nelem
      i = nodei(m)
      j = nodej(m)
      k = nodek(m)
      'set maximum difference in nodes numbers to zero
      imax = 0

      'check for maximum node difference
      isum1 = Abs(i - j)
      isum2 = Abs(i - k)
      isum3 = Abs(j - k)
      imax = isum1
      If isum2 > imax Then imax = isum2
      If isum3 > imax Then imax = isum3
      If imax > iband Then iband = imax
      Next m

      iband1 = iband + 1
      iband2 = 2 * iband + 1

ReDim a(nnode, iband2) As Double, c(nnode, iband2) As Double
Dim sum As Double, sum1 As Double, sum2 As Double, sum3 As Double, area As Double
Dim con1 As Double, con2 As Double, rbar As Double
Dim ar As Double, br As Double, cr As Double
Dim coef1 As Double, coef2 As Double, nc As Double
ReDim b(nnode) As Double, y(nnode) As Double
Dim az As Double, bz As Double, cz As Double, temp As Double
ReDim head(nnode) As Double

'determine coefficients for element equations
   For m = 1 To nelem
   i = nodei(m)
```

```
j = nodej(m)
k = nodek(m)
sum1 = rloc(i) * zloc(j) - rloc(j) * zloc(i)
sum2 = rloc(k) * zloc(i) - rloc(i) * zloc(k)
sum3 = rloc(j) * zloc(k) - rloc(k) * zloc(j)
area = (sum1 + sum2 + sum3) / 2#
rbar = (rloc(i) + rloc(j) + rloc(k)) / 3#
con1 = (3.14 * rbar) / (2# * area)
con2 = (3.14 * stor(m) * area) / (30# * delt)
ar = zloc(j) - zloc(k)
br = zloc(k) - zloc(i)
cr = zloc(i) - zloc(j)
az = rloc(k) - rloc(j)
bz = rloc(i) - rloc(k)
cz = rloc(j) - rloc(i)

'assemble the A matrix coefficients for element m into the reduced size of (nnode, iband2)

    'ith row

  coef1 = (hydr(m) * ar * ar + hydz(m) * az * az) * con1 + (6 * rloc(i) + 2 * rloc(j) + 2 * rloc(k)) * con2
    a(i, iband1) = a(i, iband1) + coef1

  coef1 = (hydr(m) * ar * br + hydz(m) * az * bz) * con1 + (2 * rloc(i) + 2 * rloc(j) + 1 * rloc(k)) * con2
    nc = iband1 + j - i
    a(i, nc) = a(i, nc) + coef1
    nc = iband1 + i - j
    a(j, nc) = a(j, nc) + coef1

  coef1 = (hydr(m) * ar * cr + hydz(m) * az * cz) * con1 + (2 * rloc(i) + 1 * rloc(j) + 2 * rloc(k)) * con2

    nc = iband1 + k - i
    a(i, nc) = a(i, nc) + coef1
    nc = iband1 + i - k
    a(k, nc) = a(k, nc) + coef1

    ' jth row

  coef1 = (hydr(m) * br * br + hydz(m) * bz * bz) * con1 + (2 * rloc(i) + 6 * rloc(j) + 2 * rloc(k)) * con2
    a(j, iband1) = a(j, iband1) + coef1

  coef1 = (hydr(m) * br * cr + hydz(m) * bz * cz) * con1 + (1 * rloc(i) + 2 * rloc(j) + 2 * rloc(k)) * con2
    nc = iband1 + k - j
    a(j, nc) = a(j, nc) + coef1
    nc = iband1 + j - k
    a(k, nc) = a(k, nc) + coef1

    ' kth row

  coef1 = (hydr(m) * cr * cr + hydz(m) * cz * cz) * con1 + (2 * rloc(i) + 2 * rloc(j) + 6 * rloc(k)) * con2
    a(k, iband1) = a(k, iband1) + coef1


'assemble the C matrix coefficients for element m in the reduced size of (nnode, iband)

    'ith row

  coef2 = (6 * rloc(i) + 2 * rloc(j) + 2 * rloc(k)) * con2
    c(i, iband1) = c(i, iband1) + coef2
```

```
      coef2 = (2 * rloc(i) + 2 * rloc(j) + 1 * rloc(k)) * con2
        nc = iband1 + j - i
        c(i, nc) = c(i, nc) + coef2
        nc = iband1 + i - j
        c(j, nc) = c(j, nc) + coef2

      coef2 = (2 * rloc(i) + 1 * rloc(j) + 2 * rloc(k)) * con2
        nc = iband1 + k - i
        c(i, nc) = c(i, nc) + coef2
        nc = iband1 + i - k
        c(k, nc) = c(k, nc) + coef2

        ' jth row

      coef2 = (2 * rloc(i) + 6 * rloc(j) + 2 * rloc(k)) * con2
        c(j, iband1) = c(j, iband1) + coef2

      coef2 = (1 * rloc(i) + 2 * rloc(j) + 2 * rloc(k)) * con2
        nc = iband1 + k - j
        c(j, nc) = c(j, nc) + coef2
        nc = iband1 + j - k
        c(k, nc) = c(k, nc) + coef2

        ' kth row

      coef2 = (2 * rloc(i) + 2 * rloc(j) + 6 * rloc(k)) * con2
        c(k, iband1) = c(k, iband1) + coef2

    Next m

'Print a
'Print #2, " a"
'For i = 1 To nnode
'For j = 1 To iband2
'Print #2, i, j, a(i, j)
'Next j
'Next i


'save a for calculation of smalq
ReDim saveda(numqbh, iband2) As Double
For i = 1 To numqbh
    For j = 1 To iband2
    saveda(i, j) = a(qhnode(i), j)
    Next j
Next i

 'Print saved a
'Print #2, "saved a"
'For i = 1 To numqbh
'For j = 1 To iband2
'Print #2, i, j, saveda(i, j)
'Next j
'Next i


' describe boundary condition for well-screen
   For i = 1 To numqbh
      For j = 1 To iband2
      a(qhnode(i), j) = 0#
```

```
    Next j
    a(qhnode(i), iband1) = 1#
  Next i

' describe boundary condition for top known-head nodes
  For i = 1 To numtbh
    For j = 1 To iband2
    a(thnode(i), j) = 0#
    Next j
    a(thnode(i), iband1) = 1#
  Next i


' compute the lu decomposition and save in a
  For i = 2 To nnode
  icount = i + iband1 - 1
  If icount > nnode Then icount = nnode
    For j = i To icount
    nc = iband1 + i - 1 - j
    temp = a(j, nc) / a(i - 1, iband1)
      For k = i To icount
      nc = iband1 + k - (i - 1)
      If nc > iband2 Then
        a(j, iband1 + k - j) = a(j, iband1 + k - j)
      Else
        a(j, iband1 + k - j) = a(j, iband1 + k - j) - temp * a(i - 1, nc)
      End If
      Next k
    nc = iband1 + i - 1 - j
    a(j, nc) = temp
    Next j
  Next i


'do loop for each time interval
Dim time As Single
ReDim crrtwt(numqbh) As Double, esthead(numqbh) As Double
Dim crrtbp As Double
ReDim savedb(numqbh) As Double, qbhead(numqbh) As Double
ReDim smallq(numqbh) As Double, leftq(numqbh) As Double
Dim largeq As Double, wvol As Double, delwt As Double, differ As Double

ReDim topsb(numtbh) As Double, tbhead(numtbh) As Double
ReDim topsq(numtbh) As Double, toplftq(numtbh) As Double
Dim toplq As Double, topwvol As Double, topdelwt As Double
Dim icount1 As Integer, icount2 As Integer
  time = 0!
  crrtbp = 0#

  For m = 1 To numqbh
  crrtwt(m) = iqbhead(m)
  Next m

  For m = 1 To numtbh
  tbhead(m) = itbhead(m)
  Next m

  For i = 1 To nnode
  head(i) = ihead(i)
  Next i
```

```
Do Until time > tmax

   femmain.text3.Text = Str(time)
   femmain.text3.Refresh

   For i = 1 To nnode
   b(i) = 0#
    icount1 = i - (iband1 - 1)
    If icount1 < 1 Then icount1 = 1
    icount2 = i + (iband1 - 1)
    If icount2 > nnode Then icount2 = nnode
     For j = icount1 To icount2
     nc = iband1 + j - i
     b(i) = b(i) + c(i, nc) * head(j)
     Next j
   Next i

'save b for calulation of smallq
   For i = 1 To numqbh
   savedb(i) = b(qhnode(i))
   Next i

' print saved b
'Print #2, "time, node, saved b"
 '     For i = 1 To numqbh
  '    Print #2, time, qhnode(i), savedb(i)
   '   Next i

  'save b for calulation of top-q
 '  For i = 1 To numtbh
  '  topsb(i) = b(thnode(i))
   ' Next i

'consider B.P. change for boundary condition at B.P. time interval
   For m = 1 To nbp
   If (Abs((time + delt) - bpintv(m)) <= (delt / 2#)) Then
   crrtbp = crrtbp + delbp(m)

   For i = 1 To numtbh
   tbhead(i) = head(thnode(i)) + delbp(m)
   Next i

    End If
    Next m

' guess boundary head after applying delta B.P. inside of the well

   For i = 1 To numqbh
   qbhead(i) = head(qhnode(i))
   esthead(i) = qbhead(i)
   Next i

   interit = 0
   Do
      For i = 1 To numqbh
      'qbhead(i) = qbhead(i) - (qbhead(i) - esthead(i)) / 10#
      'qbhead(i) = qbhead(i) - (qbhead(i) - esthead(i)) / 3#
      qbhead(i) = qbhead(i) - (qbhead(i) - esthead(i)) / 2#
      'qbhead(i) = qbhead(i) - (qbhead(i) - esthead(i)) / 100#
```

```
        'qbhead(i) = esthead(i)
        Next i

'describe boundary condition
        For i = 1 To numqbh
        b(qhnode(i)) = qbhead(i)
        Next i

        For i = 1 To numtbh
        b(thnode(i)) = tbhead(i)
        Next i

'find y of Ly=b
        y(1) = b(1) / 1#
        For i = 2 To nnode
        sum = 0#
        icount = i - (iband1 - 1)
        If icount < 1 Then icount = 1
        For j = icount To i - 1
        nc = iband1 + j - i
        sum = sum + a(i, nc) * y(j)
        Next j
        y(i) = (b(i) - sum) / 1#
        Next i

'find x of Ux=y
        head(nnode) = y(nnode) / a(nnode, iband1)
        For i = nnode - 1 To 1 Step -1
        sum = 0#
        icount = i + iband1 - 1
        If icount > nnode Then icount = nnode
        For j = i + 1 To icount
        nc = iband1 + j - i
        sum = sum + a(i, nc) * head(j)
        Next j
        head(i) = (y(i) - sum) / a(i, iband1)
        Next i

 'calculate smallq between well-screen boundary nodes
     For i = 1 To numqbh
     leftq(i) = 0#
     icount1 = qhnode(i) - (iband1 - 1)
     If icount1 < 1 Then icount1 = 1
     icount2 = qhnode(i) + (iband1 - 1)
     If icount2 > nnode Then icount2 = nnode
         For j = icount1 To icount2
         nc = iband1 + j - qhnode(i)
         leftq(i) = leftq(i) + saveda(i, nc) * head(j)
         Next j
       smallq(i) = savedb(i) - leftq(i)
       Next i

'print leftq (= saveda * head(t + delt))
         ' PRINT #2, "time, node,head, leftq,savedb, smallq"
       'FOR i = 1 TO numqbh
       'PRINT #2, time, qhnode(i), head(qhnode(i)), leftq(i), savedb(i), smallq(i)
       'NEXT i


' smallq reduction
```

```
        For i = 1 To numqbh
        If (Abs(smallq(i)) < 0.00000001) Then
        smallq(i) = 0#
        End If
        Next i


'calculate Q around well-screen
        largeq = 0#
        For i = 1 To numqbh
        largeq = largeq + smallq(i)
        Next i

'calculate the water level change due to Q
        wvol = largeq * delt
        delwt = wvol / (3.14 * (rc ^ 2#))

'calculate Q at the top
        'toplq = 0#
        'For i = 1 To numtbh
        'toplq = toplq + topsq(i)
        'Next i

'calculate the water table level change due to Q
        'topwvol = toplq * delt
        'topdelwt = 4# * topwvol / (3.14 * (800 - 2.54) ^ 2#)


'consider changed water level to estimate head of well-screen nodes
        For i = 1 To numqbh
        esthead(i) = crrtwt(i) + delwt + crrtbp
        Next i

' compute sum of the difference between the qbhead and esthead
        differ = 0#
        For i = 1 To numqbh
        differ = differ + Abs(qbhead(i) - esthead(i))
        Next i

        'Print #2, qbhead(1), esthead(1)
 interit = interit + 1
 If interit > 30 Then
 Exit Sub
 End If

    Loop Until Abs(differ) < 0.0001

 time = time + delt

'describe estimated current water level
   For i = 1 To numqbh
   crrtwt(i) = crrtwt(i) + delwt
   Next i
' simple printout of current water level for easy plotting
For m = 1 To nbp
If (Abs(time - bpintv(m)) <= (delt / 2#)) Then
Print #2, time, crrtwt(1)
End If
Next m
```

```
' simple printout of total head for easy plotting
'Print #2, time, head(qhnode(1))

'print water level change, current water level, and boundary head
   'Print #2, "time, node,water level change, current wt lvl,  current B.P.  esthead,  qbhead"
   'For i = 1 To numqbh
   'Print #2, time, qhnode(i), delwt, crrtwt(i), crrtbp, esthead(i), qbhead(i)
   'Next i

'print output for smallq at well-screen boundary node
'      FOR m = 1 TO nbp
'      IF (ABS(time - bpintv(m)) <= (delt / 2#)) THEN
'      PRINT #2, "time,  node,  smallq,     current water level"
   '           FOR i = 1 TO numqbh
    '          PRINT #2, time, qhnode(i), smallq(i), crrtwt(i)
     '         NEXT i
      ' END IF
      ' NEXT m

'print output for water level change
'      FOR m = 1 TO nbp
'      IF (ABS(time - bpintv(m)) <= (delt / 2#)) THEN
'      PRINT #2, "time,   B.P. change, flow rate (Q), water level change"
   '    PRINT #2, time, delbp(m), largeq, delwt
    '   END IF
     '  NEXT m

'print output for head with time
   'For m = 1 To nprt
   'If (Abs(time - Interval(1)) <= (delt / 2#)) Then
   'Print #2, "time      node      rloc      zloc      head"
   'For i = 1 To nnode
   'Print #2, time, i, rloc(i), zloc(i), head(i)
   'Next i
   'End If
   'Next m

Loop

Close #2
End Sub
```

## REFERENCES

Biot, M. A. 1941. General theory of three-dimensional consolidation. J. Appl. Phys. v. 12, pp. 155-164.

Bisop, A. W. 1973. The influence of an undrained change in stress on the pore pressure in porous media of low compressibility. Geotechnique. v. 23, pp. 435-442.

Bodvarsson, G. 1970. Confined fluids as strain meter. J. Geophys. Res. v.75, pp. 2711-2718.

Bouwer, D. R. and K. C. Heaton. 1978. Response of an aquifer near Ottawa to tidal forcing and the Alaskan earthquake of 1964. Can. J. Earth Sci. v. 15, pp. 331-340.

Bouwer, H. and R. C. Rice. 1976. A slug tests for determining hydraulic conductivity of unconfined aquifers with completely or partially penetrating wells. Water Resour. Res. v. 12, no. 3, pp. 423-428.

Bredehoeft, J. D. 1967. Response of well –aquifer system to earth tides. J. Geophys. Res. v. 72, pp. 3075-3087.

Carr, P. A. and van der Kamp. 1969. Determining aquifer characteristics by the tidal method. Water Resour. Res. v. 5, n. 5, pp. 1023-1031.

Clark, W. E. 1967. Computing the barometric efficiency of a well. J. Hydraul. Div., Am. Soc. Civ. Eng., v. 93 (HY4), pp. 93-98.

Cooper, H. H., J. D. Bredehoef, I. S. Papadopoulos, and R. R. Bennett. 1965. The response of well-aquifer systems to seismic waves. J. Geophys. Res. v. 70, pp. 3915-3926.

Cooper, H. H., J. D. Bredehoef, and I. S. Papadopoulos. 1967. Response of a finite diameter well to an instantaneous charge of water. Water Resour. Res. v. 3, n. 1, pp. 263-269.

Davis, D. R. and T. C. Rasmussen. 1993. A comparison of linear regression with Clark's method for estimating barometric efficiency of confined aquifers. Water Resour. Res. v. 29, n. 6, pp. 1849-1854.

Davis, R. W. 1972. Use of naturally occurring phenomena to study hydraulic diffusivities of aquitards. Water Resour. Res. v. 8, n. 2, pp. 500-507.

Edwards, K. B. and L. C. Jones. 1993. Modeling pumping tests in weathered glacial till. Journal of Hydrology. v. 150, pp. 41-60.

Freeze, R. A. and J. A. Cherry. 1979. Groundwater. Prentice Hall, Englewood Cliffs, NJ. 604 pp.

Furbish, D. J. 1988. Estimating aquifer compressibility using time series of barometric pressure and water level in an artesian well. Geol. Soc. Am. Abstr. Programs. v. 20, pp, 265.

Furbish, D. J. 1991. The response of water level in a well to a time series of atmospheric loading under confined conditions. Water Resour. Res. v. 27, n. 4, pp. 557-568.

Furbish, D. J. and M. A. Lyverse. 1988. Filtering the effects of changes in barometric pressure from records of water level in an artesian well. Geol. Soc. Am. Abstr. Programs. v. 20, pp. 265.

Gieske, A. 1986. On phase shifts and periodic well fluctuations. Geophys. J. R. Astrom. Soc. v. 86, pp. 789-799.

Gilliland, J. A. 1969. A rigid plate model of the barometric effect. Journal of Hydrology. v. 7, pp. 233-245.

Hanson, J. M. 1980. Reservoir response to tidal and barometric effects. Geotherm. Resour. Counc. Trans. V. 4, pp. 337-340.

Hare, P. W. 1998. Personal communication. General Electric Company, Corporate Environmental Programs, 1 computer Drive South, Albany, New York.

Hare, P. W. and R. E. Morse. 1997. Water-level fluctuations due to barometric pressure changes in an isolated portion of an unconfined aquifer. Groundwater. v. 35, n. 4, pp. 667-671.

Hillaker, H. 1999. Personal Communication. State Climatologist, Iowa Department of Agriculture, Johnston, Iowa.

Hsieh, P. A., J. D. Bredehoeft, and J. M. Farr. 1987. Estimation of aquifer transmissivity from phase analysis of Earth-tide fluctuation of water levels in artesian wells. Water Resour. Res. v. 23, pp. 1824-1832.

Hsieh, P. A., J. D. Bredehoeft, and S. A. Rojstaczer. 1988. Response of well-aquifer systems to earth tides: Problem revisited. Water Resour. Res. v. 24, pp. 468-472.

Huyakorn, P. S. and G. F. Pinder. 1983. Computational methods in surface flow. Academic Press, New York. 473 pp.

Hvorslev, M. J. 1951. Time lag and soil permeability in groundwater observations. U. S. Army Crops of Engrs. Exp. Station, Vicksburg, Miss. Bull. 36, 50 pp.

Hyder, Z. and Butler, J. J. 1995. Slug tests in unconfined formations: An assessment of the Bouwer and Rice technique. Ground Water. v. 33, n. 1, pp. 16-22.

Jacob, C. E. 1940. On the flow of water in an elastic artesian aquifer. Trans. Amer. Geophys. Union. v.2, pp. 574-586.

Jacob, C. E. 1950. Flow of Groundwater. Engineering Hydraulics, ed. H. Rouse. John Weily & sons. New York. pp.321-386.

Johnson, A. G., R. L. Kovach, A. Nur, and J. R. Booker. 1973. Pore pressure changes during creep events on the San Andreas Fault. J. Geophys. Res. v. 78, pp. 851-857.

Jones, L. 1993. A comparison of pumping and slug tests for estimating the hydraulic conductivity of unweathered Wisconsinan age till in Iowa. Ground Water. v. 31, no. 6, pp. 986-904.

Jones, L., T. Lemar, and C. Tsai. 1992. Results of two pumping tests in Wisconsin age weathered till in Iowa. Ground Water. v. 30, no. 4, pp. 529-538.

Keller, C. K. and G. van der Kamp. 1992. Slug tests with storage due to entrapped air. Ground Water. v. 30, no. 1, pp. 2-7.

Keller, C. K., G. van der Kamp and J. A. Cherry. 1989. A multiscale study of the permeability of a thick calyey till. Water Resour. Res. v. 25, n. 11, pp. 2299-2317.

Lemar, T. S. 1991. The application of aquifer testing evaluation techniques to oxidized till confining units in central Iowa. Ph. D. dissertation, Iowa State University, Ames, Iowa.

Marine, I. W. 1975. Water level fluctuations due to earth tides in a well pumping from slightly fractured crystalline rock. Water Resour. Res. v. 11, pp. 165-173.

Meinzer, O. E. 1928. Compressibility and elasticity of artesian aquifers. Econ. Geol. v. 23, pp. 263-291.

Munson, B. R., D. F. Young, and T. H. Okiishi. 1990. Fundamentals of fluid mechanics. John Wiley & Sons. New York. 843 pp.

Nguyen, V., and G. F. Pinder. 1984. Direct calculation of aquifer parameters in slug test analysis. In Groundwater hydraulics, ed. J. Rosenshein and G. D. Bennett. AGU Water Resour. Monogr. no. 9, pp. 222-239. Washington, D. C. American Geophysical union.

Nur, A. and J. D. Byerlee. 1971. J. Geophys. Res. An effective stress law for elastic deformation of rock with fluids. V. 76, pp. 6414-6419.

Peck, A. J. 1960. The water table as affected by atmospheric pressure. J. Geophys. Res., v. 65, pp. 2383-2388.

Pinder G. F., J. D. Bredehoeft, and H. H. Cooper, Jr. 1969. Determination of aquifer diffusivity from aquifer response to fluctuations in river stage. Water Resour. Res. v.5, n. 4, pp. 850-855.

Pinder, G. F. and E. O. Frind. 1972. Application of Galerkin's procedure to aquifer analysis. Water Resour. Res. v. 8, no. 1, pp. 108-120.

Prior, J. C., 1991, Landforms of Iowa. University of Iowa Press, pp. 153.

Rasmussen, T. C and L. A. Crawford. 1997. Identifying and removing barometric pressure effects on confined and unconfined aquifers. Ground Water. v. 35, n. 3, pp. 502-511.

Rhoads, G. M., Jr., and E. S. Robinson. 1979. J. Geophys. Res. Determination of aquifer parameters from well tides. v. 84, pp. 6071-6082.

Ritzi, R. W., S. Sorooshian, and P. A. Heieh. 1991. The estimation of fluid flow properties from the response of water levels in wells to the combined atmospheric and Earth tide forces. Water Resour. Res. v. 27, n. 5, pp. 883-893.

Rojstaczer, S. 1988a. Determination of fluid flow properties from the response of water levels in wells to atmospheric loading. Water Resour. Res. v. 24, pp. 1927-1938.

Rojstaczer, S. 1988b. The response of the water level in a well to atmospheric loading and earth tides: theory and application. Ph. D. Dissertation, Stanford University, ???, CA.

Rojstaczer, S. and D. C. Agnew. 1989. The influence of formation material properties on the response of water levels in wells to Earth tides and atmospheric loading. J. Geophys. Res. v. 94, pp. 12,403-12,411.

Rojstaczer, S. and J. P. Tunks. 1995. Field-based determination of air diffusivity using soil air and atmospheric pressure time series. Water Resour. Res. v. 31, n. 12, pp. 3337-3343.

Sen, Zekai. 1995. Applied Hydrogeology for Scientists and Engineers. CRC Press Inc, Boca Raton, Florida, 444 pp.

Seo, H. H. 1996. Hydraulic properties of Quaternary stratigraphic units in the Walnut Creek watershed. M.S. Thesis, Iowa State University, Ames, IA, 145 pp.

Simpkins, W. W. and T. B. Parkin. 1993. Hydrogeology and redox geochemistry of $CH_4$ in a late Wisconsinan till and loess sequence in central Iowa. Water Resources Res. v. 29, no. 11, pp. 3643-3657.

Supardi, S. S. 1993. Repeatability of slug test results in Wisconsinan age glacial till in Iowa. M.S. Thesis, Iowa State University, Ames, IA, 154 pp.

Terzaghi, K. V. 1923. Die Berechnung der Durchassigkeitszffer des Tones aus dem Verlauf der hydrodynamishen Spannungserscheinungen, Sitzungsber. Akad. Wiss. Wien Math Naturwiss. Kl. Abt. 2A, v. 132, pp.105.

Theis, C. V. 1935. The relation between the lowering of the piezometric surface and the rate and duration of discharge of a well using groundwater storage. Trans. Amer. Geophy. Union, v. 2, pp. 519-524.

Todd, D. K. 1959. Ground Water Hydrology. John Wiely & Sons, New York. 362 pp.

Tuinzaad, H. 1954. Influence of the atmospheric pressure on the head of artesian water and phreatic water. Assemblee generale de Rome. Association International d'Hydrologie. Publication no. 37, pp. 32-37.

Turk, L. J. 1975. Diurnal fluctuations of water tables induced by atmospheric pressure changes. Journal of Hydrology. v.26, pp. 1-16.

Van der Kamp, G. 1989. Calculation of constant –rate drawdowns from stepped-rate pumping tests. Groundwater. v. 27, pp. 175-183.

Van der Kamp, G. and J. E. Gale. 1983. Theory of earth tide and barometric effects in porous formations with compressible grains. Water Resour. Res. v. 19, n. 2, pp. 538-544.

Verruijt, A. 1969. Elastic storage of aquifers, in Flow through Porous Media, edited by R. J. M. de Wrist. Academic, New York. pp. 331-376.

Verruijt, A. 1977. Generation and dissipation of pore-water pressure in Finite Elements in Geomechanics, edited by G. Gudehus, John Wiley, New York. pp. 293-317.

Walton, W. C. 1970. Groundwater resource evaluation. McGraw-Hill, New York, 664 pp.

Wang, H. F. and M. P. Anderson. 1982. Introduction to groundwater modeling- finite difference and finite element methods. W. H. Freeman. San Francisco. 237 pp.

Weeks, E. P. 1979. Barometric fluctuation in wells tapping deep unconfined aquifers. Water Resour. Res. v. 15, n. 5, pp. 1167-1176.

Yusa, Y. 1969. The fluctuation of the level of the water table due to barometric change. Geophy. Inst. Spec. Contrib. Kyoto Univ. v. 9, pp. 15-28.

## ACKNOWLEDGMENTS

This study was initiated by the suggestion of Dr. LaDon C. Jones in the Department of Civil Engineering and he provided financial support for me to work on this research during the last three years. Acknowledgments are first due to Dr. Jones for serving as my major professor and for his critical review of the manuscript. I would also like to thank Dr. Robert Horton in the Department of Agronomy/Water Resources for his review and helpful comments on this study and Drs. Tom Al Austin, Roy Gu, and Bruce Kjartanson in the Department of Civil Engineering for their review and service as a graduate committee members.

Appreciation is due to the former graduate students Chin-Ta Tsai, Dean Olson, Sony Supardi and Dr. Carl Pederson for providing valuable field data from the Ames Till Hydrology Site (ATHS) for this study and also to Roger Bruner of Forth Environmental for helping me get the detailed picture of the buried pressure transducers at the ATHS. Special thanks go to Paul Hare of General Electric Company in New York for providing field data for Field Test 3 and to Dr. Stuart Rojstaczer of Duke University for his interest, answers to my questions and discussion on the topic of this study.

I would also like to thank all of my friends at ISU for their encouragement, impetus and friendship all the time. A very special gratitude is due to my husband, Jeong-Yun, and my family in Korea for their encouragement, patience and support. Sincere thanks are extended to my girl, Frances (**Young-Jee**), for the joy and hope that she brings into my life. I love you so much! I deeply thank the God and the Lord Jesus Christ for their unchanging love and blessings that allowed me to complete this work.